NUREG/CR-4971
EGG-2516
March 1988

Results of Semiscale Mod-2C Feedwater and Steam Line Break (S-FS) Experiment Series: Main Steam Line Break Accident Experiments

Timothy J. Boucher

F O R M A L R E P O R T

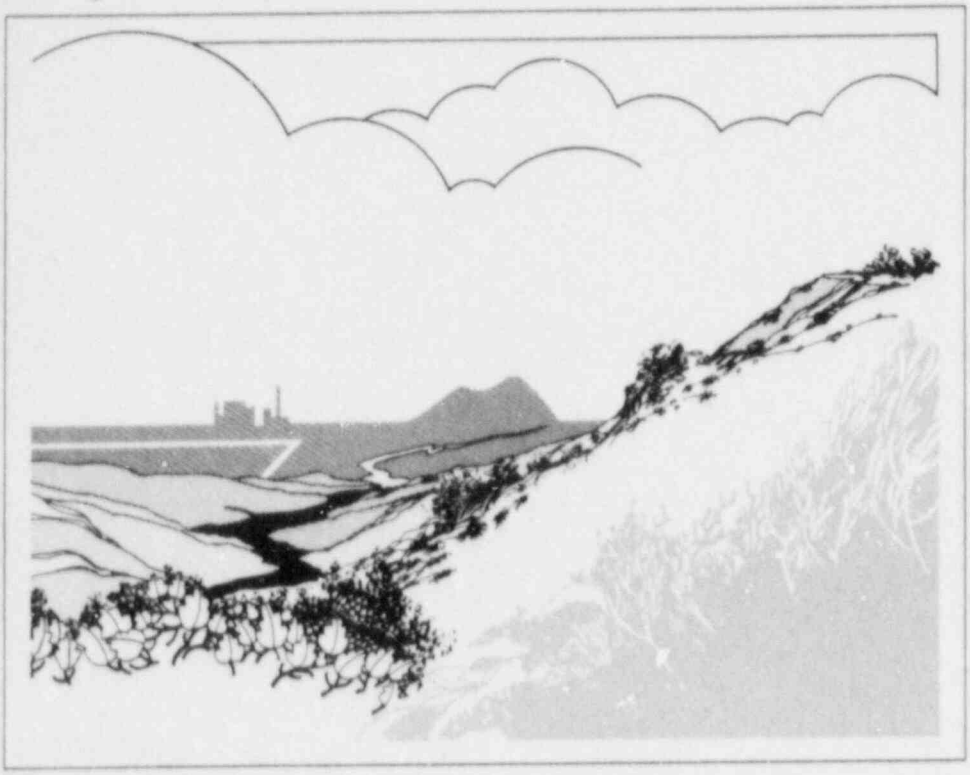

EG&G Idaho

Work performed under
DOE Contract No. DE-AC07-76ID01570

for the U.S. Nuclear
Regulatory Commission

Idaho National
Engineering Laboratory

Managed by the U.S. Department of Energy

Available from

Superintendent of Documents
U.S. Government Printing Office
Post Office Box 37082
Washington, D.C. 20013-7982

and

National Technical Information Service
Springfield, VA 22161

NUREG/CR-4971
EGG-2516
Distribution Category: R2

RESULTS OF SEMISCALE MOD-2C FEEDWATER AND STEAM LINE BREAK (S-FS) EXPERIMENT SERIES: MAIN STEAM LINE BREAK ACCIDENT EXPERIMENTS

Timothy J. Boucher

Published March 1988

EG&G Idaho, Inc.
Idaho Falls, Idaho 83415

Prepared for the
Division of Accident Evaluation
Office of Nuclear Regulatory Research
U.S. Nuclear Regulatory Commission
Washington, D. C. 20555
Under DOE Contract No. DE-AC07-76ID01570
FIN No. A6038

ABSTRACT

This report presents the results of two experiments conducted in the Semiscale Mod-2C facility which simulated main steam line break accidents at high pressure and temperature. Tests S-FS-1 and S-FS-2 simulated double-ended offset shears of the main steam line downstream and upstream, respectively, of the flow restrictor. Initial and boundary conditions were scaled from, and compounding failures and assumptions simulated, those conditions utilized for Final Safety Analysis Report (FSAR) calculations.

Primary and secondary thermal-hydraulic responses are characterized (including local secondary convective heat transfer), and the influence of the break size or location on the responses is discussed. The limiting of primary-to-secondary heat transfer by conduction heat transfer is shown to produce a trend of increased primary cooling with decreased break size, pointing out the need for further analysis for smaller break sizes. The degree of conservatism inherent in FSAR separator performance and break size and location assumptions is shown to be questionable, and the FSAR assumption of a loss of offsite power is shown to be nonconservative. The effectiveness of the recovery operations in regaining and maintaining control of the system is addressed; and main steam line break issues, including the minimum primary fluid temperatures estimated for a full-scale PWR plant, are discussed based on the results of the experiments. Finally, based on the results of the analysis, conclusions are drawn and recommendations are made for further utilization of the data. Future thermal-hydraulic computer code calculations are also considered.

EXECUTIVE SUMMARY

Although steam generator main steam line ruptures are not expected to occur often in pressurized water reactor (PWR) plants, the potential for rupture of the vessel pressure boundary due to the occurrence of pressurized thermal shock necessitates their examination. A limited amount of existing data on present-day PWR steam generators has resulted in the utilization of a large number of assumptions and simplifications in predictive calculations. Concerns exist with regard to the potential for primary system overcooling; the validity and effects of combining the assumptions and simplifications; the effectiveness of recovery procedures; and the effects of steam generator downcomer liquid level differential pressure measurement response on safety trip systems.

To address these concerns, two main steam line break (MSLB) experiments were performed in the Semiscale Mod-2C facility. The Mod-2C system is a small-scale, nonnuclear, electrically heated, high-pressure, high-temperature experimental system which simulates all of the major components of a full-scale PWR. It contains a vessel and two primary coolant loops. The affected and unaffected loops simulate one loop and three loops of a four-loop PWR, respectively. Both loops contain active steam generators and pumps, with the single-loop steam generator highly instrumented for this test series. Tests S-FS-1 and S-FS-2 simulated double-ended offset shears of the main steam line downstream and upstream, respectively, of the flow restrictor. Initial and boundary conditions were scaled from, and compounding failures and assumptions simulated, those conditions utilized for Final Safety Analysis Report (FSAR) calculations. Data from the experiments should be useful for quantifying the safety margin inherent in licensing assumptions, simplifications, and calculations, and in providing a data base of integral system response for assessment of computer codes and recovery procedure effectiveness.

The results of the analysis of the Semiscale Mod-2C MSLB data were used as a basis for addressing the principal MSLB issues and concerns, which include: (a) the relative degree of conservatism inherent in FSAR assumptions and simplifications; (b) the steam generator downcomer liquid level differential pressure measurement response effects on safety trip systems; (c) the effects of break size and location; (d) the potential for primary system overcooling; and (e) the effectiveness of recovery procedures specified in Emergency Operating Procedures (EOPs).

Final verification of the relative degree of conservatism inherent in FSAR assumptions and simplifications will require best-estimate calculations performed with a verified computer code. However, the results of the analysis of the Semiscale Mod-2C MSLB data can be used as a basis for addressing the conservatism of a number of FSAR assumptions and simplifications. Assumptions which maximize primary cooling but do not emulate the actual response exhibited by the experimental data are considered to be conservative. The Semiscale results indicate that:

- FSAR assumptions of perfect separator performance are only mildly conservative, because the rate of the primary energy removal is controlled by the conduction heat transfer across the U-tube wall, not by the break flow energy removal rate. The assumption does, however, maximize the duration of the secondary blowdown, thereby maximizing the total primary energy removal for a given break size.
- FSAR assumptions that larger break sizes produce greater primary system cooling are not conservative. The rate of the primary energy removal is controlled by the conduction heat transfer across the U-tube wall. Larger break sizes deplete the secondary inventory much more rapidly, terminating the primary energy removal much faster without substantially increasing the primary energy removal rate. The most conservative break size assumption would be a break size which produces a break flow energy removal rate which is as close as possible to the conduction-limited primary energy removal rate.
- Assuming main steam line check valve failure for FSAR calculations is conservative, since the loss of inventory from the unaffected loop steam generators prior to main steam isolation valve (MSIV) closure provides additional primary energy removal, which significantly increases the amount of the total primary cooling.
- The FSAR assumption regarding loss of offsite power at SI signal generation is not conservative, because the resulting loop

flow reductions decrease the primary convective heat transfer, reducing the net primary cooling in all of the loops.

- Configurational and fluid hydraulic response dependencies of the downcomer liquid level measurements make them suspect as conservative assumption candidates, but it is conceivable that they would produce earlier SI signal generation and thus be nonconservative.

Secondary and primary thermal-hydraulic responses are somewhat sensitive to break size and location. The main differences observed are in the timing of events and the quantitative responses. However, notable break size or location sensitivities were observed in the affected and unaffected loop steam generator primary energy removal and the primary pressure, temperature, and hydraulic responses. The affected and unaffected loop steam generator primary energy removal was much greater for the break downstream of the flow restrictor than for the break upstream of the flow restrictor. The smaller affected loop steam generator flow area for the break downstream of the flow restrictor substantially increased the duration of the primary energy removal without a substantial decrease in the primary energy removal rate. Thus, the smaller break size produced greater primary cooling, which produced notable affects on primary responses. The greater primary cooling for the break downstream of the flow restrictor produced greater primary fluid shrinkage (with the pressurizer emptying), which produced lower minimum primary pressure. The greater primary cooling also produced a lower minimum downcomer fluid temperature. These notable break size or location dependencies point out the need for assessing smaller break sizes for worst-case primary cooling considerations.

Extrapolation of Semiscale Mod-2C measured minimum downcomer fluid temperatures to those predicted for a full-scale PWR points out the need for further analysis. The measured minimum downcomer fluid temperatures for the Semiscale Mod-2C MSLB experiments are not a direct indicator of the minimum temperatures expected for a full-scale PWR. Therefore, a simple total primary energy removal versus primary fluid energy removal analysis was performed which accounted for atypical Semiscale Mod-2C metal mass and steam generator U-tube wall thickness effects. The analysis produced estimated minimum downcomer fluid temperatures substantially closer to, but still above, the 450-K pressurized thermal shock (PTS) minimum temperature limit. This result, coupled with the observed trend of lower minimum temperatures for smaller break sizes, points out the need to perform best-estimate calculations for a range of break sizes, utilizing a thermal-hydraulic computer code that has been assessed against and verified for the results of these experiments.

The automatic actions performed by the plant protective systems during the blowdown phase of the experiments left the system in a quasi-stable condition, but at conditions that did not ensure sufficient control of the system. The guidance provided by EOPs was both appropriate and effective in stabilizing and regaining control of the system for both experiments. The stabilization operations performed (SI termination, normal charging/letdown, pressurizer internal heater, and unaffected loop steam generator steam and feed operations) were very effective in stabilizing the system at conditions from which a controlled natural circulation cooldown and depressurization could be initiated. The limiting criterion in regaining control of the system for both experiments was the recovery of the pressurizer liquid level, with the break downstream of the flow restrictor case requiring the greatest amount of time to recover the level control. No upper head voiding occurred during the stabilization phase of either experiment.

The natural circulation cooldown and depressurization operations performed following system stabilization for Test S-FS-1 were very effective in cooling down and depressurizing the primary fluid system in a controlled manner. (These included normal charging/letdown, pressurizer internal heater, pressurizer auxiliary spray, and unaffected loop steam generator steam and feed with stairstep secondary pressure reduction operations.) The unaffected loop steam generator steam and feed operations with 0.71-MPa stairstep secondary pressure reductions were successful in cooling the primary fluid at about 26 K/h. However, the auxiliary feedwater flow had to be increased to the scaled maximum flow for two diesel-driven auxiliary feedwater pumps in order to maintain satisfactory control of the secondary fluid inventory at this cooldown rate. The combined operations of pressurizer auxiliary spray and internal heaters demonstrated excellent control of primary pressure and subcooled margin. An inadvertent vessel upper head void formation was due not to inappropriate recovery operations, but to the vessel upper head external heater energy addition exceeding the upper head heat loss.

Scale effects (atypical metal-mass-to-fluid-volume ratio and heat loss/heat loss mitigation) had minimal effects on the system response. The largest effect was an inadvertent vessel upper head void formation during the cooldown and depressurization due to excessive upper head heat loss mitigation. However, in general, the metal mass and heat loss effects offset each other such that the overall system response should be a reasonable indicator of the general response expected for a full-scale PWR plant. In any case, the metal masses and heat loss/heat loss mitigation for the Semiscale Mod-2C system are well characterized and can be modeled by best-estimate computer codes so that the data are well suited for code validation.

During the course of the analysis of the Semiscale Mod-2C MSLB data, a number of areas have been identified that warrant consideration for future analyses. The indicated trend in primary cooling with break size warrants further analysis with smaller break sizes. For smaller break sizes, the secondary convective heat transfer will be of greater importance in determining the primary-to-secondary heat transfer. Thus, for calculations with smaller break sizes, improvements in the secondary convective heat transfer calculation methodology will be required if thermal-hydraulic computer codes are to calculate the primary-to-secondary transient heat transfer with reasonable accuracy. This will require either modifications to existing correlations or development of a new, boiling convective heat transfer correlation based on the Semiscale Type III steam generator heat transfer data. Also, future MSLB calculations for FSARs should delay the loss of offsite power until the affected steam generator secondary has emptied. Finally, the capabilities and accuracy of codes used for best-estimate main steam line break calculations should be established using these experimental data or similar integral system experimental data before they can be used with confidence or to satisfy the proposed revision to the emergency core cooling system (ECCS) rule (10 CFR Part 50).

ACKNOWLEDGMENTS

Acknowledgment, with thanks, is given to the following individuals who have contributed to the understanding of phenomena and to the production of this report (in alphabetical order): Nello Boricelli (DOE-ID), Don Solberg (NRC), and J. R. Wolf, for their technical reviews of this report; T. H. Chen and W. A. Owca, for their analysis in the Quick Look Reports for tests S-FS-1 and S-FS-2; G. I. Johnson and N. L. Wade, for technical editing; S. L. Martin, for help with word processing; and C. C. McKenzie, for producing the computer-generated data plots. Without their assistance, this report could not have been completed in its present form.

CONTENTS

FIGURES

TABLES

RESULTS OF SEMISCALE MOD-2C FEEDWATER AND STEAM LINE BREAK (S-FS) EXPERIMENT SERIES: MAIN STEAM LINE BREAK ACCIDENT EXPERIMENTS

INTRODUCTION

The Semiscale experimental program conducted by EG&G Idaho, Inc. is part of the overall research and development program sponsored by the U.S. Nuclear Regulatory Commission (NRC) through the Department of Energy (DOE) to evaluate the behavior of pressurized water reactor (PWR) systems during hypothesized accident sequences. Its primary objective is to obtain representative integral- and separate-effects thermal-hydraulic response data to provide an experimental basis for analytical model development and assessment. The subject Semiscale Mod-2C experiments,[1] S-FS-1[2,3] and S-FS-2,[4,5] were authorized and performed under this program. The experiments simulated main steam line break (MSLB) secondary loss-of-coolant accidents (LOCAs) and were identical except for break size and location and system recovery operations. Test S-FS-1 simulated a double-ended offset shear of the main steam line downstream of the flow restrictor, whereas Test S-FS-2 simulated an identical break upstream of the flow restrictor.

This report discusses results of the simulated MSLB transients conducted in the Semiscale Mod-2C test facility and presents information pertinent to related safety issues. The Semiscale Mod-2C test facility is a small-scale, nonnuclear model of a PWR power plant. The volume and thermal power of the test loop are 1/1705 those of the reference four loop Westinghouse PWR (Trojan). The Semiscale Mod-2C facility is full height and contains the active components (core, pumps, steam generators, etc.) necessary to simulate all of the PWR components pertinent to transient response simulation and evaluation. The scenario in Semiscale for the initial phase of the tests was based on the scenario used for the Final Safety Analysis Report (FSAR) MSLB calculations (Appendix 15) for the Zion Unit No. 1 Nuclear Plant (a four-loop PWR designed by Westinghouse). Following the initial phase, plant stabilization operations were performed for both tests. Plant stabilization was followed by plant cooldown and depressurization operations for Test S-FS-1. The discussions of the responses of the primary and secondary fluid systems include descriptions of the thermal-hydraulic response and the mechanisms that drive the response. The topics pertinent to the MSLB transients and related safety concerns discussed include:

- Transient identification,
- The affected loop steam generator separator performance,
- Primary overcooling,
- The effects of break size or location,
- The effectiveness of plant automatic actions,
- The effectiveness of plant stabilization operations,
- The effectiveness of plant cooldown and depressurization operations, and
- The effects of, degree of conservatism inherent in, and applicability of FSAR assumptions.

The intent of this report is to provide insight into a number of areas. First, the general appearance of the Semiscale Mod-2C MSLB transient is presented, and the main elements of the transient are identified. This discussion will be helpful in gaining insight about the probable appearance of MSLB transients in PWR plants, although the magnitude and timing of the response for specific plants must be considered separately. Next, a detailed description and analysis of a particular transient and the driving mechanisms and thermal-hydraulic response of that transient are provided. This should improve the ability to track and assess thermal-hydraulic code calculations based on the Semiscale Mod-2C MSLB transient data. The effects of the break size and location on the system response are presented next, and the driving mechanisms affecting the response are identified. This should provide insight into the effects of break size or location on transient severity. Next, the system response to

plant stabilization, cooldown, and depressurization operations are discussed; and the driving mechanisms affecting the response are identified. This should provide insight into the effectiveness of the operations specified in Emergency Operating Procedures (EOPs) in stabilizing and recovering the plant following a MSLB. Pertinent MSLB issues are discussed next in light of the results of these tests. Major emphasis is placed on the test results relative to FSAR assumptions, current licensing concerns, and EOPs. This should provide insight into the relative effects, degree of conservatism inherent in, and applicability of several MSLB FSAR assumptions; the extent of primary system cooling; and, the effectiveness of the EOPs for recovering and cooling down the plant.

The overall organization of this report is as follows. Following this introduction, the historical background for these tests is discussed. This is followed by a brief system description and discussion of experimental procedure. Next, the general areas outlined above are presented, followed by a discussion of the conclusions drawn based on the results of the MSLB tests. Finally, recommendations for additional uses of the data are provided, followed by a list of references and appendices containing a detailed system description, test conduct information, and additional test data.

HISTORICAL BACKGROUND

Although ruptures of steam generator main steam lines are not expected to occur often in PWR plants, the potential consequences of these events necessitates their examination. Failures of steam turbine exhaust lines, caused by steam erosion, have occurred in a number of PWR plants.[6] Although these events have not been severe, they indicate the potential for the occurrence of more severe steam line rupture events. Steam line break transients lead to excessive cooldowns of the primary coolant systems and eventually to possible repressurization once the heat sink is lost. Although concerns regarding possible recriticality power excursions have been identified, the emphasis in the nuclear industry is on concerns related to pressurized thermal shock phenomena.[7] The associated threat to the integrity of the PWR pressure boundary necessitates examination of steam line break events.

Due to the limited data base on present-day PWR steam generators and associated systems, a large number of assumptions and simplifications are employed when performing calculations to predict system responses to MSLB transients. Foremost is an assumption regarding the separator performance. Such assumptions and simplifications may preclude accurate prediction of actual system response or combine to distort overall behavior. Verification of the response predicted by thermal-hydraulic computer codes requires performing best-estimate MSLB calculations utilizing a computer code that has been assessed for these types of events. While significant information on integral system response was provided by two MSLB experiments[8,9] performed in 1982 in the Semiscale Mod-2A facility, lack of sufficient steam generator secondary side measurements made code assessment impractical. Hence, a need for experimental data required to allow assessment of computer codes for steam line break events was identified by the NRC.[a] The need for experimental data on primary-to-secondary heat transfer response and separator performance during MSLB accidents has been identified and included in the Westinghouse Model Boiler (MB-2)[10] and Japanese Atomic Energy Research Institute (JAERI) Rig of Safety Assessment (ROSA-IV) Large-Scale Test Facility[b] experimental safety research programs.

With this background information in mind, the steam line break experiments performed during the Semiscale Mod-2C feedwater and steam line break (FS) experiment series were chosen to provide data within a representative range of typical PWR conditions, break sizes and locations, and operating scenarios with appropriate conservatisms incorporated. The MSLB test parameters were scaled from a Westinghouse four-loop plant. The boundary and initial conditions were consistent with those in Reference 11. Data from the experiments will be useful in quantifying the safety margin inherent in licensing assumptions, simplifications, and calculations, and in providing a data base of integral system response for assessment of computer codes. The heat transfer data from the Semiscale Mod-2C integral system MSLB experiments will also be complemented by heat transfer data from the MB-2 program single-component steam generator MSLB experiment and the ROSA-IV program integral-system MSLB experiment. The combined data from these programs will cover a wide range of scale [1/48 volume scale for ROSA-IV (LSTF); 1/159 volume scale for MB-2; and 1/1705 volume scale for Semiscale Mod-2C] and should allow assessment of the effects of scale on the heat transfer phenomena observed.

In terms of reactor operation and plant behavior, major concerns regarding steam line break events include: the effects of compounding system failures on recovery procedures; and the effect of steam generator downcomer liquid level differential pressure measurement response to flow out of the break on related safety trip systems.[a] The incorrect choice of recovery procedures may lead to primary fluid system voiding and eventual core uncovering. Break location and size may also alter system behavior and transient severity. Improperly indicated steam generator downcomer liquid levels could result in delayed reactor and turbine trips, delayed main steam isolation valve (MSIV) closures, delayed safety injection (SI) signals, and delayed initiation of auxiliary feedwater injection. The steam line break experiments performed addressed the concerns and effects of the aforementioned variables.

---

a. R. J. Mattson to O. E. Bassett, "Additional Semiscale and RELAP5 Needs for DSI," January 11, 1982.

b. Minutes of the Sixth JAERI/ROSA-IV Program Technical Review Meeting, April 23-24, 1987, Attachment J-15.

a. A Memo of Conservation, J. S. Martinell to Jack Guttman (NRC Licensing), "Feedline/Steamline Break Issues," June 17, 1983.

SYSTEM DESCRIPTION AND EXPERIMENTAL PROCEDURE

System Description

The facility configuration required for the FS test series is the Semiscale Mod-2C system. A more detailed description of the facility as configured and instrumented for the MSLB tests is contained in Appendix A of this report and in Reference 12. Briefly, the system is scaled from a reference four-loop PWR system based on the core power ratio, 2(MWth)/3411(MWth).[13] Component elevations, dynamic pressure heads, and liquid distributions were maintained as similar as practical.

The two-loop test configuration consisted of the vessel, with a 25-rod, electrically heated core, and external downcomer, tube-and-shell steam generators, and associated loop piping with circulation pumps. The affected loop (in which the MSLB occurs) is scaled to represent one loop of a four-loop PWR, and the unaffected loop represents three loops of a four-loop PWR. The Mod-2C system consists of the Mod-2B system with several modifications, the foremost of which is a new Type III steam generator in the affected loop. The Type III steam generator design incorporates a downcomer that is outside the tube bundle and riser sections. In this manner, component mass inventory and fluid property (including density/void fraction) information was obtained.

The design also includes a steam dome with separator equipment which provides steam exit qualities of at least 90% during full-power, steady-state operations. Component flow areas, volumes, lengths, and pressure drops have been sized to simulate a Westinghouse Model 51 steam generator. Temperature measurements from the primary fluid, U-tube outside wall, and secondary fluid were normalized to provide heat transfer data for the tests. Measurement spool pieces in the upper and lower downcomer and the riser provided fluid hydraulics data for the tests.

Experimental Procedure

The two MSLB tests performed during the FS test series simulated transients initiated by a double-ended offset shear of a steam generator main steam line both downstream (S-FS-1) and upstream (S-FS-2) of the flow restrictor. The initial conditions and sequences of events were specified to simulate the initial conditions and assumptions used for the FSAR calculations (Appendix 15) for the Zion Unit 1 Nuclear Plant (a Westinghouse design four-loop PWR).[11] A more detailed discussion of the initial conditions and sequences of events for the MSLB tests is contained in Appendix A of this report.

A greatly detailed discussion of the experimental procedure for the steam line break tests is contained in References 2, 3, 4, 5 and 12. Briefly, the initial conditions for the tests represented the "hot standby" conditions (thought to produce the most severe primary cooling) used for the Zion Unit 1 FSAR calculations. Many of the assumptions made for the Zion Unit 1 plant FSAR calculations were also used for these tests, including:

- Failure of the check valve in the main steam line of the affected steam generator,
- Safety injection (SI), MSIV closure, and main feedwater isolation signals generated based on low affected steam generator secondary pressure,
- Loss of offsite power, causing primary coolant pump trips and delaying SI and auxiliary feedwater availability, was assumed to occur at SIS,
- Degraded HPIS and charging flows were assumed such that only one train of SI was available,
- Auxiliary feedwater was assumed to be supplied only to the unaffected steam generators.

Compensation for environmental heat loss was provided through heat addition with trace heaters on the exterior of the pressure boundary and through augmentation of the core power.

EXPERIMENTAL RESULTS

This section presents an interpretive description of important thermal-hydraulic phenomena associated with Semiscale Mod-2C MSLB Tests S-FS-1 and S-FS-2. The discussion is aimed toward aiding code development and assessment efforts, EOP effectiveness analysis efforts, and FSAR assumption analysis efforts. Therefore, discussion concentrates on the phenomena which are either of a particular challenge to code application or are pertinent to EOP effectiveness and FSAR assumption analysis efforts, or both.

Most of this section refers to data from Test S-FS-1, which simulated a double-ended offset shear downstream of the flow restrictor. Following an overview of the gross system response during the blowdown phase of a MSLB secondary LOCA, the secondary system response during the blowdown phase is discussed along with the mechanisms driving the response. Included in the discussion on secondary response during the blowdown phase are the pressure, hydraulic, and thermal responses for both secondaries (with emphasis on the affected loop steam generator and its local heat transfer response). Next, the primary system response associated with the secondary response is discussed, along with the mechanisms driving the response. Included in the discussion on primary response during the blowdown phase are pressure, hydraulic, and thermal responses.

The influence of break size and location on the blowdown phase of a MSLB secondary LOCA is then discussed. Included in this discussion are the secondary and primary thermal-hydraulic response comparisons and the driving mechanisms. Next, the effectiveness of plant stabilization operations is discussed for Tests S-FS-1 and S-FS-2. Included in this discussion are the primary and secondary pressure, temperature, and fluid inventory responses to plant stabilization operations as taken from EOPs. The system response to plant cooldown and depressurization operations for Test S-FS-1 is then discussed. Included in this discussion are the primary and secondary pressure, temperature, and fluid inventory responses to plant cooldown and depressurization operations, as taken from EOPs. Finally, based on the results of these tests, pertinent MSLB issues are discussed. Major emphasis is placed on the test results relative to FSAR assumptions, current licensing concerns, and EOP-specified recovery operations.

Overview of a Steam Generator Main Steam Line Break

Preliminary to the detailed discussion of Tests S-FS-1 and S-FS-2 results, this section presents a qualitative overview of the gross system response to a MSLB secondary LOCA, with special emphasis on major events that affect the primary energy balance and, thus, transient severity. System response during a double-ended offset shear MSLB is characterized as a secondary depressurization with total loss of the affected loop steam generator secondary fluid mass inventory and substantial loss of the unaffected loop steam generator secondary fluid mass inventory (due to the failed main steam line check valve), as shown in Figure 1. The affected loop steam generator secondary fluid mass inventory is controlled by the fluid mass balance formed by the flow out of the break and the main feedwater flow. The unaffected loop steam generator secondary fluid mass inventory is controlled by the fluid mass balance formed by flow past the failed main steam line check valve, main feedwater flow, and auxiliary feedwater flow. As shown in Figure 1, the loss of mass from the secondaries causes a rapid depressurization of the affected loop steam generator, while the unaffected loop steam generator experiences a somewhat slower depressurization early in the transient due to less subcooling of the secondary downcomer fluid. Once the subcooling is removed from the secondary downcomer fluid, the depressurization rates decrease slightly and are nearly identical. These depressurizations continue until the low affected loop steam generator secondary pressure trip setpoint is reached (at about 21 s in Figure 1), initiating the SI and MSIV closure signals. The depressurization of the unaffected loop steam generator is halted when the MSIV fully closes, isolating the unaffected loop steam generator and causing a slight repressurization of the secondary. The affected loop steam generator continues to depressurize until the generator is essentially empty (at about 110 s in Figure 1). The remainder of the blowdown phase of the transient is characterized by the unaffected loop steam generator auxiliary feedwater recovering the secondary inventory and providing cooling which aids in stabilizing the unaffected loop steam generator secondary pressure and the primary system fluid temperature.

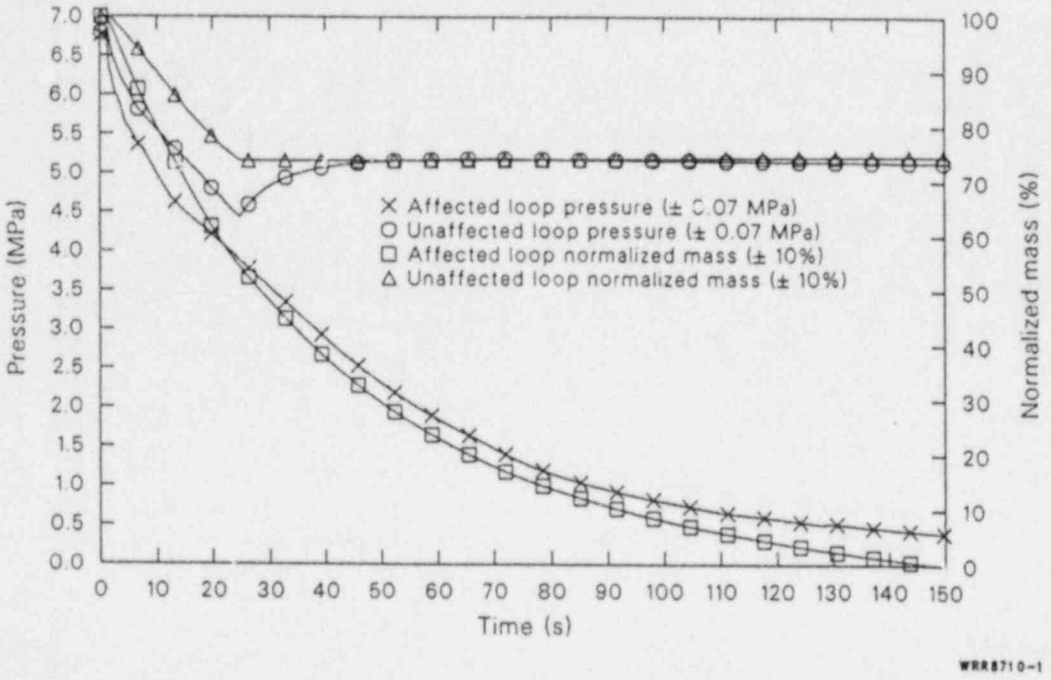

Figure 1. Affected and unaffected loop steam generator secondary pressures and normalized secondary fluid mass inventories during the blowdown phase of a double-ended offset shear downstream of the flow restrictor MSLB transient.

The primary fluid system response is a rapid cooldown in response to the increased primary-to-secondary heat transfer during the MSLB secondary LOCA. As shown in Figure 2, the primary fluid rapidly cools down as the primary-to-secondary heat transfer increases in the affected and unaffected loop steam generators. This causes the primary fluid to shrink and rapidly depressurize, with the depressurization rate increasing due to the emptying of the pressurizer (at about 17 s in Figure 2). The primary cooldown continues until the primary coolant pumps coast to a stop at about 52 s after the loss of offsite power (i.e., about 52 s after the SI signal is generated), with the minimum fluid temperature occurring in the loop cold legs. The primary system response after this point is governed primarily by the SI and auxiliary feedwater flows. The SI flow enters the primary fluid system and initiates refilling of the pressurizer (at about 86 s in Figure 2). This results in a very gradual increase in the pressurizer liquid level, which continues until operator actions are taken to terminate SI flow. The cold (300 K) SI flow also provides minor primary fluid energy removal which aids the unaffected loop steam generator auxiliary feedwater in stabilizing the average fluid temperature during the initial phase of the transient. The remainder of the blowdown phase of the transient is characterized by the SI flow slowly increasing the pressurizer liquid inventory, and the primary fluid system pressure and temperature slowly increasing as the primary heats slightly. No upper head voiding occurs, and the primary fluid system remains subcooled.

At the end of the blowdown phase of the transient, the primary and secondary systems are sufficiently stable to allow transient identification and plant stabilization and recovery operations to begin.

Secondary System Response to a Steam Generator Main Steam Line Break

Understanding the secondary fluid system thermal-hydraulic response during a MSLB secondary LOCA is important, because the cooling of the primary fluid system is controlled by the secondary response. Basically, the primary thermal response is controlled by an overall energy balance involving core power, primary-to-secondary heat transfer, and heat loss. There are several characteristic inflection

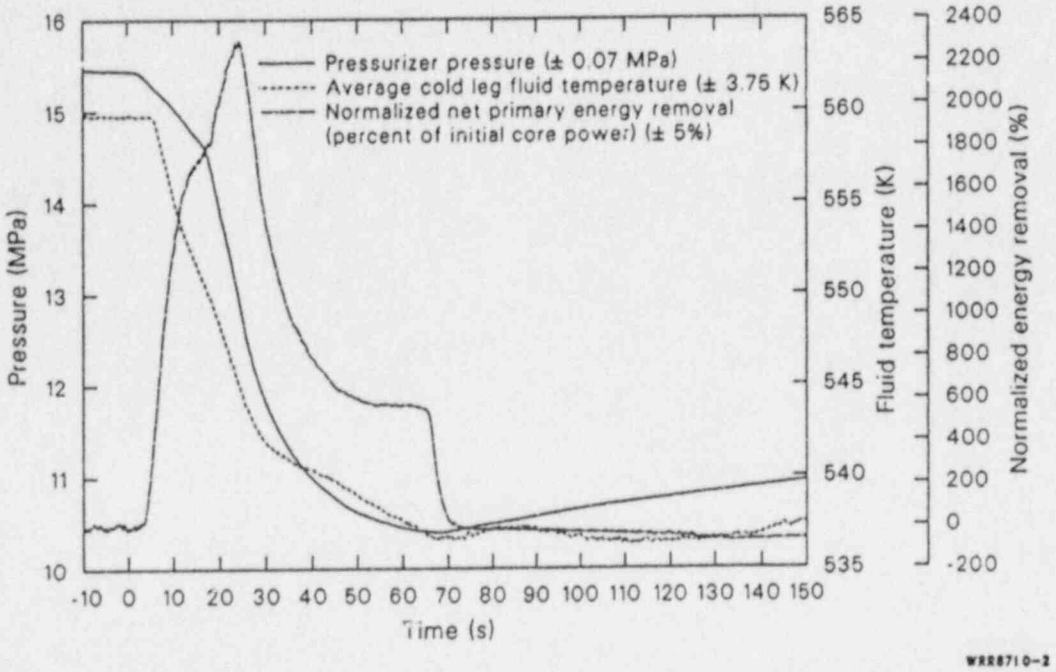

Figure 2. Normalized primary fluid system energy removal, pressurizer pressure, and average cold leg fluid temperature during the blowdown phase of a double-ended offset shear downstream of the flow restrictor MSLB transient.

points in the secondary fluid system thermal-hydraulic response to a MSLB secondary LOCA. The causes of these inflection points are discussed in this section. The general sequence of events affecting the secondary response are outlined first. This is followed by discussions of the pressure response, hydraulic response, and thermal response for both secondaries, with major emphasis on the affected loop steam generator. Since both of the MSLB experiments had similar basic secondary thermal-hydraulic responses, this discussion refers to Test S-FS-1 data only. Break size and location effects will be discussed later.

General Secondary Response. The occurrence of a double-ended offset shear of a steam generator main steam line downstream of the flow restrictor produced severe effects on the steam generator secondaries. The steam line break initiated the transient at 0 s. Compounded by failure of the affected loop steam generator steam line check valve, the unaffected, as well as affected, loop steam generator experienced loss of inventory. Secondary fluid, originally at 6.76 MPa, flowed from the steam generators through the break flow nozzles and into the catch tanks. The primary energy removal was substantially increased for both secondaries due to the break flow energy removal. The loss of mass produced significant depressurization of both secondaries until the low affected loop steam generator secondary pressure signal was generated, initiating MSIV closure. Following MSIV closure, the depressurization of the unaffected loop steam generator secondary was halted. The affected loop steam generator continued to depressurize until it emptied, decoupling from the primary system. The unaffected loop steam generator slowly refilled with auxiliary feedwater and slowly repressurized.

Secondary Pressure Response. The secondary pressure responses are characterized by a number of inflection points associated with changes in the mass and energy balances. As shown in Figure 3, the loss of mass from the secondaries caused a rapid depressurization of the affected and unaffected loop steam generators. The marked decreases in depressurization rates (at 5.8 MPa in the unaffected loop steam generator and 4.7 MPa in the affected loop steam generator) were due to initially subcooled downcomer fluid reaching saturation conditions. The secondary depressurizations following these points were very similar due to the

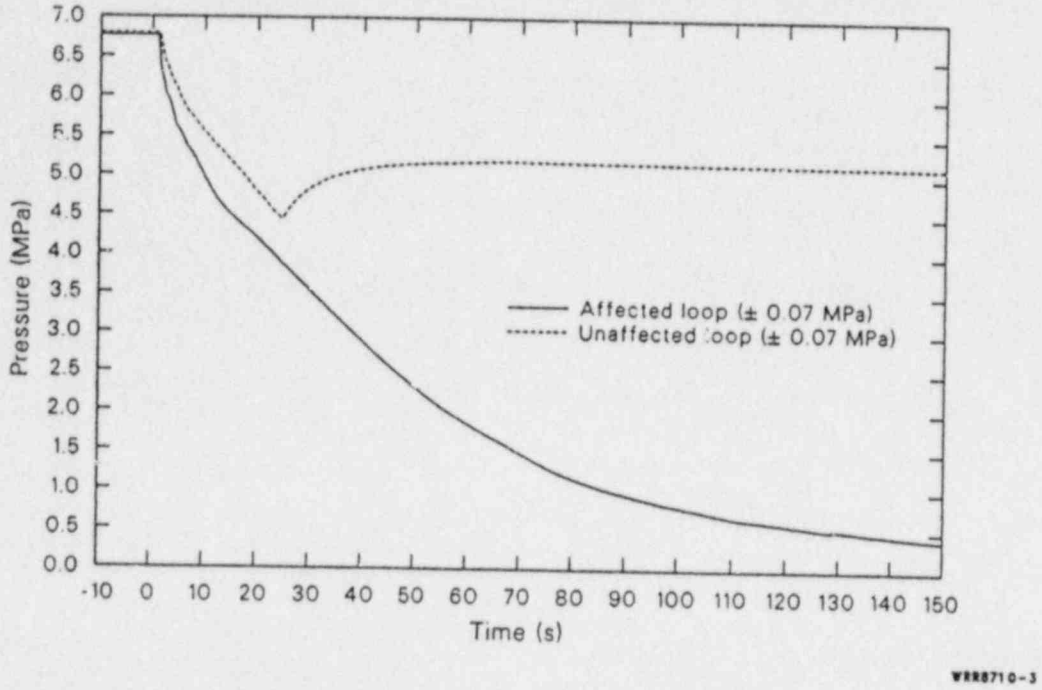

Figure 3. Affected and unaffected loop steam generator secondary pressures during the blowdown phase of MSLB Test S-FS-1 (-10 to 150 s).

simulated break configuration. For a double-ended offset shear downstream of a flow restrictor with concurrent check valve failure, the flow from each secondary is limited only by its own flow restrictor. Therefore, the break-flow-to-secondary-volume ratio is the same for each secondary, resulting in similar depressurization rates. The low affected loop steam generator secondary pressure trip setpoint of 4.14 MPa was reached at about 21 s. This initiated the SI and MSIV closure signals. The depressurization of the unaffected loop steam generator was halted when the MSIV fully closed at about 27 s. Following MSIV closure, the unaffected loop steam generator experienced a slight repressurization due to energy addition from the primary fluid system in the absence of secondary feeding and steaming. The affected loop steam generator continued to depressurize until the generator was essentially empty at about 110 s; it became essentially decoupled from the primary fluid system for the remainder of the transient. The unaffected loop steam generator secondary pressure continued to experience a very gradual increase due to the primary energy addition exceeding the auxiliary feedwater energy removal. At the end of the blowdown phase of the transient, the secondary pressures were fairly stable.

Secondary Hydraulic Response. The hydraulic response of the affected loop steam generator secondary fluid system to a double-ended offset shear of the main steam line downstream of the flow restrictor is characterized by a rapid voiding of the entire secondary. Because the affected loop steam generator was not steaming at initial conditions and injection of auxiliary feedwater into the affected loop steam generator was disallowed (simulating the response of an automatic faulted secondary detection system), the secondary mass balance was affected only by the break flow. The simulated MSLB initiated the loss of secondary inventory, which severely affected secondary hydraulic characteristics. As shown in Figure 4, the break flow peaked at about 1 s as the critical flow was established. The break effluent from the steam generator consisted of two-phase fluid early in the transient, followed by single-phase steam for the remainder of the blowdown, as shown in Figure 5. The transition of the break flow from a two-phase mixture to single-phase steam produced slight

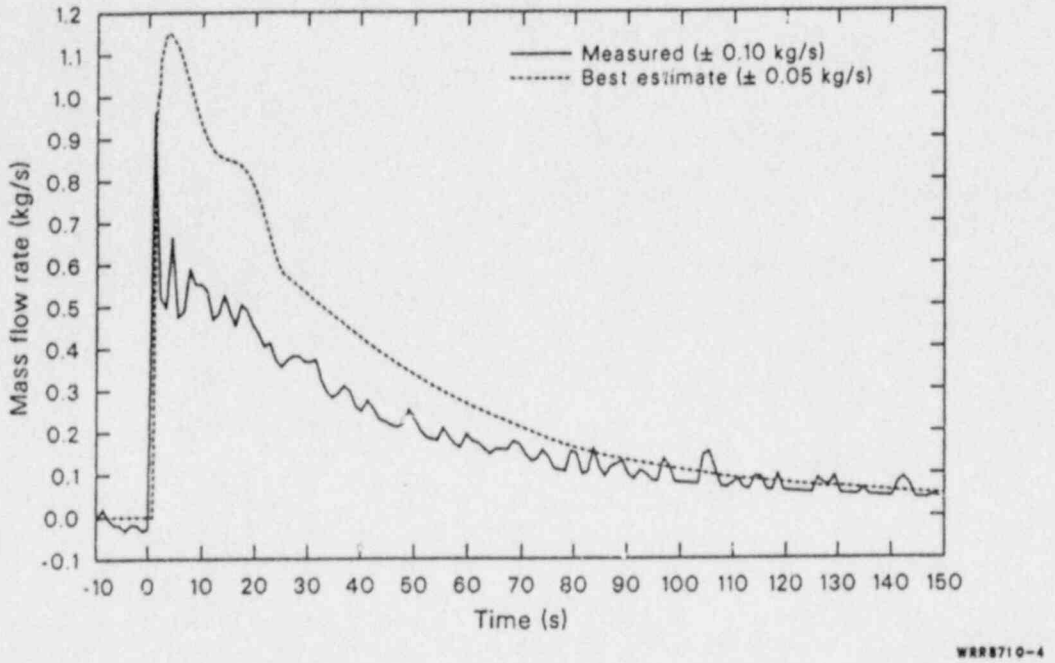

Figure 4. Affected loop steam generator measured and best-estimate break mass flow rates during the blowdown phase of MSLB Test S-FS-1 (-10 to 150 s).

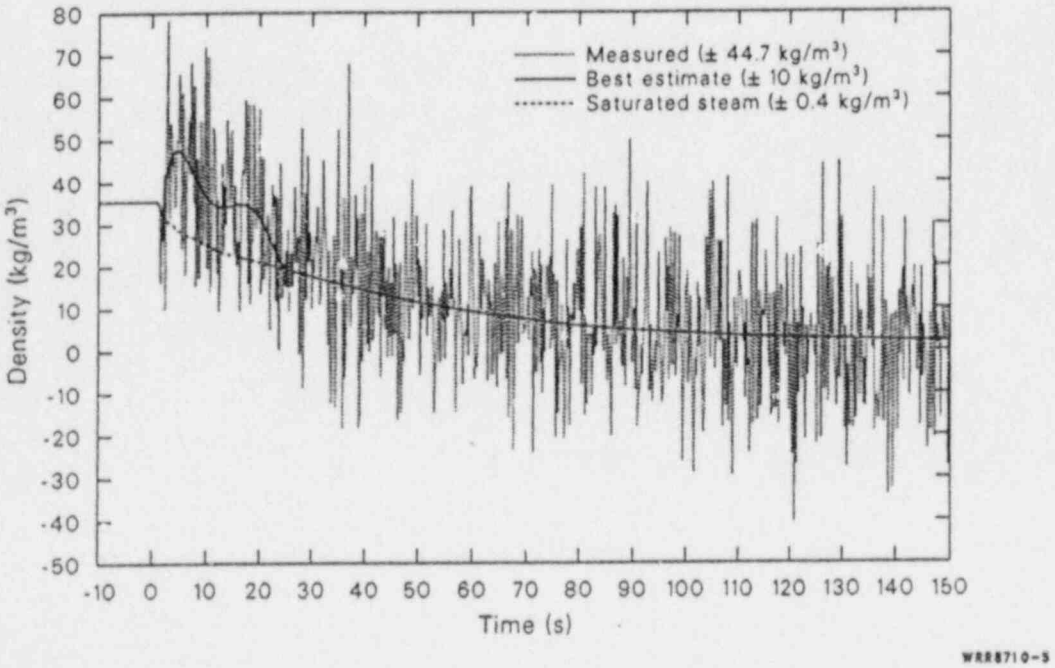

Figure 5. Affected loop steam generator measured and best-estimate break fluid and saturated steam densities during the blowdown phase of MSLB Test S-FS-1 (-10 to 150 s).

variations in the steam generator secondary depressurization rate (Figure 3). During the initial part of the blowdown, the break flow was of sufficient magnitude to cause the flow in the affected loop steam generator upper downcomer to reverse and the flow at the top of the riser to increase (Figures 6 and 7). The riser flow was not of sufficient magnitude to prevent the lower downcomer flow from reversing (Figure 8), causing a period of split flow in the tube bundle. The high mass flow rates in the affected loop steam generator and the rapid depressurization caused flow reversal in the separator drain lines, as indicated by the negative differential pressures in Figure 9, and degraded the performance of the steam separator. This allowed the two-phase mixture to exit the steam dome until the flows were reduced to within the range of the steam separator capabilities. The minimum void fraction measured at the break was about 0.97, which represents a homogeneous flow quality of about 0.58 (Figure 10). Thus, separator efficiency was decreased significantly by the high mass flow rates and the drain line flow reversals. As the affected loop steam generator secondary depressurized, the break flow decreased, ending the upper and lower downcomer flow reversals and decreasing the component mass-flow rates. The component flows continued to decrease until the secondary fluid inventory was depleted at about 110 s. The affected loop steam generator secondary component flows remained stagnant for the remainder of the transient, since the secondary fluid inventory remained depleted with no auxiliary feedwater injection occurring.

The MSLB transient condition resulted in nonuniform rates of inventory reduction for the affected loop steam generator downcomer and tube bundle regions, as shown in Figures 11 and 12. The initial reduction in the total secondary mass inventory involved a more rapid rate of reduction in the tube bundle mass inventory than in the downcomer mass inventory. The rapid depressurization of the affected loop steam generator secondary caused the secondary fluid to flash and, aided by the loss of inventory, resulted in early voiding of the tube bundle section (Figure 13). The entire tube bundle region secondary fluid inventory changed to an all-vapor condition (void fraction of 1.0) as the tube bundle liquid inventory was finally depleted. This altered the secondary convective heat transfer significantly but did not severely affect the primary-to-secondary heat transfer, since the transient heat transfer was almost totally controlled by the conduction heat transfer across the tube wall. The altering of the secondary convective heat transfer would, however, become more important for cases of smaller-sized breaks where the secondary depressurization and temperature reduction rates are not of sufficient magnitude to cause conduction limiting across the U-tube wall. Thus, accurate modeling of the entire secondary fluid system flow areas, volumes, and hydraulic resistances and accurate calculation of the intercomponent as well as the break mass flow rates become more important for ensuring accurate prediction of the heat transfer response during a MSLB transient as the MSLB size is reduced.

The secondary fluid hydraulic response of the unaffected loop steam generator was affected by the mass balance for the secondary. The mass balance was affected by the loss of inventory past the failed main steam line check valve and the feedwater flow. The simulated MSLB concurrent with main steam line check valve failure initiated the loss of secondary inventory, severely affecting secondary hydraulic characteristics. As shown in Figure 14, the break flow peaked at about 1 s as critical flow was established. The break effluent from the steam generator consisted of two-phase fluid early in the transient, followed by single-phase steam for the remainder of the blowdown, as shown in Figure 15. The transition of the break flow from a two-phase mixture to single-phase steam produced slight variations in the steam generator secondary depressurization rate (Figure 3). During the initial part of the blowdown, the break flow was of sufficient magnitude to produce flow through the steam separator, which exceeded the separating capabilities of the separator. This allowed the two-phase mixture to exit the steam dome until the flows were reduced to within the range of the steam separator capabilities. As the unaffected loop steam generator secondary depressurized, the break flow decreased, decreasing the flow through the separator. The minimum void fraction measured at the break was about 0.95, which represents a homogeneous flow quality of about 0.41 (Figure 16). Thus, the separator efficiency was decreased significantly by the high mass-flow rates. Following the low affected loop steam generator secondary pressure trip, the unaffected loop steam generator feedwater flow was terminated, the MSIV was closed, and auxiliary feedwater flow was initiated. Main feedwater flow had little effect on the secondary mass balance, since both the flow ("hot standby" represents about 1.5% of full-power conditions) and the time required for termination (about 22 s) were minimal. The MSIV

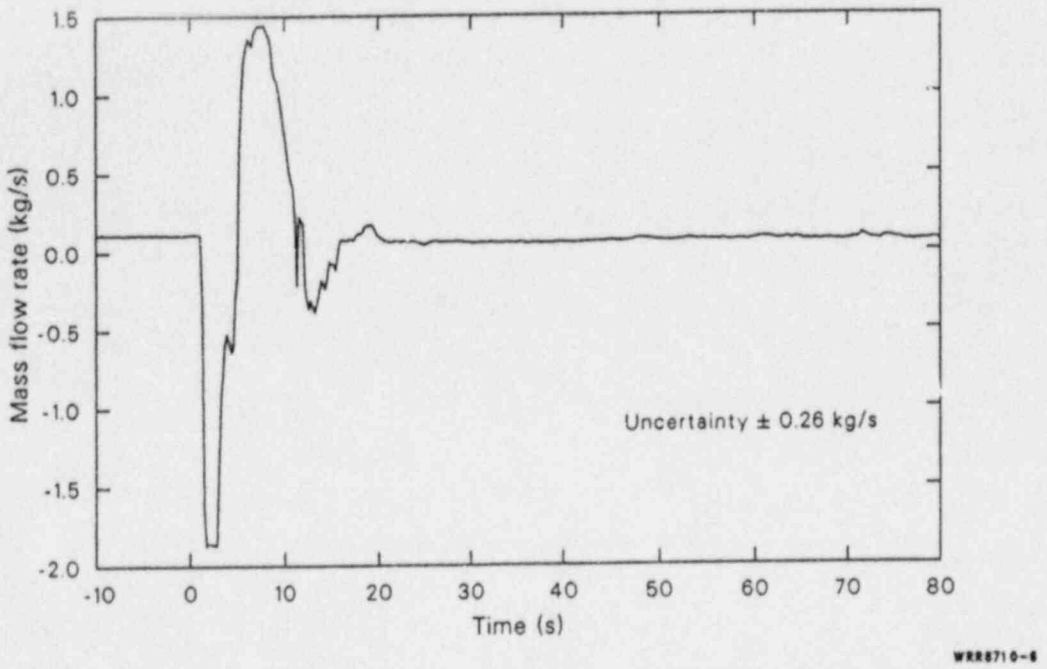

Figure 6. Affected loop steam generator upper downcomer mass flow rate during the blowdown phase of MSLB Test S-FS-1 (-10 to 80 s).

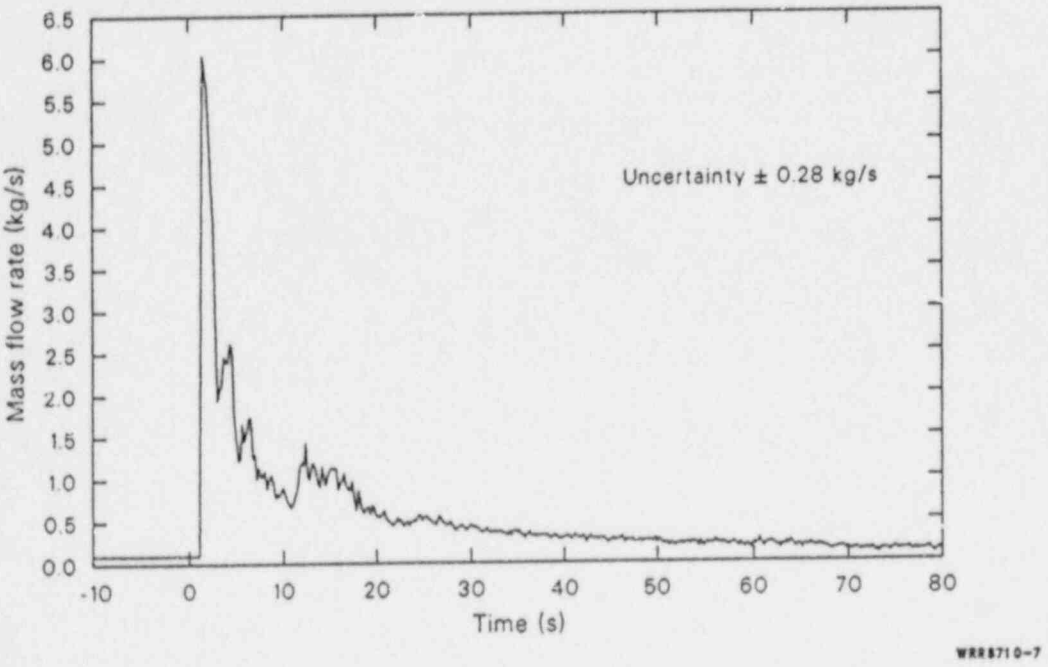

Figure 7. Affected loop steam generator riser mass flow rate during the blowdown phase of MSLB Test S-FS-1 (-10 to 80 s).

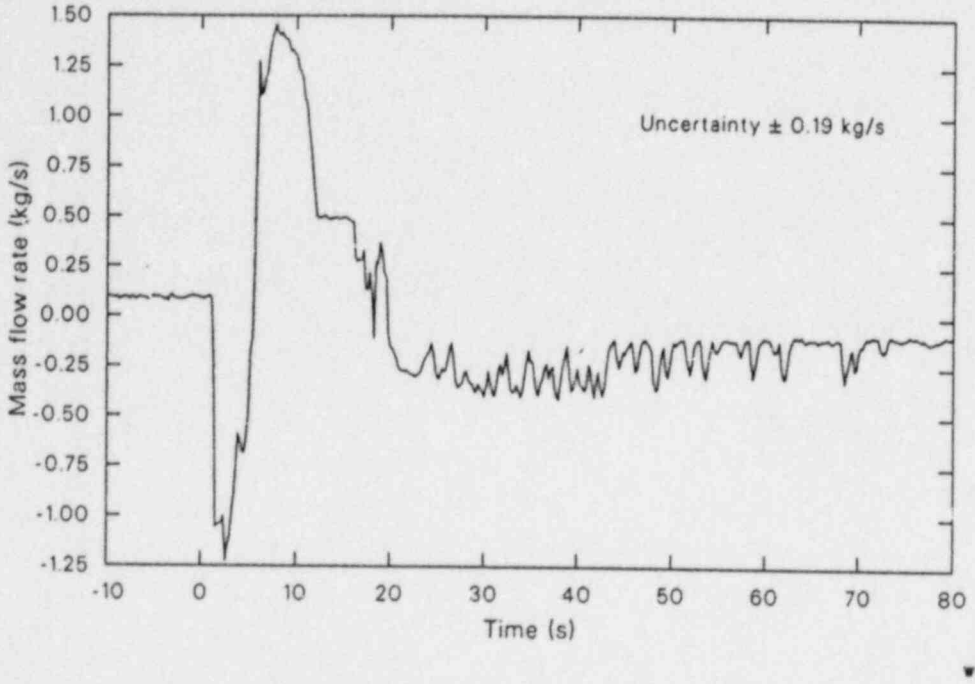

Figure 8. Affected loop steam generator lower downcomer mass flow rate during the blowdown phase of MSLB Test S-FS-1 (-10 to 80 s).

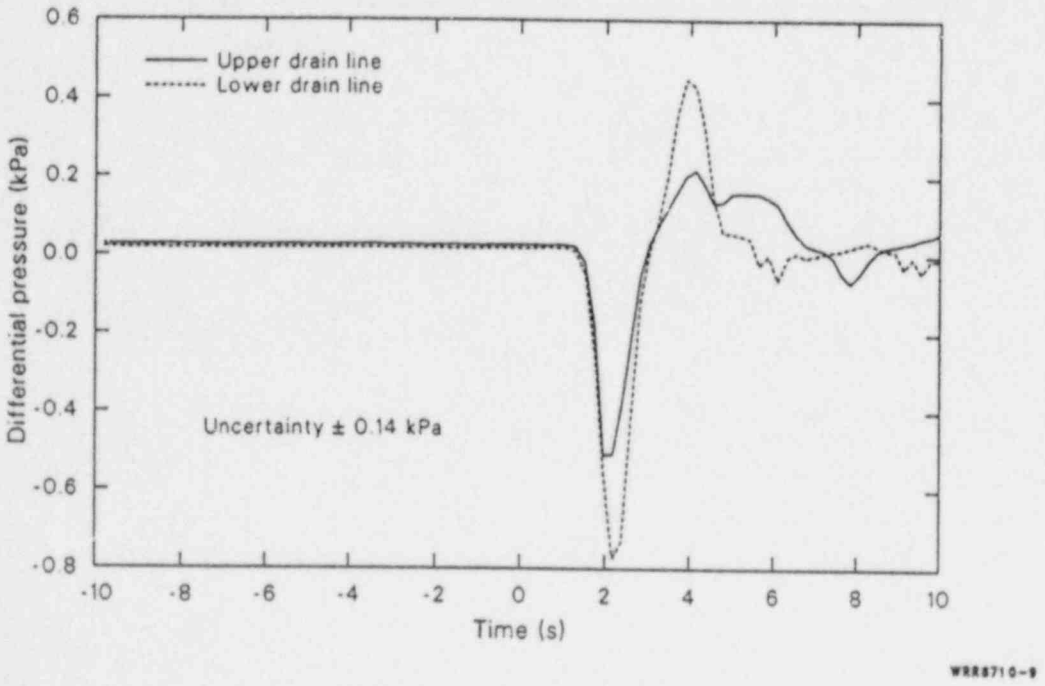

Figure 9. Affected loop steam generator separator drain line differential pressures (indicative of flow direction) during the blowdown phase of MSLB Test S-FS-1 (-10 to 10 s).

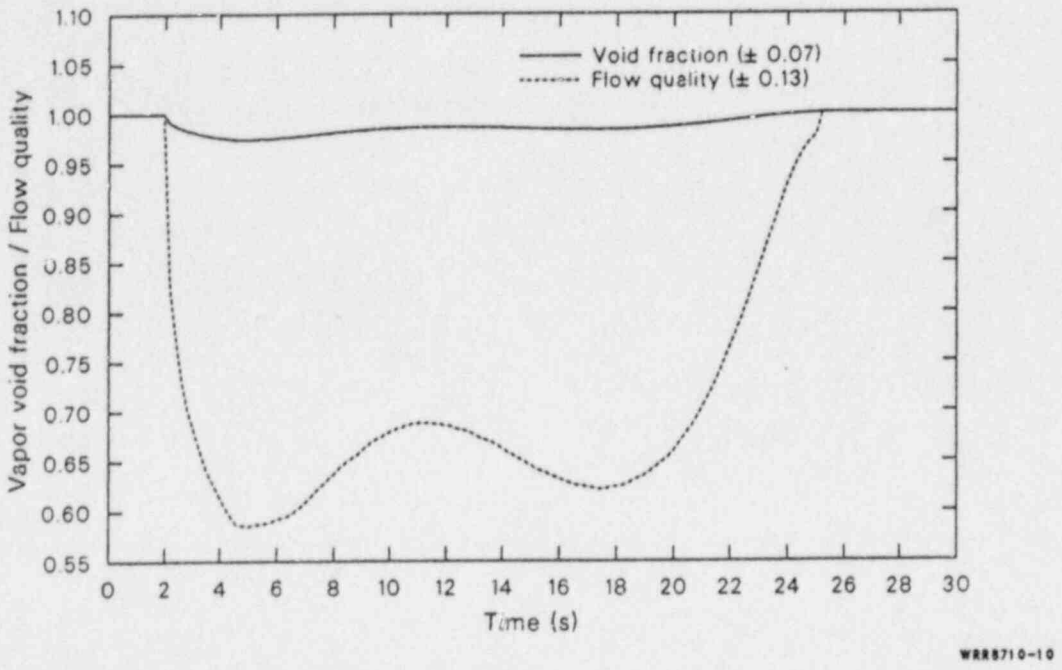

Figure 10. Affected loop steam generator break effluent best-estimate vapor void fraction and homogeneous flow quality during the blowdown phase of MSLB Test S-FS-1 (0 to 30 s).

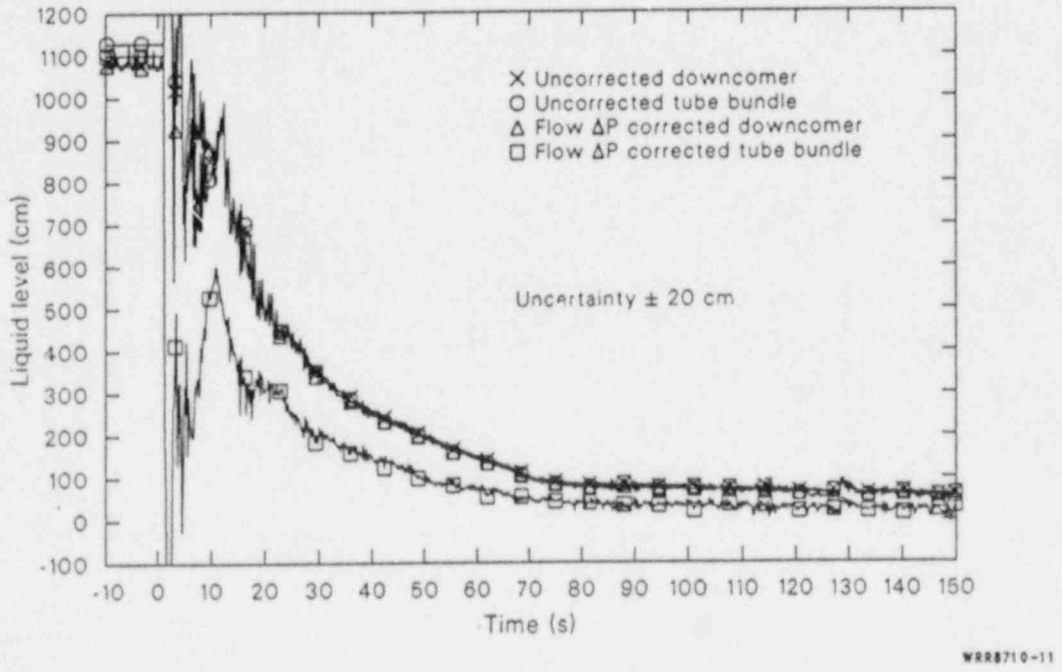

Figure 11. Affected loop steam generator overall downcomer and tube bundle interfacial liquid levels during the blowdown phase of MSLB Test S-FS-1 (-10 to 150 s).

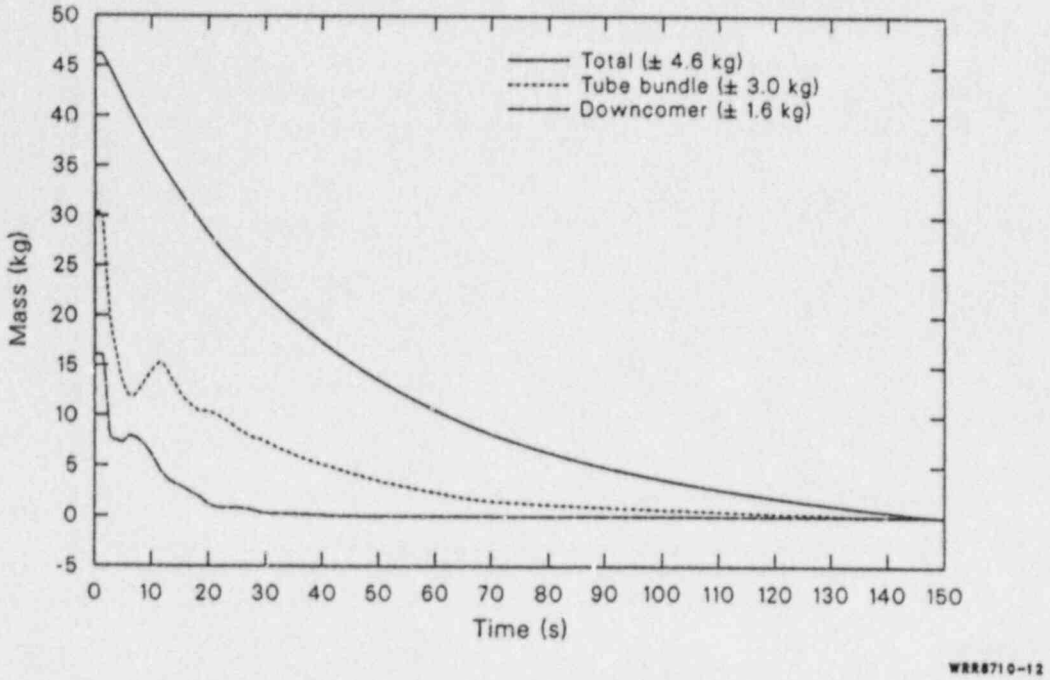

Figure 12. Affected loop steam generator total, downcomer, and tube bundle secondary fluid mass inventories dur ng the blowdown phase of MSLB Test S-FS-1 (0 to 150 s).

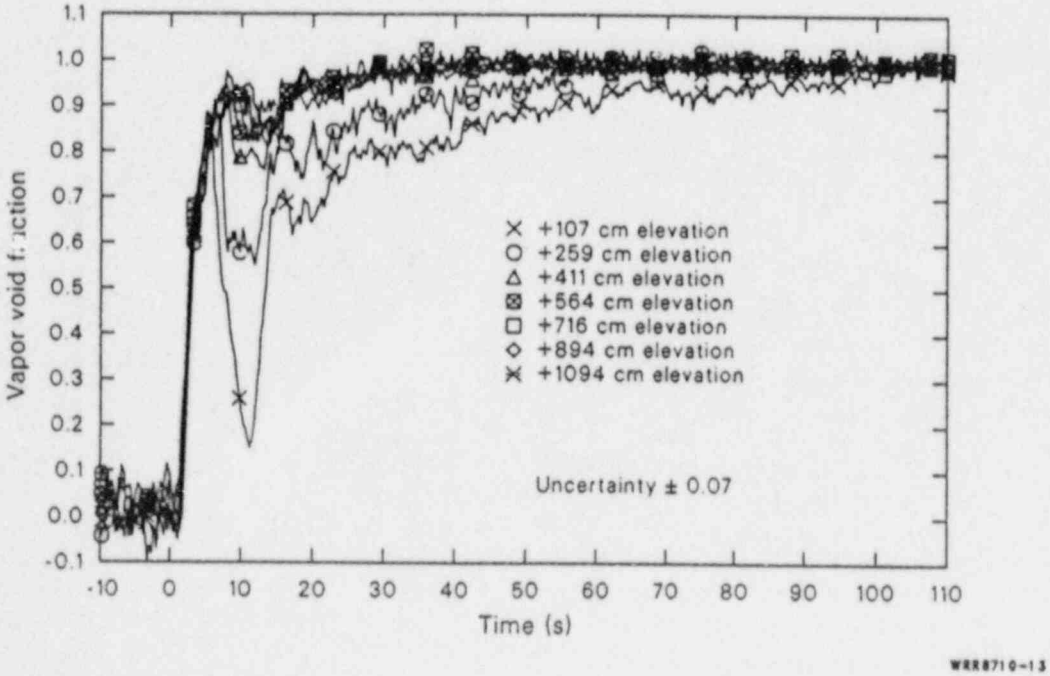

Figure 13. Affected loop steam generator tube bundle secondary fluid vapor void fractions during the blowdown phase of MSLB Test S-FS-1 (-10 to 110 s).

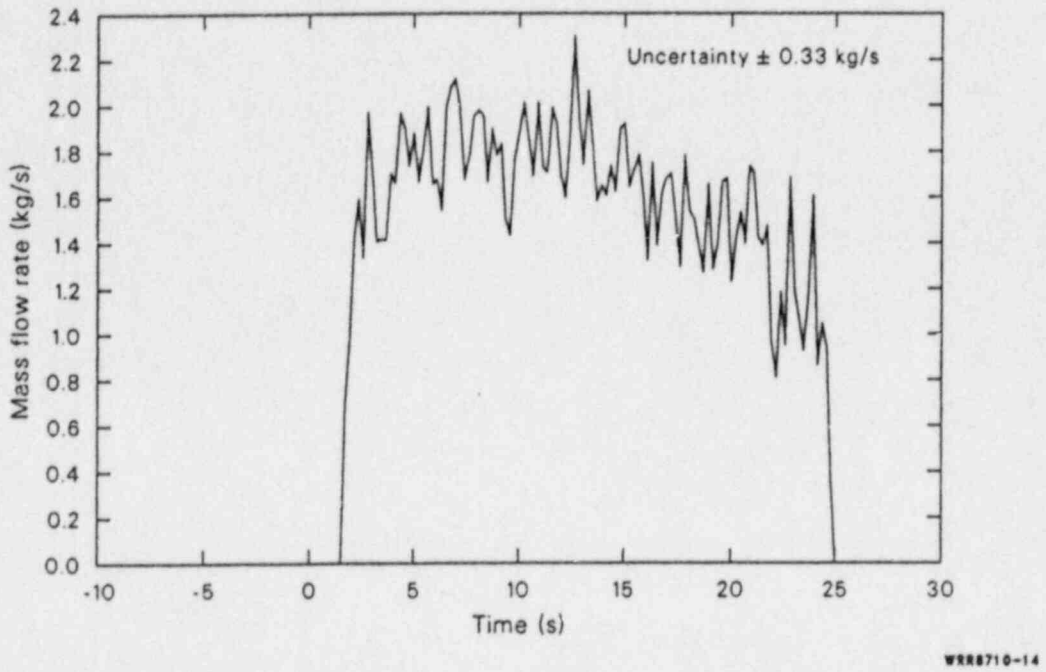

Figure 14. Unaffected loop steam generator break mass flow rate during the blowdown phase of MSLB Test S-FS-1 (-10 to 30 s).

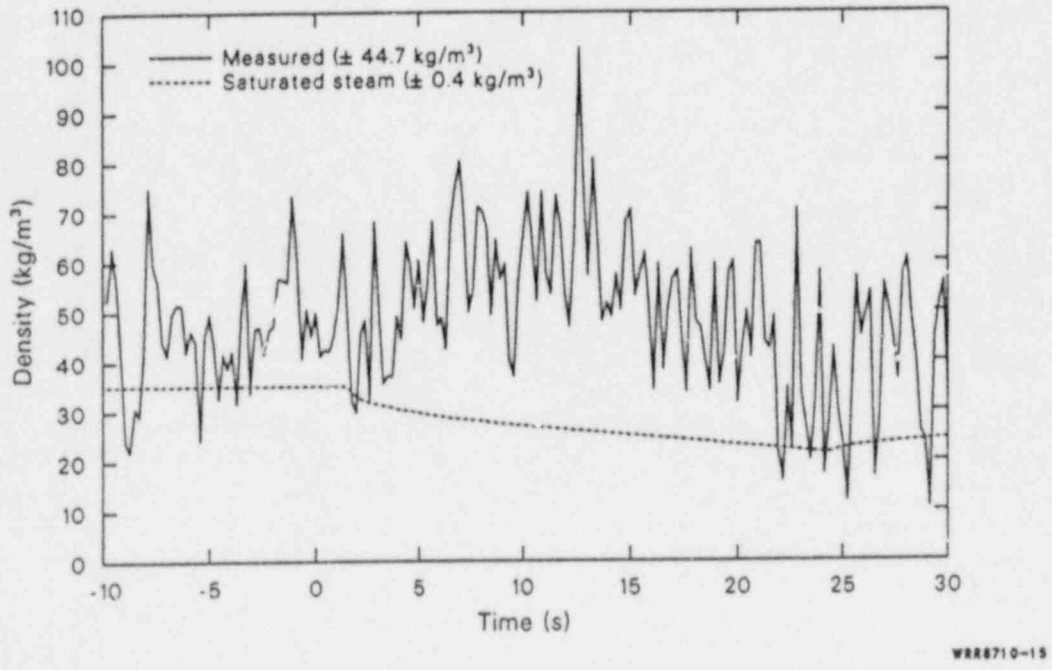

Figure 15. Unaffected loop steam generator break fluid and saturated steam densities during the blowdown phase of MSLB Test S-FS-1 (-10 to 30 s).

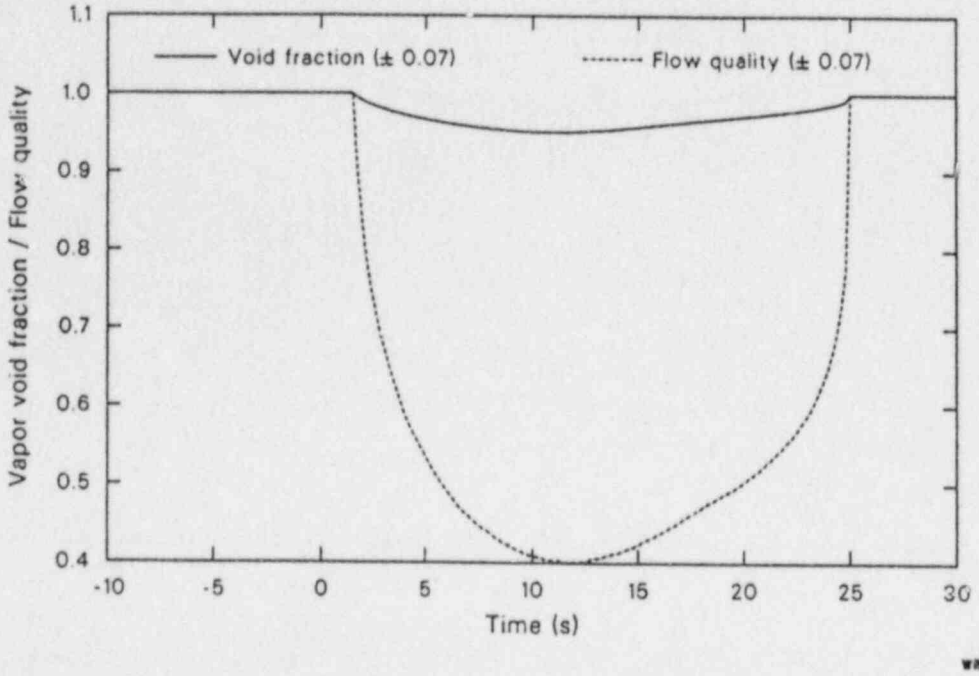

Figure 16. Unaffected loop steam generator break effluent best-estimate vapor void fraction and homogeneous flow quality during the blowdown phase of MSLB Test S-FS-1 (-10 to 30 s).

closure halted the loss of secondary inventory with the inventory at its minimum value of about 60% of the initial mass. Recovery of the secondary inventory was then initiated by auxiliary feedwater injection, as indicated by the liquid level response (Figure 17). At the end of the blowdown phase of the test, the secondary inventory had recovered to about 64% of the initial mass.

Secondary Thermal Response. The thermal response of the affected loop steam generator secondary fluid system to a double-ended offset shear of the main steam line downstream of the flow restrictor is characterized by a rapid increase in the primary-to-secondary heat transfer. As shown in Figure 18, the affected loop steam generator primary-to-secondary heat transfer increased rapidly until loop flow reductions began due to the loss of offsite power. The primary-to-secondary heat transfer then decreased somewhat as the U-tube primary side convective heat transfer coefficients decreased (Figure 19), but remained high due to the decreasing secondary fluid saturation temperature (Figure 20) and the increased secondary convective heat transfer coefficients (Figure 21 and Figures B-1 through B-7). While the affected loop steam generator primary energy removal increased substantially, it was at least an order of magnitude below the energy removal capacity associated with the break flow (Figure 18). These observed trends in the primary-to-secondary heat transfer provide insight into the mechanisms controlling the amount of primary cooling which occurs during a MSLB secondary LOCA.

The mechanisms which control the amount of primary cooling provided by the affected loop steam generator during a MSLB transient are the primary convective heat transfer, the conduction heat transfer across the U-tube wall, and the secondary convective heat transfer. The affected loop steam generator primary-to-secondary heat transfer during Test S-FS-1 was obviously limited by some mechanism, since the primary energy removal was at least an order of magnitude below the energy removal capacity associated with the break flow. During the initial part of the blowdown, both the primary and secondary convective heat transfer coefficients remained constant after undergoing a step change increase at transient initiation. The primary-to-secondary fluid temperature differences were constantly increasing, however, as the secondary fluid temperatures constantly

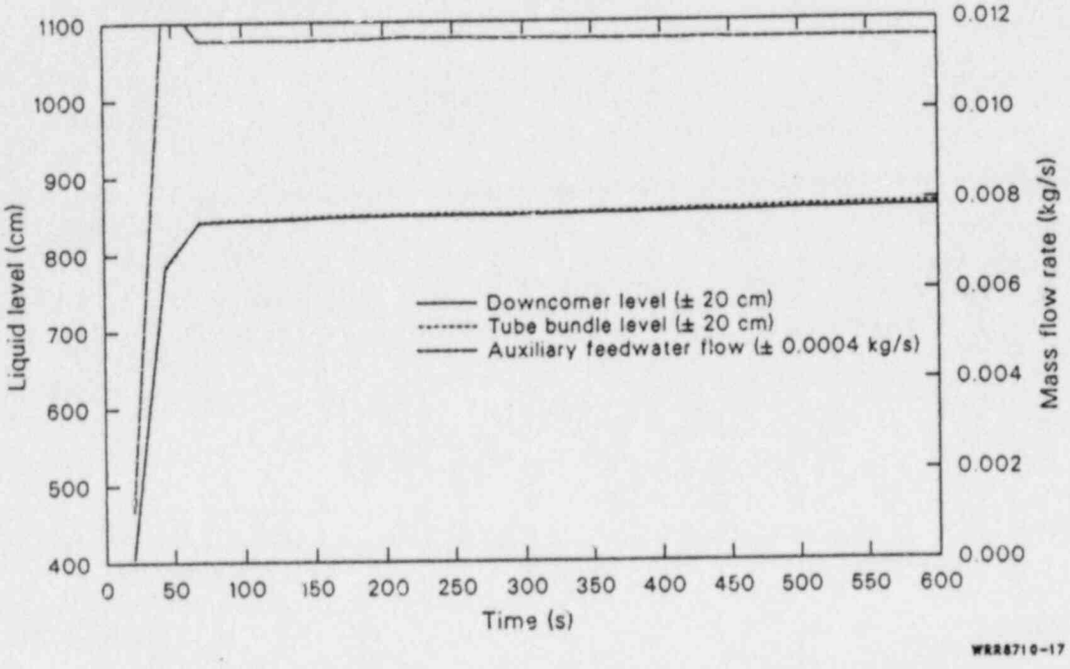

Figure 17. Unaffected loop steam generator overall downcomer and tube bundle collapsed liquid levels and auxiliary feedwater mass flow rate during the blowdown phase of MSLB Test S-FS-1 (0 to 600 s).

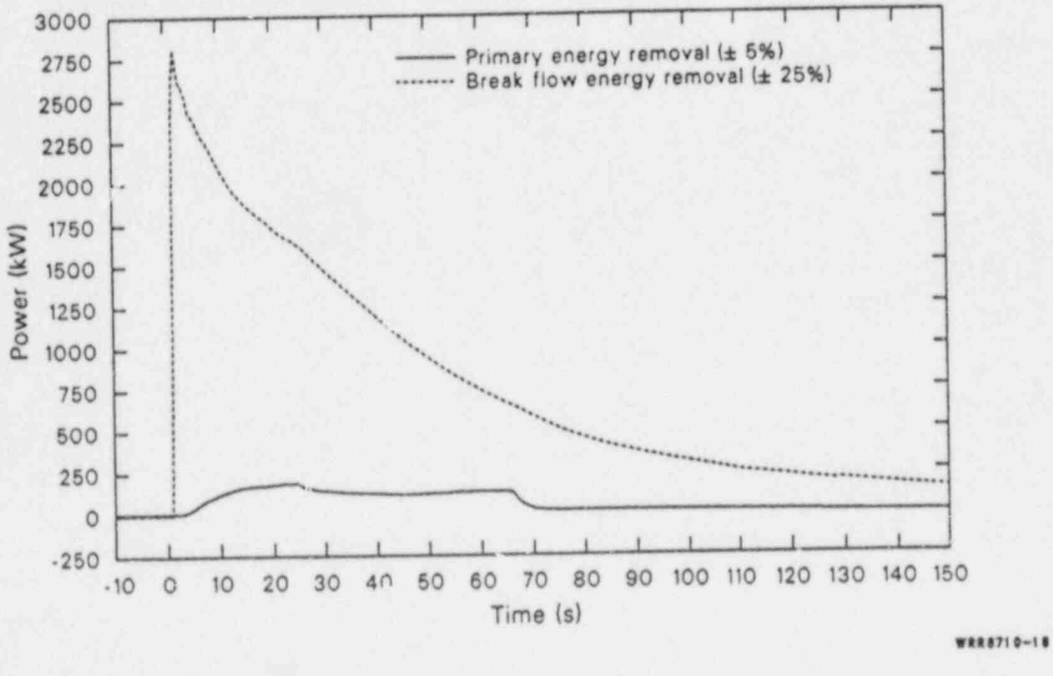

Figure 18. Affected loop steam generator primary and break flow energy removal during the blowdown phase of MSLB Test S-FS-1 (-10 to 150 s).

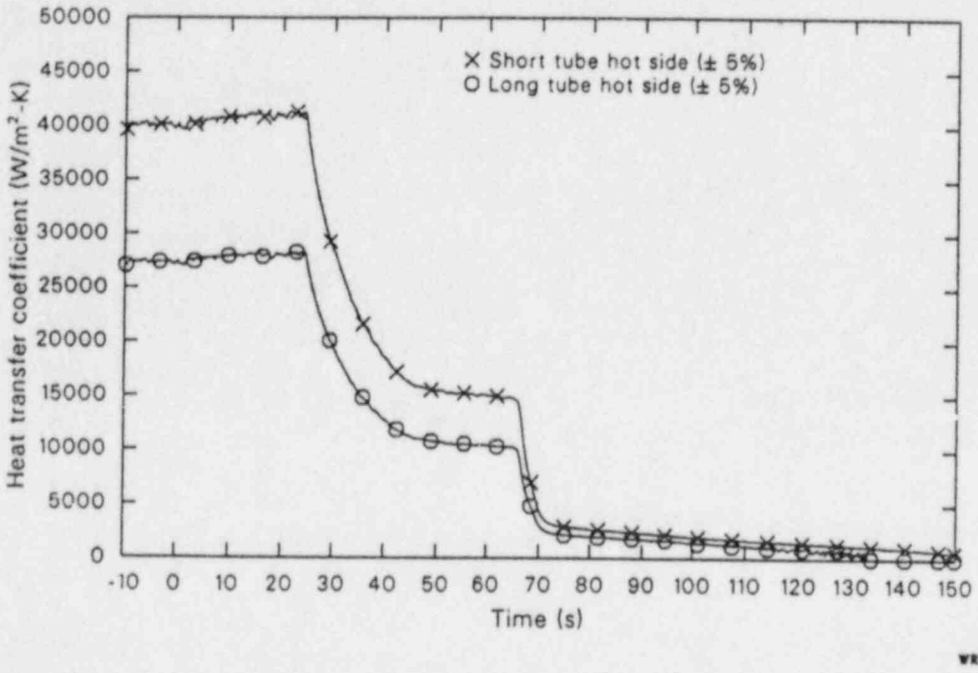

Figure 19. Affected loop steam generator primary convective heat transfer coefficients at the 61-cm elevation during the blowdown phase of MSLB Test S-FS-1 (-10 to 150 s).

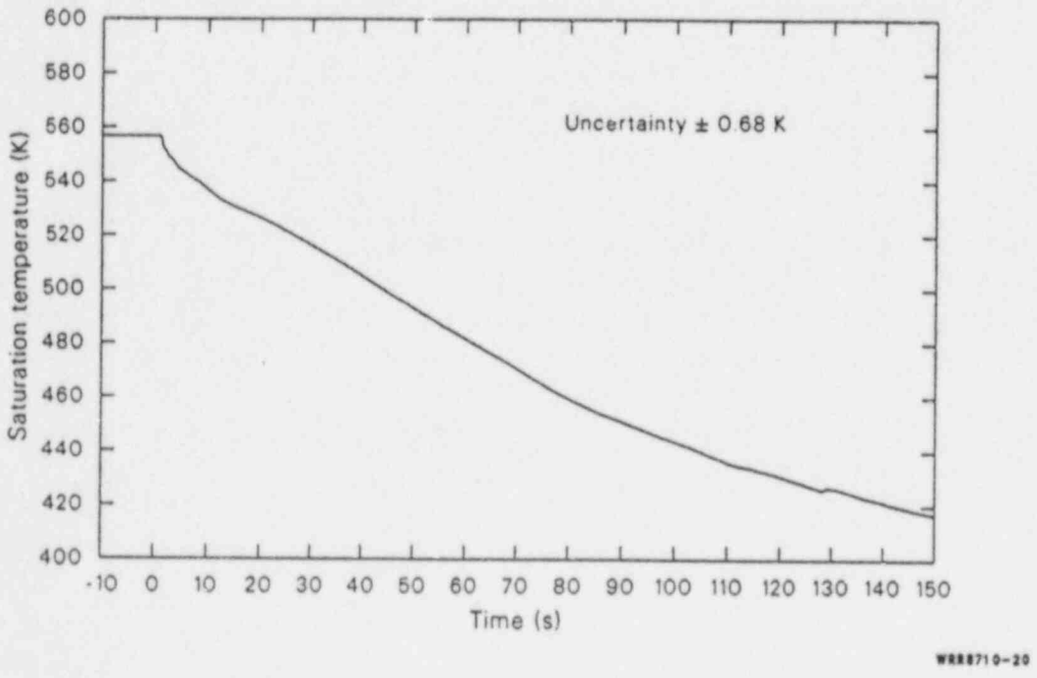

Figure 20. Affected loop steam generator secondary fluid saturation temperature during the blowdown phase of MSLB Test S-FS-1 (-10 to 150 s).

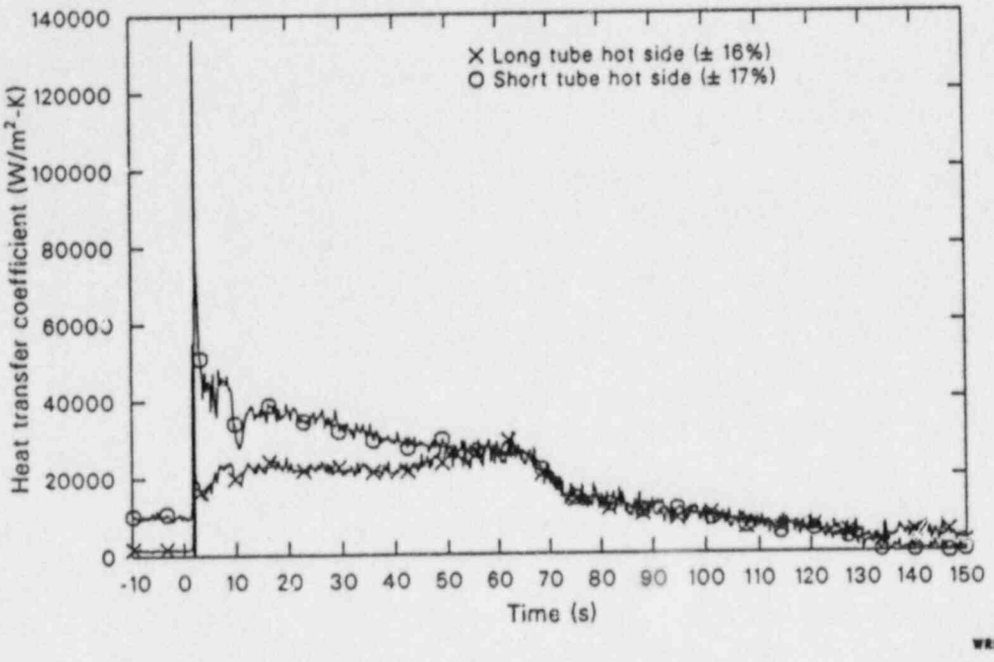

Figure 21. Affected loop steam generator secondary convective heat transfer coefficients at the 61-cm elevation during the blowdown phase of MSLB Test S-FS-1 (-10 to 150 s).

decreased. The primary-to-secondary heat transfer during this part of the blowdown was therefore limited by the conduction heat transfer across the U-tube wall. During the period of primary coolant pump coastdowns, the primary convective heat transfer coefficients were constantly decreasing. The primary-to-secondary heat transfer during this part of the blowdown was therefore limited by the conduction heat transfer and the primary convective heat transfer. Eventually, the primary-to-secondary heat transfer was limited by the primary convective heat transfer when the primary coolant pumps coasted to a stop. The secondary convective heat transfer coefficients rapidly degraded to zero when the liquid inventory was depleted (i.e., the local secondary convective heat transfer coefficients rapidly degraded to zero when the local vapor void fractions reached a value of 1.0). Therefore, the primary-to-secondary heat transfer would have eventually been limited by the secondary convective heat transfer, had the primary coolant pumps not been tripped off.

The purpose of assumptions applied to MSLB transient simulations and calculations is to produce the maximum amount of primary cooling. Assumptions which maximize primary cooling are considered to be conservative assumptions. Based on the preceding discussion, invaluable insight can be gained into the relative degree of conservatism inherent in MSLB simulation assumptions. The assumed loss of offsite power at SI causes loop flow reduction, which decreases primary convective heat transfer. Because primary cooling is decreased by reducing primary convective heat transfer, loss of offsite power should not be considered to be a conservative assumption. While perfect separator performance assumptions provide the maximum energy removal capacity associated with the break flow, the primary-to-secondary heat transfer is limited by the conduction heat transfer across the U-tube wall such that the primary energy removal is much less than the energy removal capacity associated with the break flow. Therefore, the break fluid energy removal which results from an assumed separator performance has minimal direct effect upon the primary energy removal.

A greater effect of assuming perfect separation is that it decreases the rate of the secondary mass loss, depressurization, and secondary fluid saturation temperature reduction. This increases the duration of the conduction heat transfer across the U-tube wall, the secondary convective heat transfer, and,

the primary-to-secondary heat transfer. The same effect would be achieved by decreasing the break size so that the break flow energy removal rate is as close as possible to the conduction limited primary-to-secondary heat transfer rate. In this manner, the effect of the secondary break flow energy removal on primary cooling would be maximized. Thus, the primary cooling caused by the affected steam generator during a MSLB transient would be maximized by:

- Either not simulating the loss of offsite power or delaying the simulated loss of offsite power until after the secondary convective heat transfer has degraded to zero (after the affected loop steam generator secondary is empty),
- Assuming perfect separation (although the effect of this assumption is minimal), and
- Decreasing the break size such that the break flow energy removal rate is as close as possible to the conduction-limited primary-to-secondary heat transfer rate.

Because the primary-to-secondary heat transfer during a MSLB transient is conduction-limited, the steam generator U-tube thermal conductivity (which is dependent upon the type of material and the material temperature) and wall thickness play a key role in determining the amount of primary cooling. The Type III affected loop steam generator U-tube material and material temperatures are typical of the Westinghouse Model 51 steam generator. However, the Type III steam generator U-tube walls are 0.165-cm thick, whereas the Westinghouse Model 51 steam generator U-tube walls are 0.124-cm thick. The 0.165-cm tube wall thickness in the Type III steam generator allows approximately 20% less conduction heat transfer across the U-tube wall than would occur for a 0.124-cm thick wall with the same primary-to-secondary temperature difference. The primary cooling produced by the affected loop steam generator during the simulated MSLB transient was therefore approximately 20% less than would have occurred with the 0.124-cm thick U-tube walls in a Westinghouse Model 51 steam generator.

The initial depressurization rate of the affected loop steam generator secondary (Figure 3) was affected by the initial subcooling of the secondary fluid. The affected loop steam generator was not subject to mixing in stratification layer (Figure 22). The initial depressurization rate was therefore more rapid due to initial subcooling of the downcomer fluid before the liquid could flash to vapor. The secondary vapor generation was not sufficient to replace the vapor lost out of the break, causing the initial depressurization rate to be more rapid. The initial secondary depressurization rate was therefore more rapid due to initial subcooling of the downcomer fluid.

The affected loop steam generator decoupled from the primary fluid system following the loss of inventory. With no auxiliary feedwater injection, the secondary fluid system remained devoid of fluid, and had no further effect on the primary fluid system.

The thermal response of the unaffected loop steam generator secondary fluid system to a double-ended offset shear of the main steam line downstream of the flow restrictor with concurrent check valve failure is also characterized by a rapid increase in the primary-to-secondary heat transfer. As shown in Figure 23, the unaffected loop steam generator primary-to-secondary heat transfer increased rapidly until MSIV closure terminated the loss of inventory via the break. Concurrent with MSIV closure, the loop flow reductions began due to the loss of offsite power. The primary-to-secondary heat transfer then decreased significantly as the U-tube primary and secondary side convective heat transfer decreased. Here again, although the unaffected loop steam generator primary energy removal increased substantially, it was at least an order of magnitude below the energy removal capacity associated with the break flow (Figure 23). These observed trends in the primary-to-secondary heat transfer are similar to those observed for the affected loop steam generator, indicating that the mechanisms controlling the amount of primary cooling which occurs are similar for both steam generators.

Although the mechanisms which control the amount of primary cooling provided by both the affected and unaffected loop steam generators are the same, the interaction of the mechanisms is different. Like the affected loop steam generator, the unaffected loop steam generator primary-to-secondary heat transfer during Test S-FS-1 was obviously limited by some mechanism, since the primary energy removal was at least an order of magnitude below the energy removal capacity associated with the break flow. The primary-to-secondary heat transfer during the initial part of the blowdown was limited by conduction heat transfer across the U-tube wall, as with the affected loop steam generator. However, primary-to-secondary heat transfer was next limited by secondary convective heat transfer due to the isolation of the secondary at MSIV

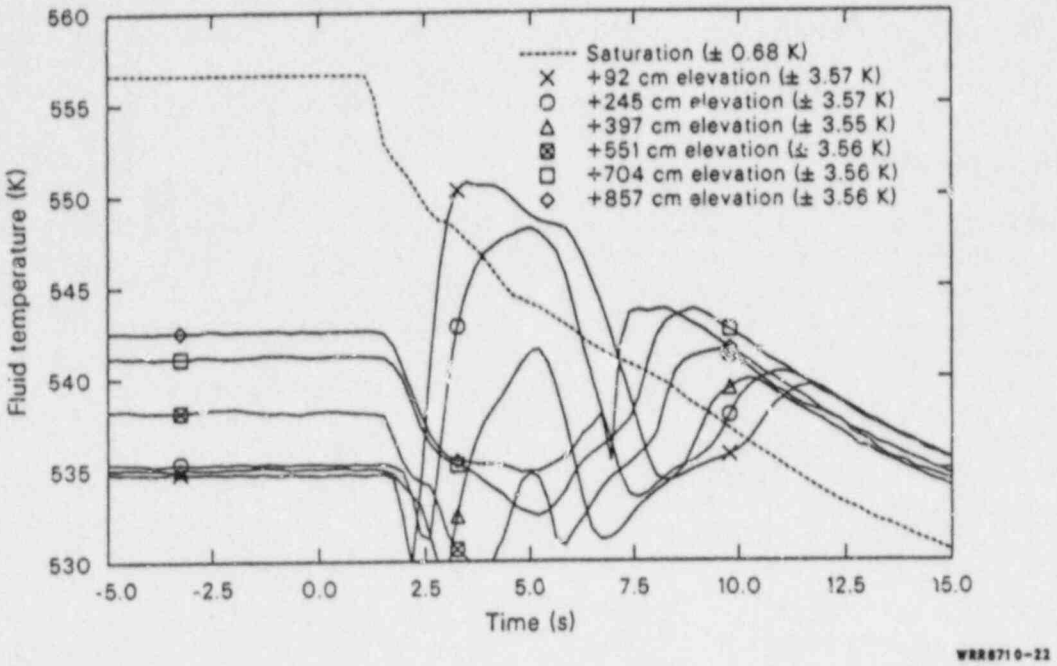

Figure 22. Affected loop steam generator downcomer fluid and saturation temperatures during the blowdown phase of MSLB Test S-FS-1 (-5 to 15 s).

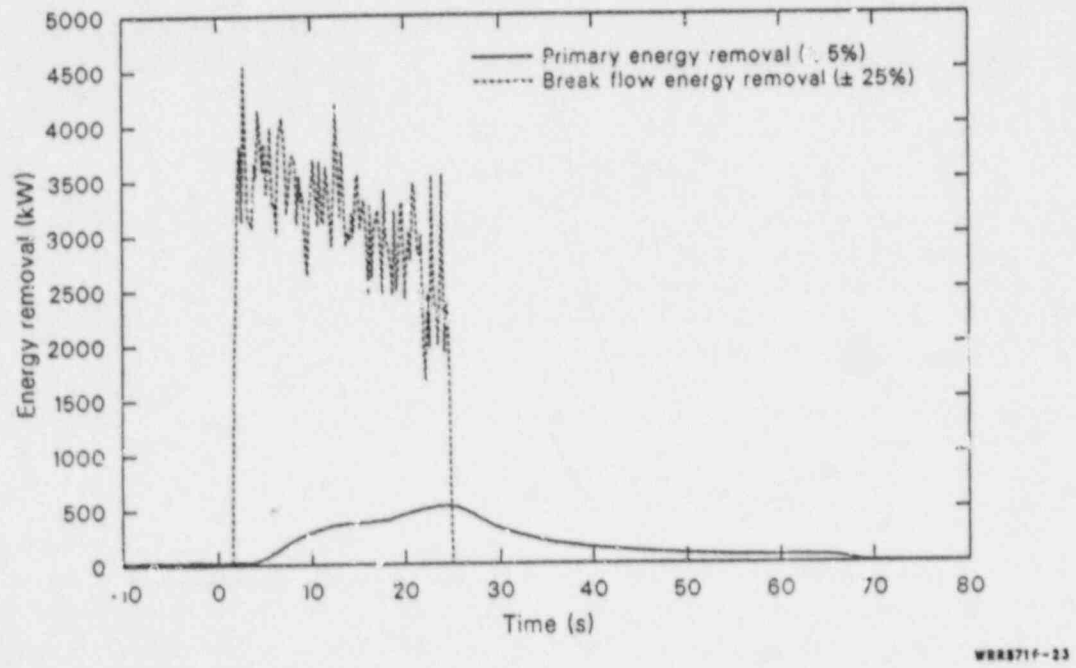

Figure 23. Unaffected loop steam generator primary and break flow energy removal during the blowdown phase of MSLB Test S-FS-1 (-10 to 80 s).

closure. During the pump coastdown part of the blowdown, primary-to-secondary heat transfer was limited by both the secondary and primary convective heat transfer. These observations also provide useful guidance for making MSLB transient simulation assumptions which will produce the maximum amount of primary cooling.

The earlier discussion of MSLB calculation assumptions and their effect on primary cooling also applies for the unaffected loop steam generator. However, the effect of the main steam line check valve failure was not discussed. The unaffected loop steam generator provided significant cooling of the primary coolant system, which added to the cooling provided by the affected loop steam generator. This substantially increased the cooling of the primary coolant system. Therefore, the failed main steam line check valve assumption maximizes the primary cooling and should be considered a conservative assumption.

The initial depressurization rate of the unaffected loop steam generator secondary (Figure 3) was also affected by the initial subcooling of the secondary fluid. The unaffected loop steam generator secondary fluid exhibited some slight stratification and subcooling in the downcomer (Figure 24) at initial conditions. The initial subcooling had the same effect on unaffected loop steam generator secondary depressurization as it did on steam generator secondary depressurization in the affected loop. Here again, the initial secondary depressurization rate was more rapid due to initial subcooling of the downcomer fluid.

Following the SI signal, the unaffected loop steam generator main feedwater flow was terminated, the MSIV was closed, and auxiliary feedwater injection was initiated. Termination of the unaffected loop steam generator main feedwater had virtually no effect on the secondary response. The energy removal via the break flow completely overshadowed the loss of energy removal associated with the main feedwater termination. The MSIV closure terminated the energy removal via the break, causing the secondary to gradually heat and repressurize. The energy removal provided by the auxiliary feedwater aided in minimizing secondary heating and pressurization.

Primary System Response to a Steam Generator Main Steam Line Break

Understanding the primary fluid system thermal-hydraulic response during a MSLB secondary LOCA is important, because the degree of cooling of the primary fluid system depends upon the thermal-hydraulic response to the increased heat sink. The primary thermal-hydraulic response is determined by the primary energy and mass balances. There are several characteristic inflection points in the primary fluid system thermal-hydraulic response to a MSLB secondary LOCA. The causes of these inflection points are discussed in this section. The general sequence of events affecting the primary response is outlined first. This is followed by discussions of the pressure, hydraulic, and thermal responses for the primary fluid system. Since both of the MSLB experiments had similar basic primary thermal-hydraulic responses, this discussion refers to Test S-FS-1 data only. As with the secondary response discussion, break size and location effects will be discussed later.

General Primary Response. The occurrence of a double-ended offset shear of a steam generator main steam line downstream of the flow restrictor produces severe effects on the primary fluid system. The MSLB initiated the transient at 0 s. The primary fluid system response is a rapid cooldown due to increased primary-to-secondary heat transfer during the secondary LOCA. The primary fluid rapidly cools down as the affected and (due to the failed main steam line check valve) unaffected loop steam generator primary-to-secondary heat transfer increases. This causes the primary fluid to shrink and rapidly depressurize, with the depressurization rate increasing when the pressurizer empties. The cooldown and depressurization of the primary system moderates slightly following isolation of the unaffected loop steam generator due to MSIV closure at SI. However, the cooldown and depressurization continues until the primary coolant pumps coast to a stop about 52 s later (due to loss of offsite power at SI), with the minimum fluid temperature occurring in the loop cold legs. The primary system response for the remainder of the blowdown phase of the transient is characterized by SI flow slowly increasing the pressurizer liquid inventory and providing slight primary cooling, which aids the unaffected loop steam generator auxiliary feedwater in moderating primary pressure and temperature. The primary fluid system pressure and temperature increase slowly as the primary heats slightly and the pressurizer slowly refills. No voiding of the primary fluid system was observed during the blowdown phase of the transient.

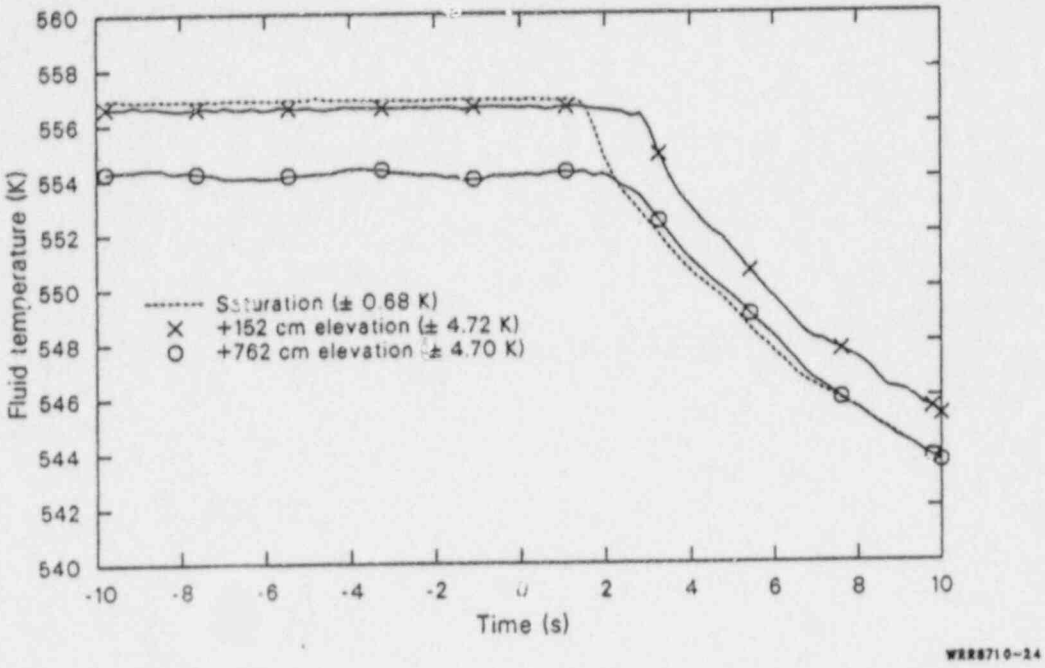

Figure 24. Unaffected loop steam generator downcomer fluid and saturation temperatures during the blowdown phase of MSLB Test S-FS-1 (-10 to 10 s)

Primary Pressure Response. The primary pressure response is characterized by a number of inflection points associated with changes in the energy balance and fluid distribution. As shown in Figure 25, the MSLB secondary LOCA created an energy imbalance, which resulted in immediate, rapid depressurization (about 0.05 MPa/s) of the primary fluid system. The rate of depressurization increased at about 17 s as the vapor generation in the pressurizer was halted due to the emptying of the pressurizer. The depressurization of the primary fluid system continued (at about 0.23 MPa/s) until the affected loop steam generator secondary pressure SI low setpoint was reached. The resulting MSIV closure decreased the unaffected loop steam generator primary-to-secondary heat transfer slightly, which caused a slight decrease in the rate of primary depressurization starting at about 24 s. The rate of depressurization continued to decrease as the loop flows decreased due to the primary coolant pump coastdowns following loss of offsite power at SI. The minimum primary cold leg pressure of 10.41 MPa occurred at about 73 s, when the primary coolant pumps coasted to a stop. The primary then pressurized slowly due to primary energy addition and compression of the pressurizer vapor space as the SI flow slowly refilled the pressurizer. The rate of pressurization moderated slightly as the loops changed to the natural circulation mode of heat transfer. For the remainder of the blowdown phase of the transient, the primary continued to pressurize slowly, as it slowly heated and the pressurizer slowly filled.

Primary Hydraulic Response. The hydraulic response of the primary fluid system during a MSLB secondary LOCA is characterized as a rapid shrinkage of fluid out of the pressurizer. As the primary energy removal via the affected and unaffected loop steam generators increases, the primary fluid cools down and shrinks out of the pressurizer, as shown in Figure 26. The rate of the shrinkage is determined by initial primary pressure and temperature, initial pressurizer vapor volume, the energy balance, and the pressurizer surge line hydraulic resistance. The initial primary pressure and temperature determine the initial energy content of the primary fluid system. The amount of the primary fluid shrinkage (decrease in the fluid specific volume) is determined by the integrated energy removal from the primary fluid and the initial energy content of the primary fluid. The rate of primary fluid shrinkage is determined primarily by the rate of energy removal and the vapor generation

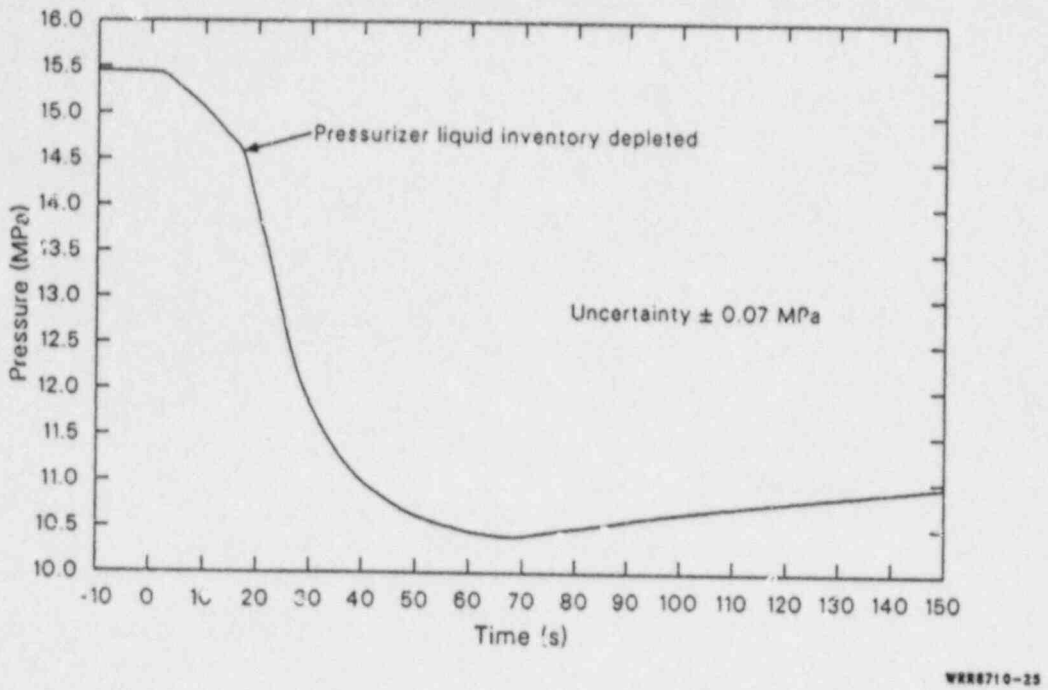

Figure 23. Pressurizer pressure during the blowdown phase of MSLB Test S-FS-1 (-10 to 150 s).

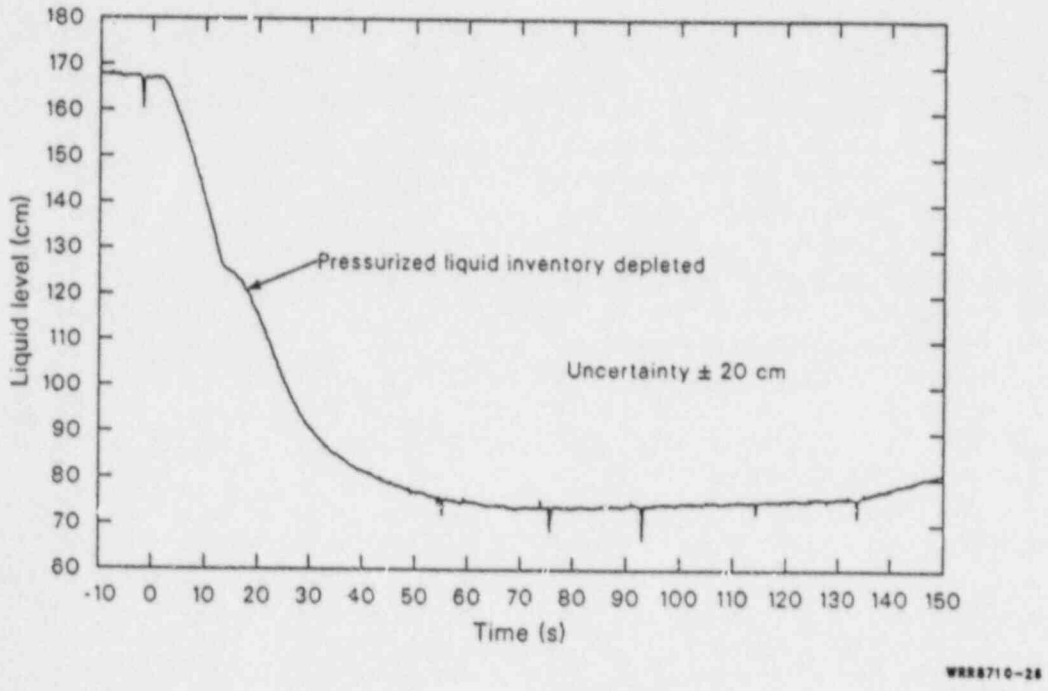

Figure 26. Pressurizer overall collapsed liquid level during the blowdown phase of MSLB Test S-FS-1 (-10 to 150 s).

in the pressurizer due to the depressurization (the impetus for the shrinkage) and the resistance to flow through the pressurizer surge line (the resistance to the expansion). It is also determined to some extent by the initial energy content of the primary fluid system. The basic mechanism involves the primary fluid energy content decreasing due to the energy removal. The decreased energy content produces a decreased fluid specific volume and fluid pressure, which causes a pressure gradient between the pressurizer and the primary loop hot leg. The primary fluid then flows out of the pressurizer at a rate determined by the pressure difference, the fluid specific volume, and the surge line hydraulic resistance. As the fluid flows out of the pressurizer, the decreasing fluid volume expands the vapor volume, increasing the vapor-specific volume and depressurizing the pressurizer. This is moderated somewhat by the flashing of liquid to vapor as the pressurizer depressurizes. During the rapid shrinkage of fluid out of the pressurizer, the predominant factors determining the pressure differential between the primary loop and the pressurizer are the rate of energy removal from the primary system fluid and the surge line hydraulic resistance. For a given surge line resistance, the greater the rate of primary energy removal, the greater the pressure difference developed due to the greater volumetric rate of fluid shrinkage through the surge line from the pressurizer. For a given primary energy removal rate, the greater the surge line hydraulic resistance, the greater the pressure difference required to accommodate the volumetric rate of fluid shrinkage through the surge line out of the pressurizer. The shrinkage of fluid out of the pressurizer continued until the pressurizer emptied at about 17 s. The primary fluid shrinkage continued until the primary coolant pumps coasted to a stop about 52 s after loss of offsite power. The fluid then expands as the primary system heats and the fluid specific volume increases. The primary fluid mass inventory increases as the SI flow enters the primary and refills the pressurizer. For the remainder of the blowdown phase of the transient, the primary fluid flows into the pressurizer from the loop hot leg under the influence of the continued heating provided by the core power and the mass addition provided by the SI flow.

Primary Thermal Response. The thermal response of the primary fluid system during a MSLB secondary LOCA is characterized as a rapid cooldown of primary fluid. As shown in Figure 27, as the affected and unaffected loop heat sinks rapidly increase, the primary energy balance is lost and energy is removed from the primary fluid, causing the fluid to rapidly cool. This continues until about 48 s after SI and MSIV closure, when the primary coolant pumps are tripped off and allowed to coast to a stop (simulating loss of offsite power at SI), reducing the affected and unaffected loop steam generator primary energy removal rates to a level below the level of the core power. The minimum downcomer fluid temperature (average cold leg fluid temperature) reached was about 536 K at about 69 s. This is well above the pressurized thermal shock (PTS) minimum temperature limit of 450 K.

Primary cooling was limited somewhat due to the thicker U-tube walls in the Type III steam generator, but the effect on the measured minimum average cold leg fluid temperature was minimal. During the period of primary cooldown, the primary fluid average temperature (Figure 28) decreased from 560 to 542 K, while the primary fluid pressure decreased from 15.50 to 10.39 MPa. This represents a total primary energy removal during the cooldown of about 10,570 kJ. As discussed in the secondary thermal response section, the thicker U-tube walls in the Type III steam generator (0.165 cm versus 0.124 cm) reduced the conduction heat transfer through the wall by about 20%, which reduced the net primary energy removal somewhat. If 0.124-cm thick U-tube walls had been used for the Type III steam generator, the net primary energy removal would have been about 11,490 kJ. This would have decreased the primary fluid average temperature to about 540 K, assuming the same primary pressure decrease. Correspondingly, the minimum average cold leg fluid temperature would have been about 534 K, still well above the PTS limit. Thus, while the thicker U-tube walls in the Type III steam generator limited the primary cooling somewhat (about 9%), the effect on the measured minimum downcomer fluid temperature was minimal.

The primary fluid system thermal response moderated following MSIV closure and loop flow reductions, as the unaffected loop steam generator primary energy removal via the break was terminated, and the system changed to a natural circulation mode of heat transfer. As natural circulation flow was being established, the primary fluid was gradually heating, as evidenced by the average fluid temperature increase. Once the natural circulation flow was established, as evidenced by the unaffected loop hot-leg-to-cold-leg temperature difference reaching a maximum, the rate of system

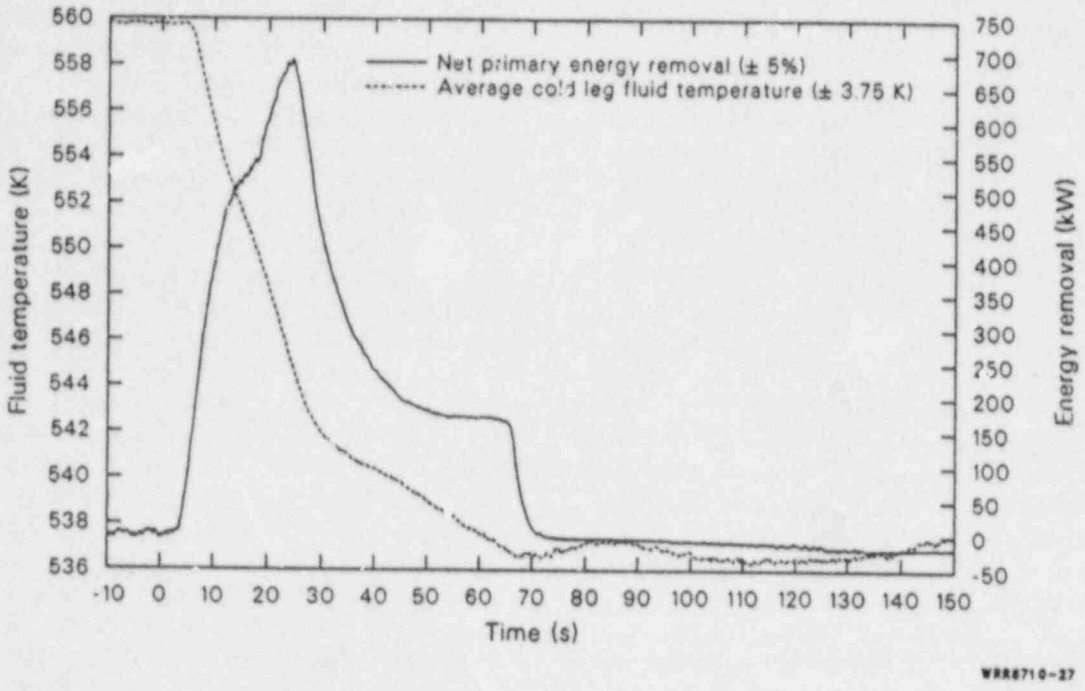

Figure 27. Primary fluid system energy removal and average cold leg fluid temperature during the blowdown phase of MSLB Test S-FS-1 (-10 to 150 s).

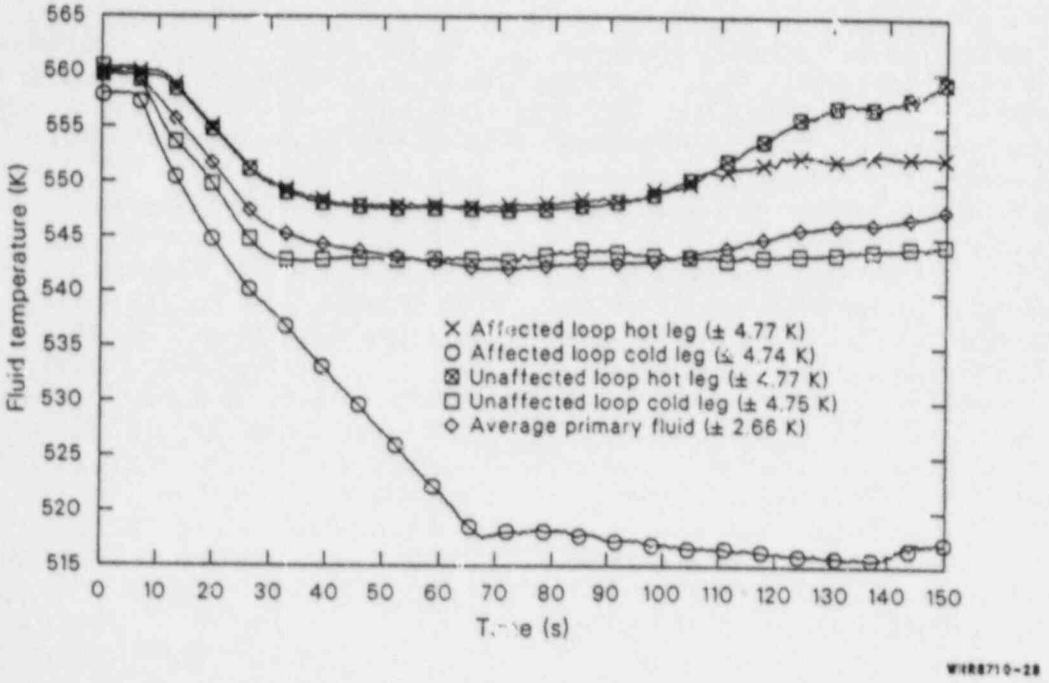

Figure 28. Affected and unaffected loop hot and cold leg and average primary fluid system temperatures during the blowdown phase of MSLB Test S-FS-1 (0 to 150 s).

heating moderated. The system continued to heat due to the core power (1.5% of full power) exceeding the unaffected loop steam generator auxiliary feedwater energy removal capacity. This caused the primary fluid thermal response to exhibit very gradual heating through the end of the blowdown phase.

Influence of Main Steam Line Break Size or Location on System Response

Concerns exist with respect to the effects of the break size or location on the primary and secondary system responses to a MSLB secondary LOCA. MSLB calculations performed for the Zion Unit One Nuclear Plant FSAR, Appendix 15, showed a definite sensitivity of calculated primary cooling to the break size or location. In this section, the effects of break size or location on transient severity are addressed by comparing first the secondary and then the primary fluid system thermal-hydraulic responses for double-ended offset shears of the main steam line downstream (Test S-FS-1) and upstream (Test S-FS-2) of the flow restrictor, with concurrent main steam line check valve failure. The discussion is organized into two subsections, with one subsection covering secondary fluid system response and the other covering primary fluid system response.

Effects of Break Size or Location on Secondary Response. As discussed earlier, the cooling of the primary fluid system is controlled by the secondary response to the MSLB secondary LOCA. Therefore, it is important to understand the effects of the MSLB size or location on the secondary thermal-hydraulic response in order to understand the relative severity of the resulting primary cooling. Both of the MSLB experiments had similar basic thermal-hydraulic responses. However, several differences in the responses are worthy of note. Comparisons of the general secondary system responses to the general sequences of events are discussed first. This is followed by comparisons of the secondary pressure responses, hydraulic responses, and thermal responses for both secondaries, with major emphasis on the affected loop steam generator.

General Secondary Response Comparisons. The general secondary responses for the MSLB experiments were qualitatively the same. The major differences observed are in the timing of events and the quantitative responses. For both break sizes and locations, the occurrence of the break produced severe effects on the steam generator secondary. In both cases, the unaffected loop steam generator also experienced a loss of inventory and increased primary energy removal, due to flow past the failed main steam line check valve to the break before MSIV closure. Following MSIV closure, the unaffected loop steam generator slowly refilled with auxiliary feedwater and repressurized. The affected loop steam generator emptied and decoupled from the primary.

Secondary Pressure Response Comparisons. The secondary pressure responses exhibited the same basic trends for both break sizes and locations, with the major differences occurring in the magnitudes of the parameters and the timing of events. In both cases, the secondary pressure responses are characterized by a number of inflection points associated with changes in the mass and energy balances. As shown in Figure 29, the loss of mass from the secondaries caused a rapid depressurization of the affected and unaffected loop steam generators. Both cases exhibited the marked decreases in depressurization rates as the initially subcooled downcomer fluid reached saturation conditions. For the break upstream of the flow restrictor (Test S-FS-2), the flow from the affected loop steam generator represented flow limited only by the steam generator exit piping flow area; whereas, the flow from the unaffected loop steam generator represented flow limited by the affected loop steam line flow restrictor. As discussed earlier, for the break downstream of the flow restrictor (Test S-FS-1), the flow from the affected loop steam generator represented flow limited by the affected steam line flow restrictor. At the same time, the flow from the unaffected loop steam generator represented flow from three steam generators (with the flow from each limited by its respective flow restrictor).

The larger affected loop steam generator steam line break flow area for Test S-FS-2 caused the secondary to depressurize faster, as shown in Figure 29. Similarly, the smaller unaffected loop steam generator steam line break flow area for Test S-FS-2 caused the slower secondary depressurization shown in the figure. The faster affected loop steam generator secondary depressurization during Test S-FS-2 resulted in a much earlier SI signal. The low affected loop steam generator secondary pressure trip setpoint of 4.14 MPa was reached

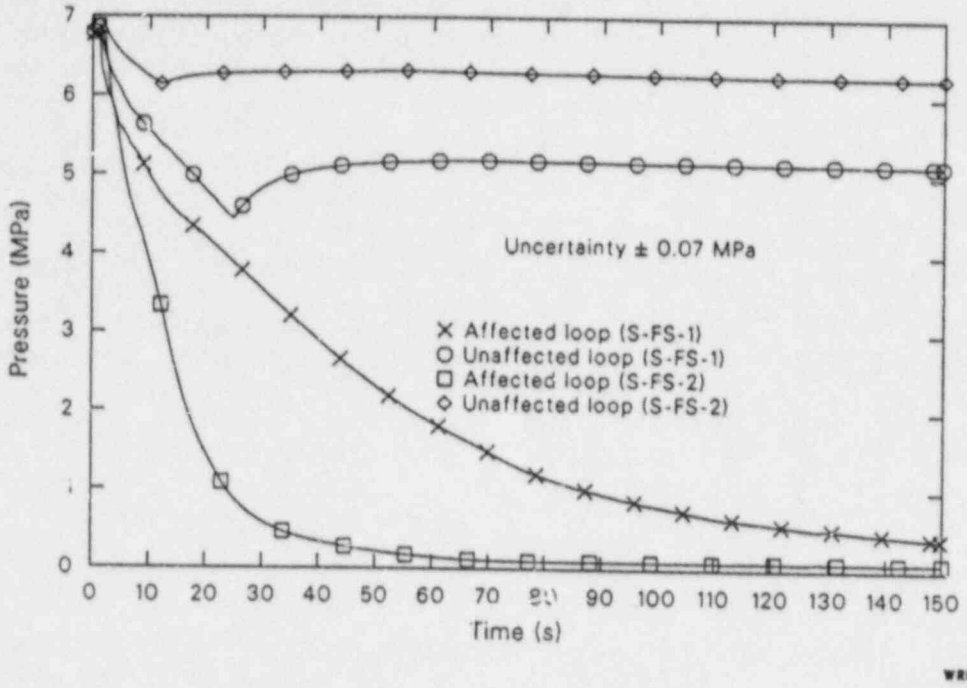

Figure 29. Comparisons of affected and unaffected loop steam generator secondary pressures during the blowdown phases of MSLB Tests S-FS-1 and S-FS-2.

at about 7.6 s during Test S-FS-2 and about 21 s during Test S-FS-1. In both cases, the SI signal initiated SI and MSIV closure signals. The depressurization of the unaffected loop steam generator was halted in both cases when the MSIV fully closed at about 4 s after SI. In both cases, the unaffected loop steam generator experienced a slight repressurization following MSIV closure due to energy addition from the primary fluid system in the absence of secondary feeding and steaming. The affected loop steam generator continued to depressurize in both cases until the generator was essentially empty at about 50 s (during Test S-FS-2) and about 110 s (during Test S-FS-1). In both cases, the affected loop steam generator became essentially decoupled from the primary fluid system for the remainder of the transient. The unaffected loop steam generator secondary pressure continued to experience a very gradual increase due to the primary energy addition exceeding the auxiliary feedwater energy removal in both cases. At the end of the blowdown phase of both transients, the secondary pressures were fairly stable.

Secondary Hydraulic Response Comparisons. The secondary hydraulic responses exhibited the same basic trends for both cases. The hydraulic response of the affected loop steam generator secondary fluid system to a double-ended offset shear of the main steam line either upstream or downstream of the flow restrictor is characterized by a rapid voiding of the entire secondary. Because the affected loop steam generator was not steaming at initial conditions and injection of auxiliary feedwater into the affected loop steam generator was disallowed (simulating the response of an automatic faulted secondary detection system), the secondary mass balance was affected only by the break flow. The simulated MSLB initiated the loss of secondary inventory, producing severe effects on the secondary hydraulic characteristics in both cases. The break flow peaked at about 1 s in both cases as critical flow was established (Figures 4 and 30). The break effluent from the steam generator consisted of two-phase fluid early in both transients, followed by single-phase steam for the remainder of the blowdown (Figures 5 and 31). The larger break mass-flow rate for Test S-FS-2 resulted in greater measured liquid content of the break effluent. The transitions of the break flows from two-phase mixture to single-phase steam produced slight variations in the steam generator secondary depressurization rates (Figure 29) for both cases. During the initial part of both blowdowns,

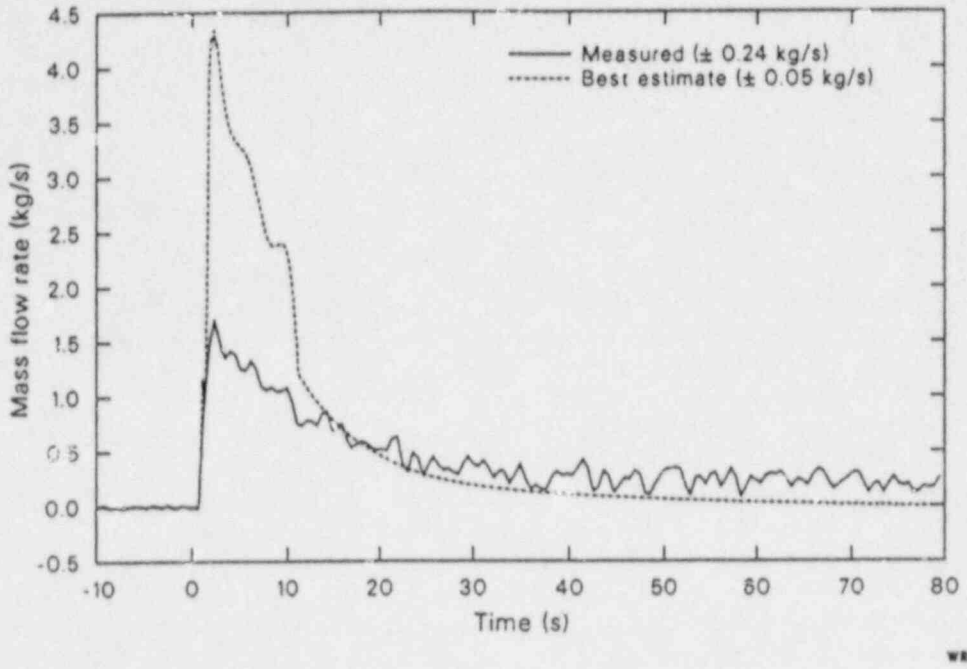

Figure 30. Affected loop steam generator measured and best-estimate break mass flow rates during the blowdown phase of MSLB Test S-FS-2 (-10 to 80 s).

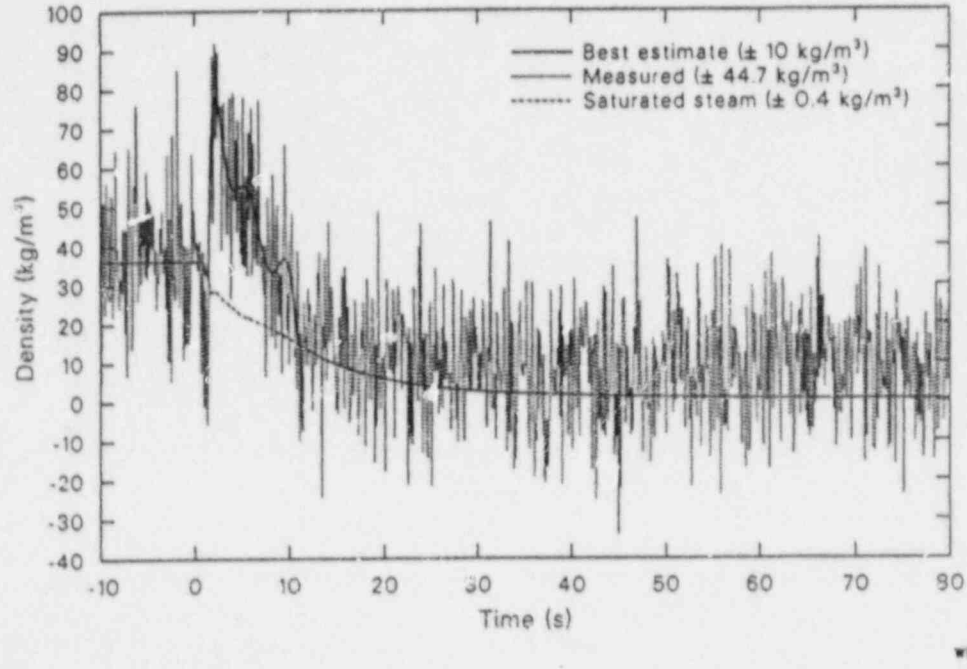

Figure 31. Affected loop steam generator measured and best-estimate break fluid and saturated steam densities during the blowdown phase of MSLB Test S-FS-2 (-10 to 80 s).

the break flows were of sufficient magnitude to cause the flow in the affected loop steam generator upper downcomer to reverse and the flow at the top of the riser to increase (Figures 32 and 33). One difference was noted in the lower downcomer flow response. The greater riser flow for the break upstream of the flow restrictor (Test S-FS-2) prevented the lower downcomer flow from reversing as it did for Test S-FS-1 (Figure 34). In both tests, the high-mass flow rates in the affected loop steam generator and the rapid depressurizations caused flow reversals in the separator drain lines, as indicated by the negative differential pressures in Figure 35. This degraded the performance of the steam separator, which allowed two-phase mixtures to exit the steam dome in both cases until the flows were reduced to within the range of the steam separator capabilities. The minimum void fractions measured at the break were about 0.93 (for Test S-FS-2) and 0.97 (for Test S-FS-1), representing homogeneous flow qualities of about 0.34 and 0.58, respectively (Figure 36). Thus, separator efficiency was decreased significantly by the high mass-flow rates and the drain line flow reversals in both cases, with the lowest efficiency observed for the largest break size (Test S-FS-2). In both cases, as the affected loop steam generator secondary depressurized, the break flow decreased, ending the upper downcomer flow reversal and decreasing the component mass-flow rates. The component flows continued to decrease in both cases until the secondary fluid inventory was depleted (at about 50 s in Test S-FS-2 and about 110 s in Test S-FS-1). The affected loop steam generator secondary component flows remained stagnant for the remainder of both transients, since the secondary fluid inventories remained depleted with no auxiliary feedwater injection occurring.

The MSLB transient condition resulted in nonuniform rates of inventory reduction for the affected loop steam generator downcomer and tube bundle regions for both cases (Figures 11, 37, 12 and 38). In both cases, the initial reduction in the total secondary mass inventory involved a more rapid rate of reduction in the tube bundle mass inventory than in the downcomer mass inventory. The rapid depressurization of the affected loop steam generator secondary caused the secondary fluid to flash and, aided by the loss of inventory, resulted in early voiding of the tube bundle section (Figures 13 and 39). In both cases, the entire tube bundle region secondary fluid inventory changed to an all-vapor condition (void fraction of 1.0) as the tube bundle liquid inventory was finally depleted. This altered the secondary convective heat transfer significantly in both cases but did not severely affect the primary-to-secondary heat transfer, since the transient heat transfer in both cases was almost totally controlled by the conduction heat transfer across the tube wall. The altering of the secondary convective heat transfer would, however, become more important for smaller-break-size cases where the secondary depressurization and temperature reduction rates are not of sufficient magnitude to cause conduction limiting across the U-tube wall. Thus, accurate modeling of the entire secondary fluid system flow areas, volumes, and hydraulic resistances and accurate calculation of the intercomponent, as well as the break mass flow rates, becomes more important for ensuring accurate prediction of the heat transfer response during a MSLB transient as the MSLB size is reduced.

The secondary fluid hydraulic response of the unaffected loop steam generator was similar for both break sizes and locations, with the major differences occurring in the magnitudes of the parameters and the timing of events. The simulated MSLB concurrent with main steam line check valve failure initiated the loss of secondary inventory, severely affecting secondary hydraulic characteristics in both cases. As shown in Figure 40, the break flows peaked at about 1 s as critical flow was established. A significant difference was observed in the response of the unaffected loop steam generator steam separator to the different break flows. For the break downstream of the flow restrictor (Test S-FS-1), the break effluent from the steam generator consisted of two-phase fluid early in the transient, followed by single-phase steam for the remainder of the blowdown, as shown in Figure 15. However, for the break upstream of the flow restrictor (Test S-FS-2), the break effluent remained essentially single-phase steam during the blowdown, as shown in Figure 41. Since the break flow remained single-phase vapor during Test S-FS-2, secondary depressurization did not exhibit the slight variations observed for Test S-FS-1 (Figure 29). The smaller break flow area for the break upstream of the flow restrictor (Test S-FS-2) limited the break flow to that within the range of the unaffected loop steam generator-steam separator capabilities. This allowed the break effluent to remain single-phase vapor during Test S-FS-2, whereas a two-phase mixture exited the steam dome during Test S-FS-1. The minimum void fractions measured at the break were about 1.0 for Test S-FS-2 and about 0.95 for Test S-FS-1, which represent homogeneous flow qualities of about 1.0 and 0.41, respectively

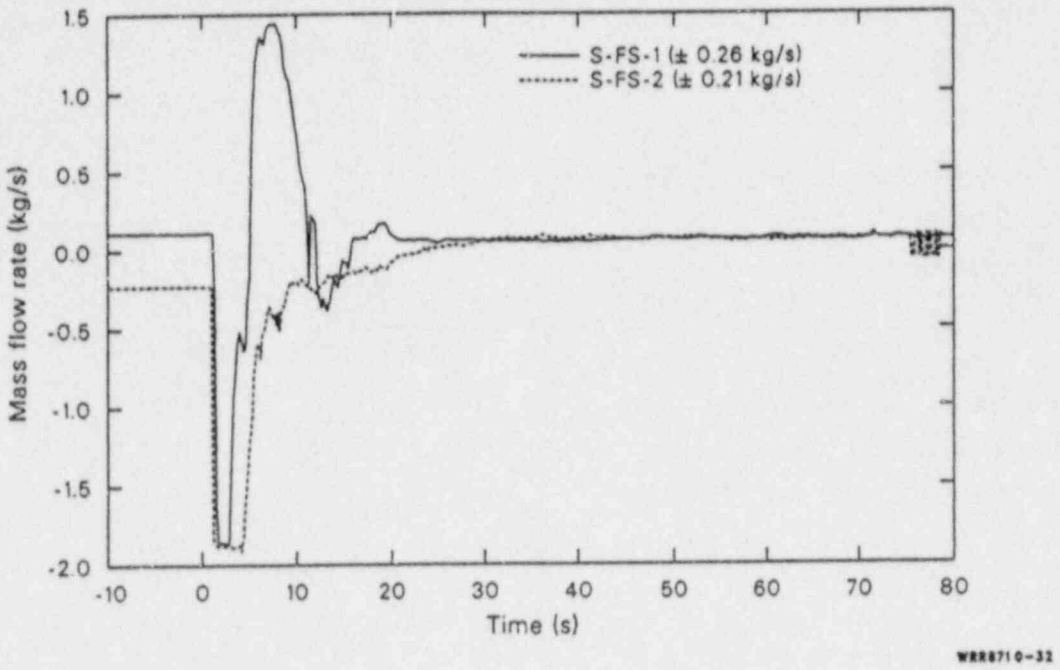

Figure 32. Comparisons of affected loop steam generator upper downcomer mass flow rates during the blowdown phases of MSLB Tests S-FS-1 and S-FS-2.

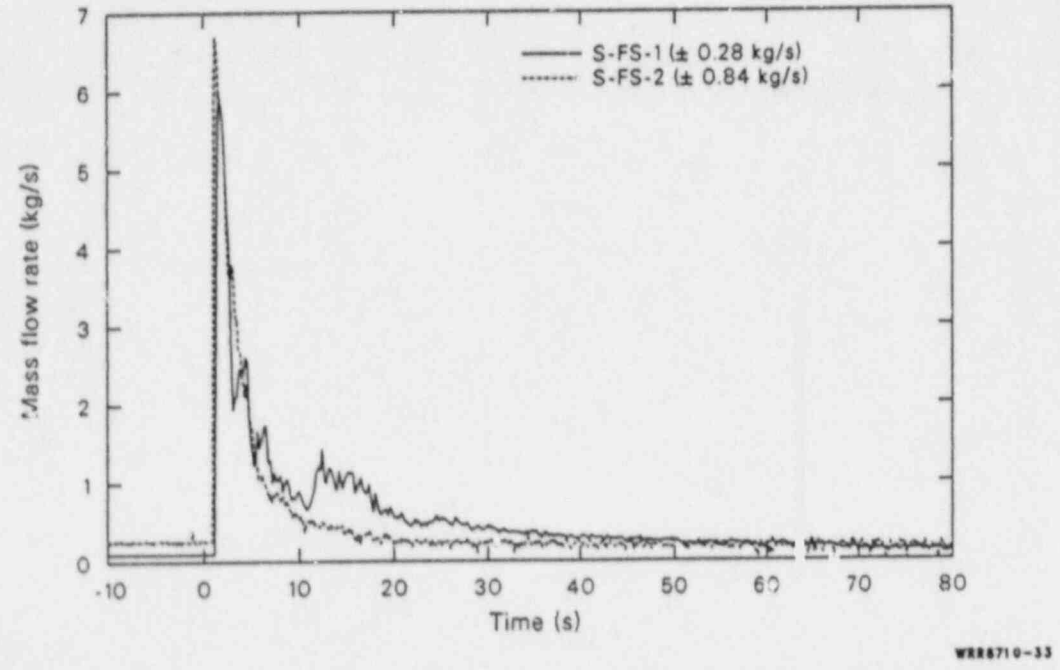

Figure 33. Comparisons of affected loop steam generator riser mass flow rates during the blowdown phases of MSLB Tests S-FS-1 and S-FS-2.

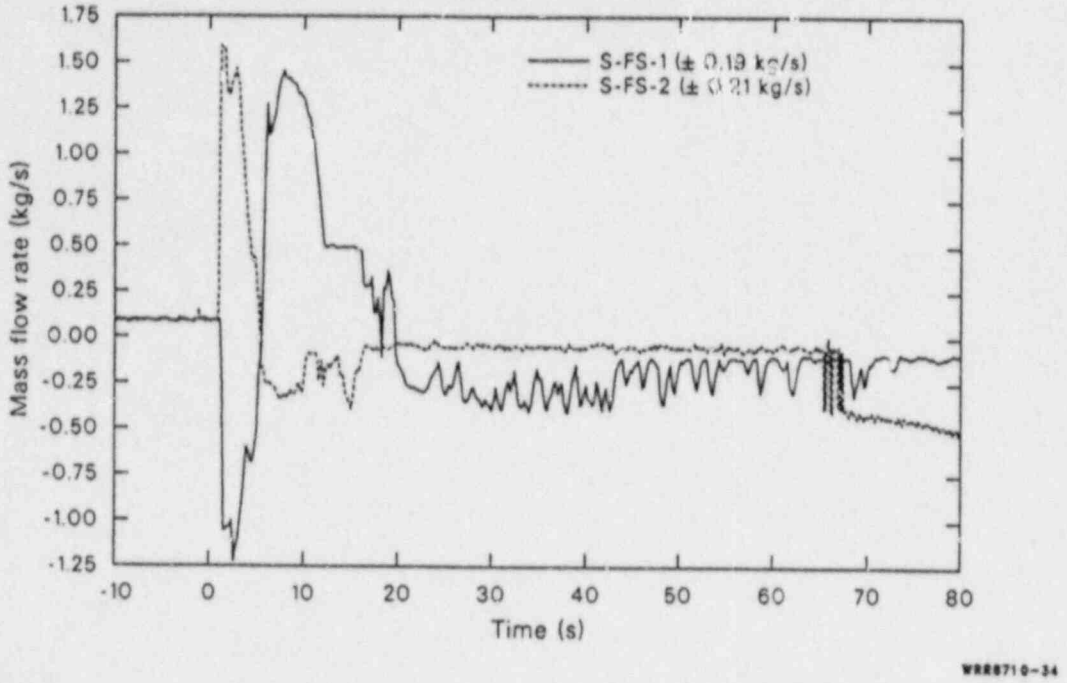

Figure 34. Comparisons of affected loop steam generator lower downcomer mass flow rates during the blowdown phases of MSLB Tests S-FS-1 and S-FS-2.

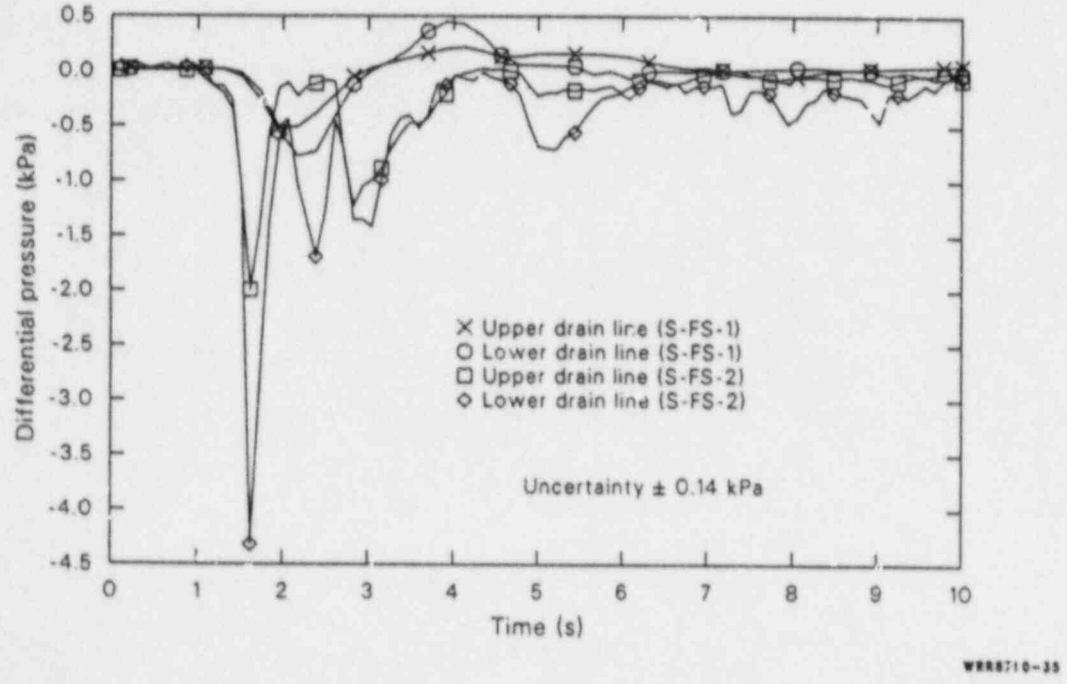

Figure 35. Comparisons of affected loop steam generator separator drain line differential pressures (indicative of flow direction) during the blowdown phases of MSLB Tests S-FS-1 and S-FS-2.

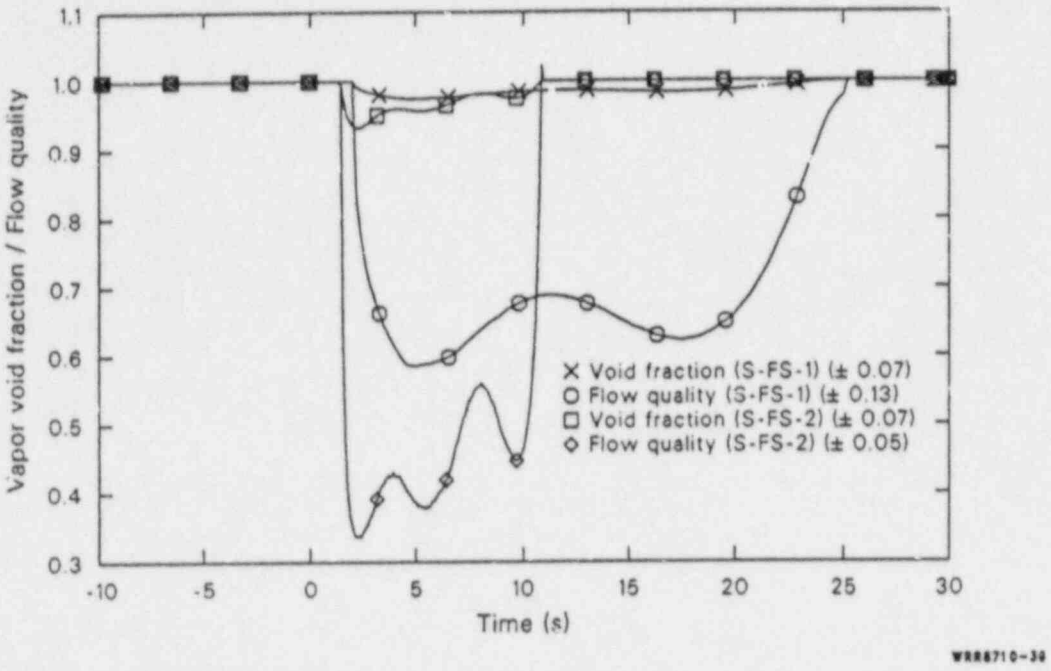

Figure 36. Comparisons of affected loop steam generator break effluent vapor void fractions and homogeneous flow qualities during the blowdown phases of MSLB Tests S-FS-1 and S-FS-2.

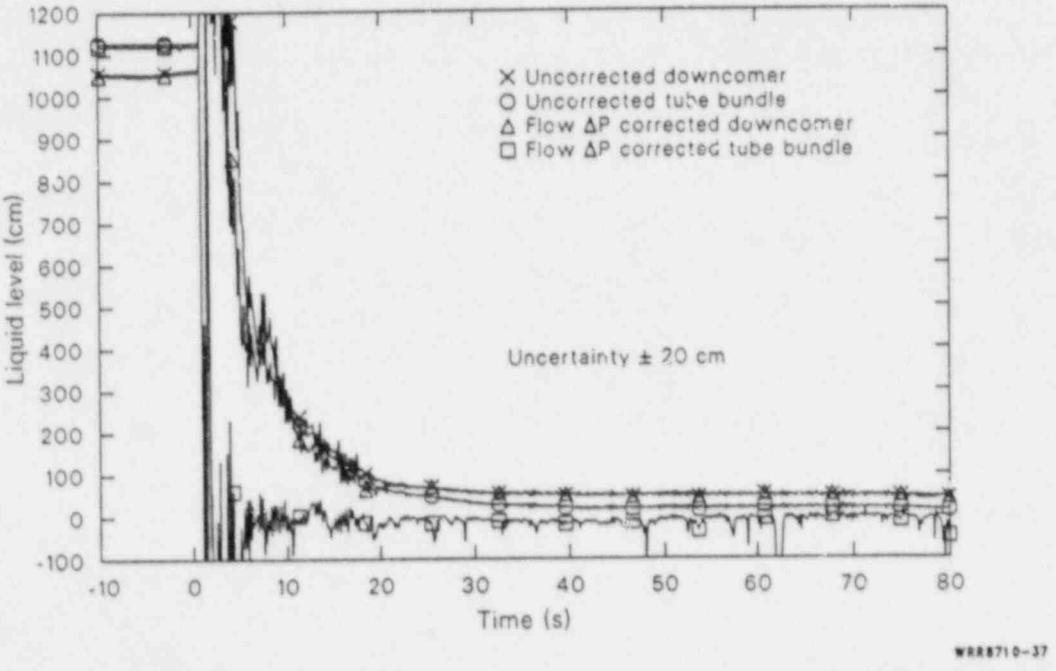

Figure 37. Affected loop steam generator overall downcomer and tube bundle interfacial liquid levels during the blowdown phase of MSLB Test S-FS-2 (-10 to 80 s).

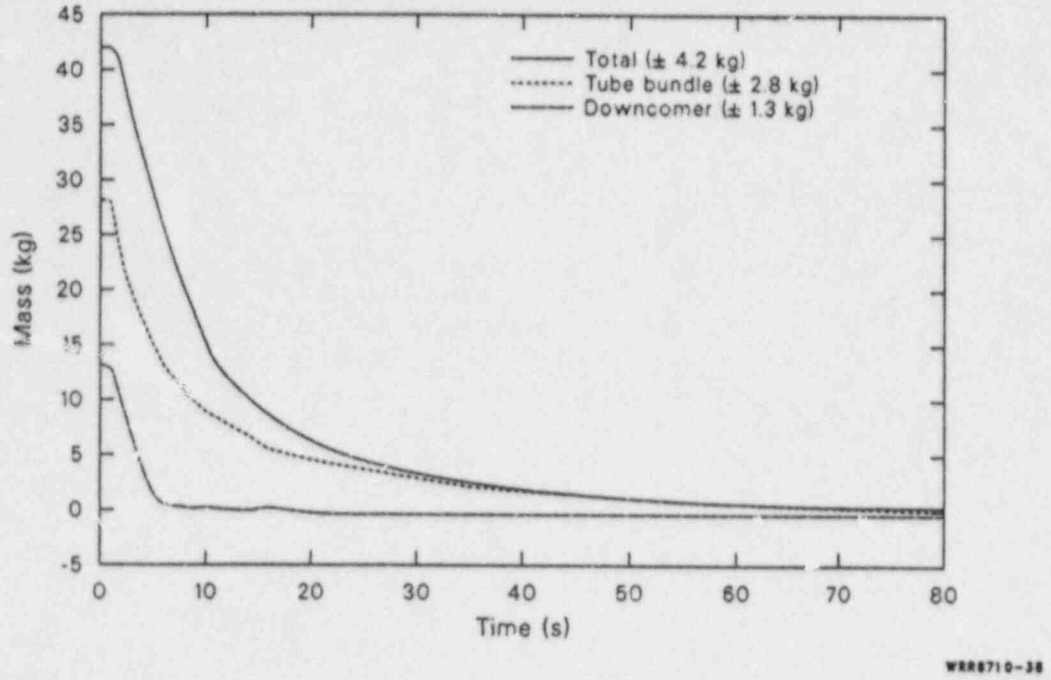

Figure 38. Affected loop steam generator total, downcomer, and tube bundle secondary fluid mass inventories during the blowdown phase of MSLB Test S-FS-2 (0 to 80 s).

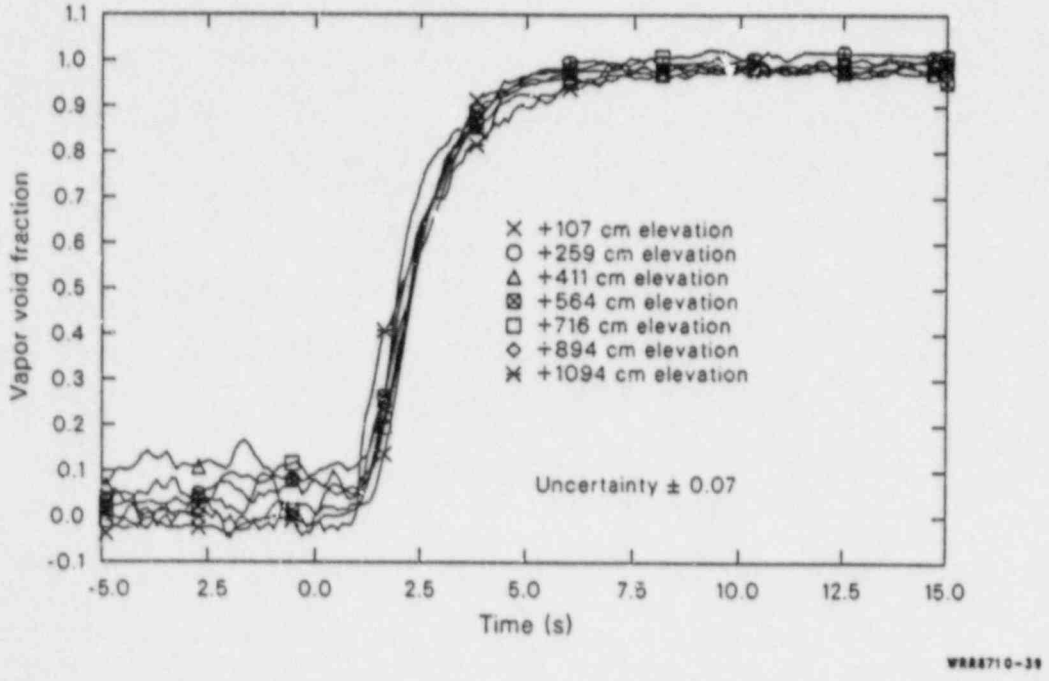

Figure 39. Affected loop steam generator tube bundle secondary fluid vapor void fractions during the blowdown phase of MSLB Test S-FS-2 (-5 to 15 s).

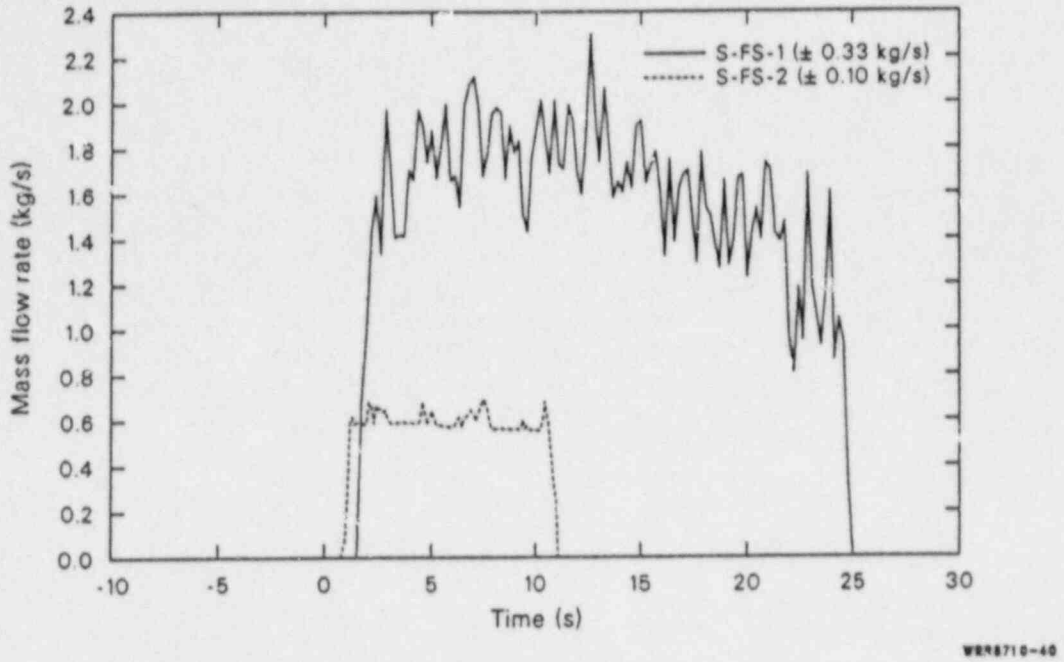

Figure 40. Comparisons of unaffected loop steam generator break mass flow rates during the blowdown phases of MSLB Tests S-FS-1 and S-FS-2.

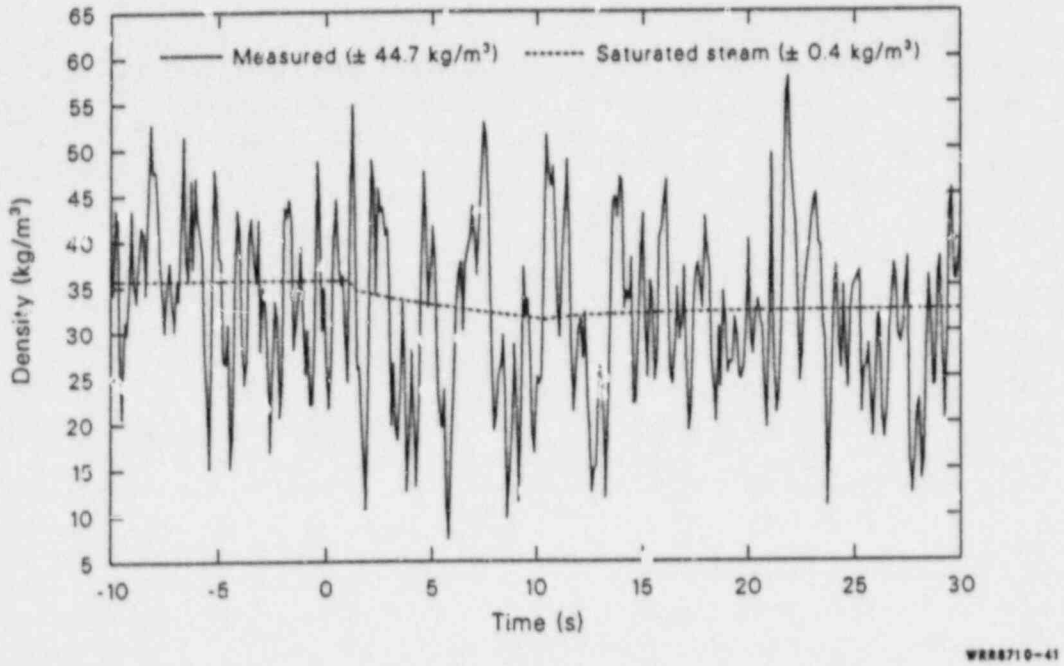

Figure 41. Unaffected loop steam generator break fluid density and saturated steam density during the blowdown phase of MSLB Test S-FS-2 (-10 to 30 s).

(Figure 42). Thus, separator efficiency was decreased significantly by the high mass-flow rates during Test S-FS-1, but was not affected by the lower mass-flow rates during Test S-FS-2. Following the low affected loop steam generator secondary pressure trip, unaffected loop steam generator feedwater flow was terminated, the MSIV was closed, and auxiliary feedwater flow was initiated in both cases. Main feedwater flow had little effect on the secondary mass balance in either case, since the flow was minimal ("hot standby," representing about 1.5% of full power conditions) and the time required for termination was minimal (about 8 s during Test S-FS-2 and about 22 s during Test S-FS-1). The MSIV closure halted the loss of secondary inventory, with the inventory at its minimum value of about 97% and 60% of the initial mass for Tests S-FS-2 and S-FS-1, respectively. In both cases, recovery of the secondary inventory was then initiated by auxiliary feedwater injection, as indicated by the liquid level responses (Figure 43). At the end of the blowdown phase of Tests S-FS-2 and S-FS-1, the secondary inventories had recovered to about 102% and 64%, respectively, of the initial mass.

Secondary Thermal Response Comparisons. The measured secondary thermal responses for both break sizes and locations are very similar. The thermal response of the affected loop steam generator secondary fluid system to a double-ended offset shear of the main steam line either upstream or downstream of the flow restrictor is characterized by a rapid increase in the primary-to-secondary heat transfer. As shown in Figure 44, for both cases, the affected loop steam generator primary-to-secondary heat transfer increased rapidly until the loop flow reductions began due to the loss of offsite power. The primary-to-secondary heat transfer then decreased somewhat as the U-tube primary side convective heat transfer coefficients decreased (Figures 19 and 45), but remained high due to the decreasing secondary fluid saturation temperature (Figure 46) and the increased secondary convective heat transfer coefficients (Figures 21, 47, and B-1 through B-14). In both cases, while the affected loop steam generator primary energy removal increased substantially, it was at least an order of magnitude below the energy removal capacity associated with the break flow (Figure 44).

The observed trends in the primary-to-secondary heat transfer were very similar for the two different break size and location cases. Both cases exhibit the same controlling mechanisms (i.e., primary convective heat transfer, conduction heat transfer across the U-tube wall, and secondary convective heat transfer), with only minor differences in the interaction of the mechanisms. The affected loop steam generator primary-to-secondary heat transfer during both tests was obviously limited by some mechanism, since the primary energy removal was at least an order of magnitude below the energy removal capacity associated with the break flow. During the initial part of the blowdown, both primary and secondary convective heat transfer coefficients remained constant after undergoing a step-change increase at transient initiation. The primary-to-secondary-fluid temperature differences were constantly increasing, however, as the secondary fluid temperatures constantly decreased. The primary-to-secondary heat transfer during this part of the blowdown was therefore limited by the conduction heat transfer across the U-tube wall. During the period of primary coolant pump coastdowns, primary convective heat transfer coefficients were constantly decreasing. The primary-to-secondary heat transfer during this part of the blowdown was therefore limited by the conduction heat transfer and the primary convective heat transfer. Eventually, the primary-to-secondary heat transfer was limited by the primary convective heat transfer when the primary coolant pumps coasted to a stop. The secondary convective heat transfer coefficients rapidly degraded to zero when the liquid inventory was depleted (i.e., the local secondary convective heat transfer coefficients rapidly degraded to zero when the local vapor void fractions reached a value of 1.0). This produced some secondary convection heat transfer limiting in the upper elevations of the secondary for Test S-FS-2, but no real secondary convective heat transfer limiting during Test S-FS-1. However, in both cases, the primary-to-secondary heat transfer would have eventually been limited by the secondary convective heat transfer had the primary coolant pumps not been tripped off.

As discussed previously, the purpose of assumptions applied to MSLB transient simulations and calculations is to produce the maximum amount of primary cooling. Assumptions which maximize the primary cooling are considered to be conservative assumptions. Based on the preceding discussions, invaluable insight can be gained into the relative degree of conservatism inherent in MSLB simulation assumptions. The assumed loss of offsite power at SI causes loop flow reduction, which decreases primary convective heat transfer. Because

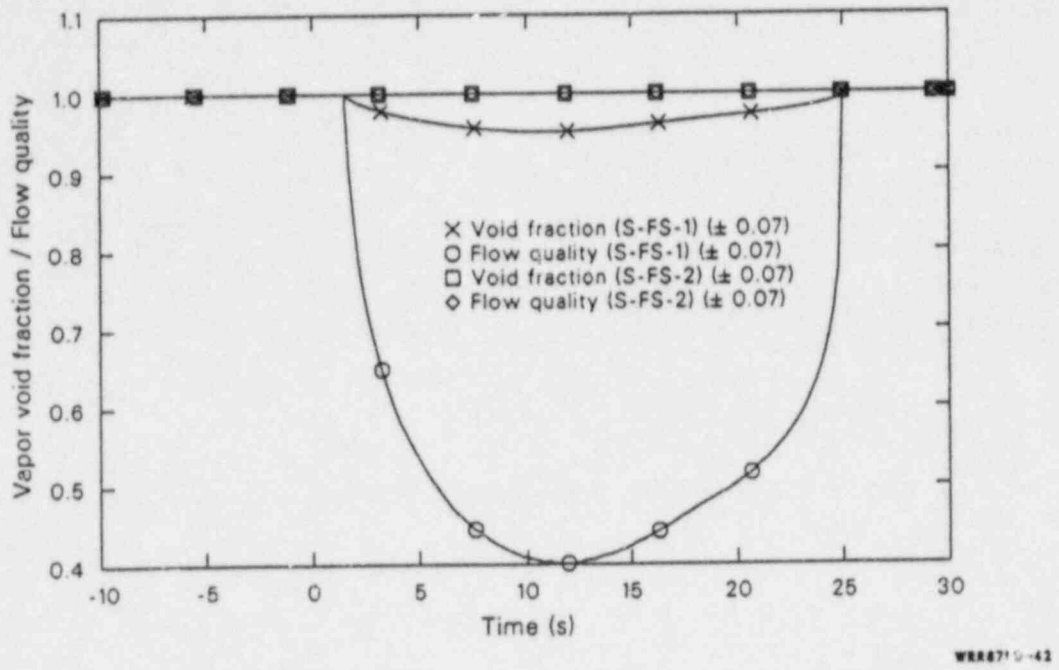

Figure 42. Comparisons of unaffected loop steam generator break effluent vapor void fractions and homogeneous flow qualities during the blowdown phases of MSLB Tests S-FS-1 and S-FS-2.

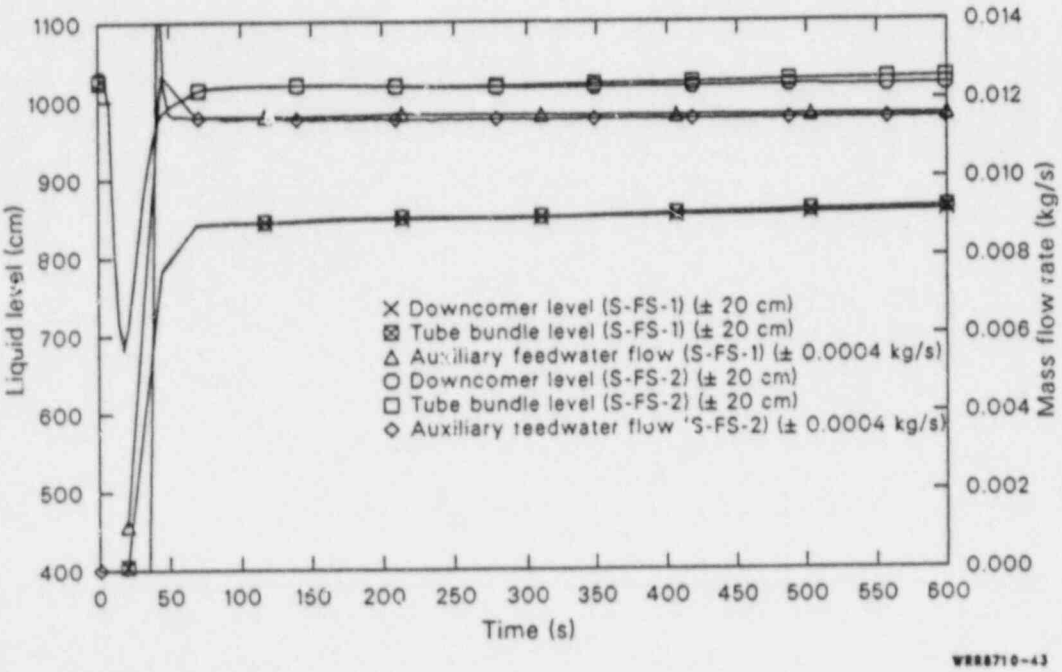

Figure 43. Comparisons of unaffected loop steam generator overall downcomer and tube bundle collapsed liquid levels and auxiliary feedwater mass flow rates during the blowdown phases of MSLB Tests S-FS-1 and S-FS-2.

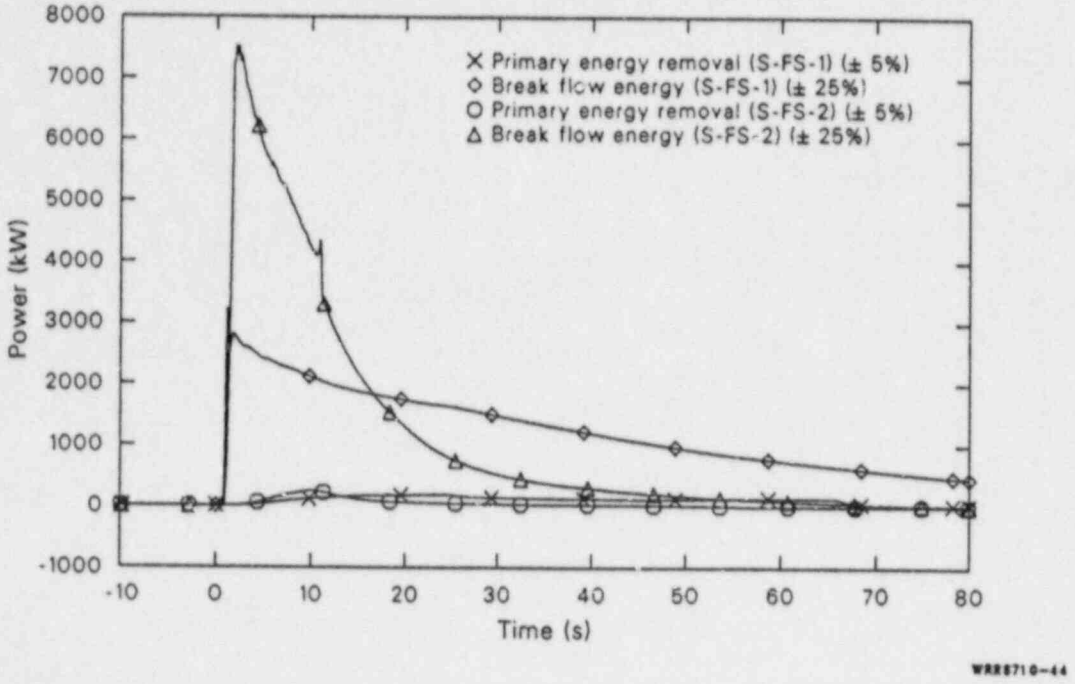

Figure 44. Comparisons of affected loop steam generator primary-to- secondary heat transfer and break flow energy during the blowdown phases of MSLB Tests S-FS-1 and S-FS-2.

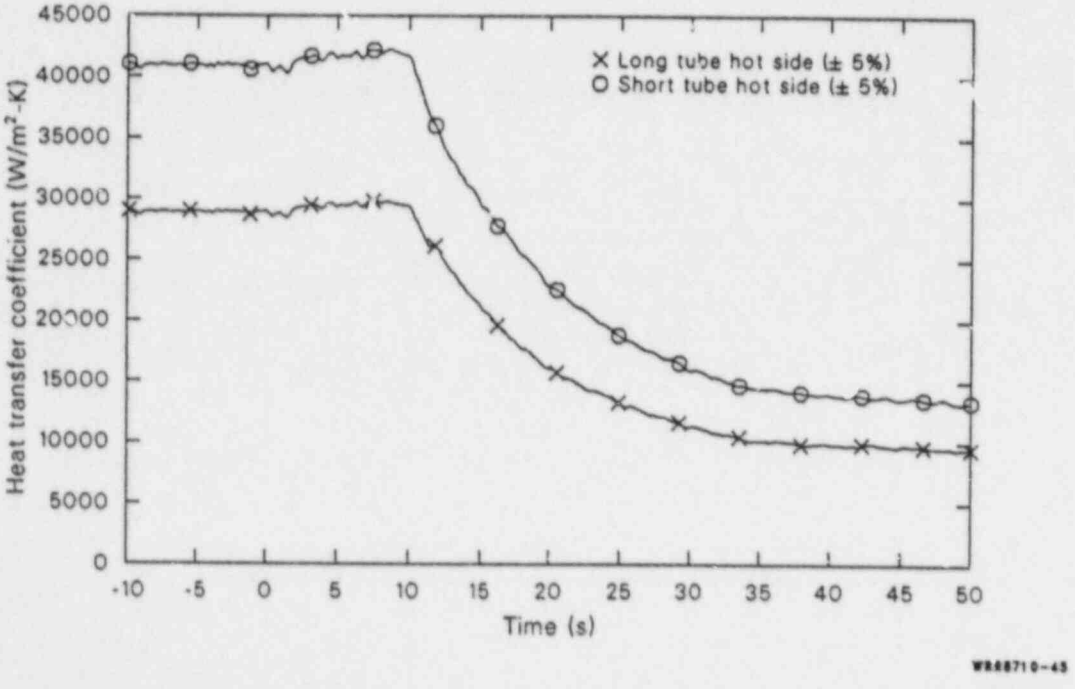

Figure 45. Affected loop steam generator primary convective heat transfer coefficients at the 61-cm elevation during the blowdown phase of MSLB Test S-FS-2 (-10 to 50 s).

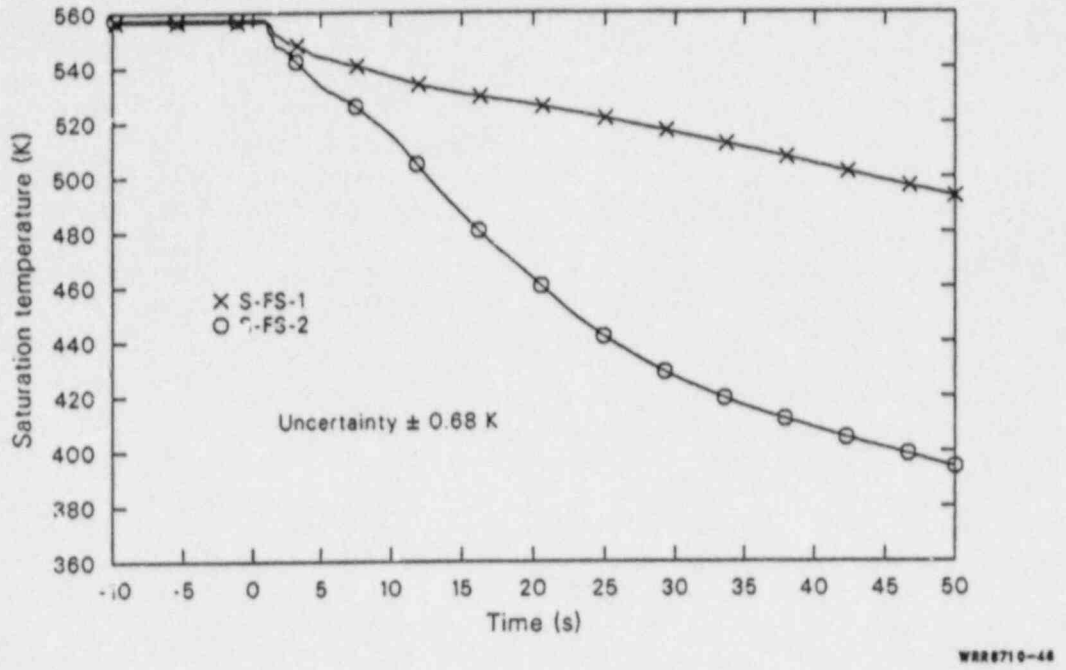

Figure 46. Comparisons of affected loop steam generator secondary fluid saturation temperatures during the blowdown phases of MSLB Tests S-FS-1 and S-FS-2.

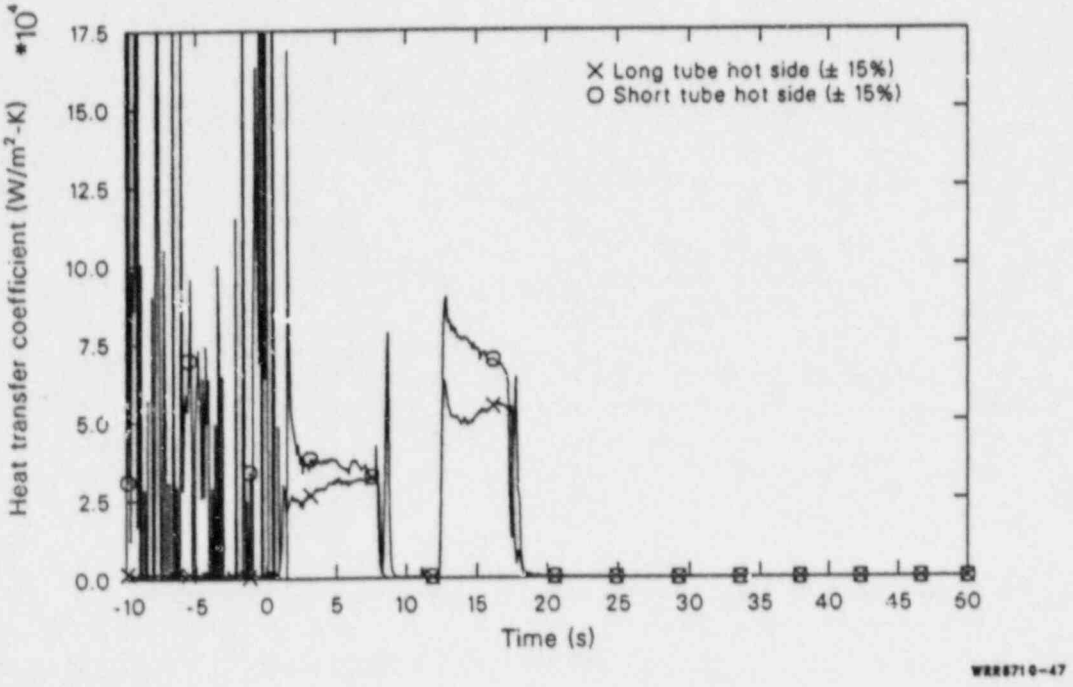

Figure 47. Affected loop steam generator secondary convective heat transfer coefficients at the 61-cm elevation during the blowdown phase of MSLB Test S-FS-2 (-10 to 50 s).

the primary cooling is decreased by reducing primary convective heat transfer, loss of offsite power should not be considered to be a conservative assumption.

Assuming perfect separation provides the maximum energy removal capacity associated with break flow. However, primary-to-secondary heat transfer is limited by conduction heat transfer across the U-tube wall such that the primary energy removal is much less than the energy removal capacity associated with the break flow. Therefore, the break fluid energy removal which results from an assumed separator performance has minimal direct effect upon the primary energy removal. A greater effect of assuming perfect separation is that it decreases the rate of the secondary mass loss, depressurization, and secondary fluid saturation temperature reduction. This increases the duration of conduction heat transfer across the U-tube wall, secondary convective heat transfer, and primary-to-secondary heat transfer. The same effect would be achieved by decreasing the break size so that the break flow energy removal rate is as close as possible to the conduction-limited primary-to-secondary heat transfer rate. In this manner, the effect of the secondary break flow energy removal on the primary cooling would be maximized. This is evidenced by the fact that the total primary energy removal via the affected loop steam generator was much greater for the break downstream of the flow restrictor (Test S-FS-1) than for the break upstream of the flow restrictor (Test S-FS-2). Thus, the primary cooling caused by the affected steam generator during an MSLB transient would be maximized by: either not simulating the loss of offsite power or delaying the simulated loss of offsite power until after secondary convective heat transfer has degraded to zero (after the affected loop steam generator secondary is empty), assuming perfect separation (although the effect of this assumption is minimal); and, decreasing the break size such that the break flow energy removal rate is as close as possible to the conduction-limited primary-to-secondary heat transfer rate.

The primary-to-secondary heat transfer during both of the MSLB transients was conduction-limited. Therefore, as discussed previously, the steam generator U-tube thermal conductivity played a key role in determining the amount of primary cooling. The Type III affected loop steam generator U-tube material and material temperatures are typical of the Westinghouse Model 51 steam generator; however, the Type III steam generator U-tube walls are 0.165-cm thick, whereas the Westinghouse Model 51 steam generator U-tube walls are 0.124-cm thick. The 0.165-cm tube wall thickness in the Type III steam generator allows approximately 20% less conduction heat transfer across the U-tube wall than would occur for a 0.124-cm thick wall with the same primary-to-secondary temperature difference. The primary cooling produced by the affected loop steam generator during both simulated MSLB transients was therefore approximately 20% less than would have occurred with the 0.124-cm thick U-tube walls in a Westinghouse Model 51 steam generator.

In both cases, the initial depressurization rate of the affected loop steam generator secondary (Figure 29) was affected by the initial subcooling of the secondary fluid. The affected loop steam generator was not steaming at initial conditions in either test, resulting in stratification and subcooling in the downcomer (Figures 22 and 48). The initial subcooling delayed the onset of flashing in both cases, causing a rapid initial depressurization rate.

The affected loop steam generator decoupled from the primary fluid system following the loss of inventory in both cases. With no auxiliary feedwater injection, the secondary fluid system remained devoid of fluid and had no further effect on the primary fluid system.

The thermal response of the unaffected loop steam generator secondary fluid system to a double-ended offset shear of the main steam line (either upstream or downstream of the flow restrictor with concurrent check valve failure) is also characterized by a rapid increase in the primary-to-secondary heat transfer. As shown in Figures 23 and 49, the unaffected loop steam generator primary-to-secondary heat transfer increased rapidly in both cases until MSIV closure terminated the loss of inventory via the break. Concurrent with MSIV closure, the loop flow reductions began due to the loss of offsite power. The primary-to-secondary heat transfer then decreased significantly in both cases as the U-tube primary and secondary side convective heat transfer decreased. Here again, although the unaffected loop steam generator primary energy removal increased substantially in both cases, it was at least an order of magnitude below the energy removal capacity associated with the break flow (Figures 23 and 49). These observed trends in the primary-to-secondary heat transfer are similar to those observed for the affected loop steam generator and indicate that the mechanisms controlling the amount of primary cooling are similar for both steam generators in each experiment.

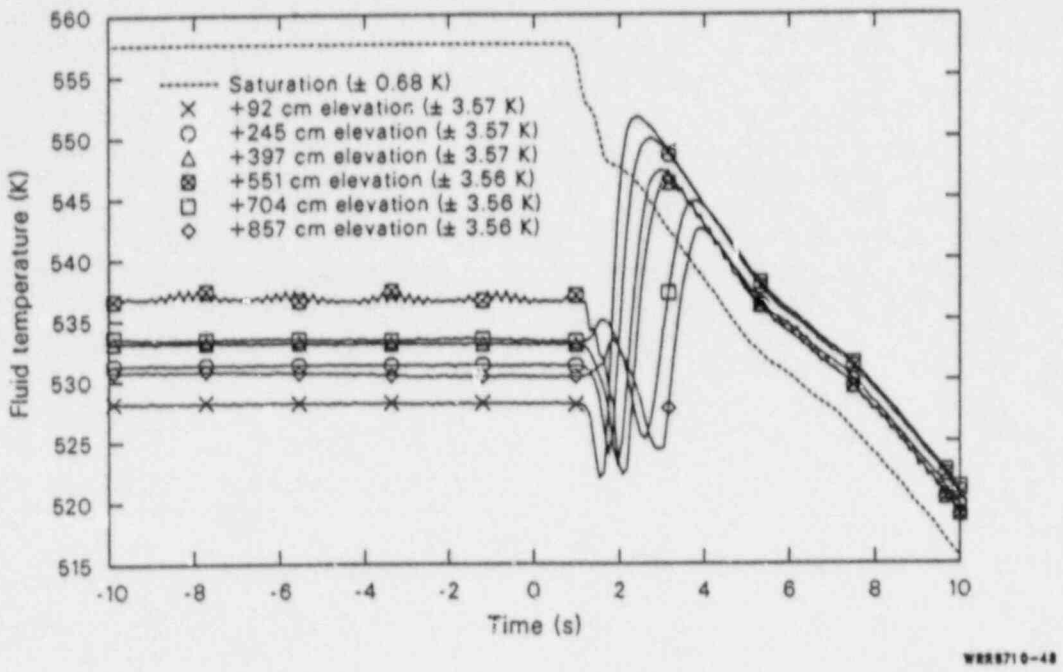

Figure 48. Affected loop steam generator downcomer fluid temperatures and saturation temperature during the blowdown phase of MSLB Test S-FS-2 (-10 to 10 s).

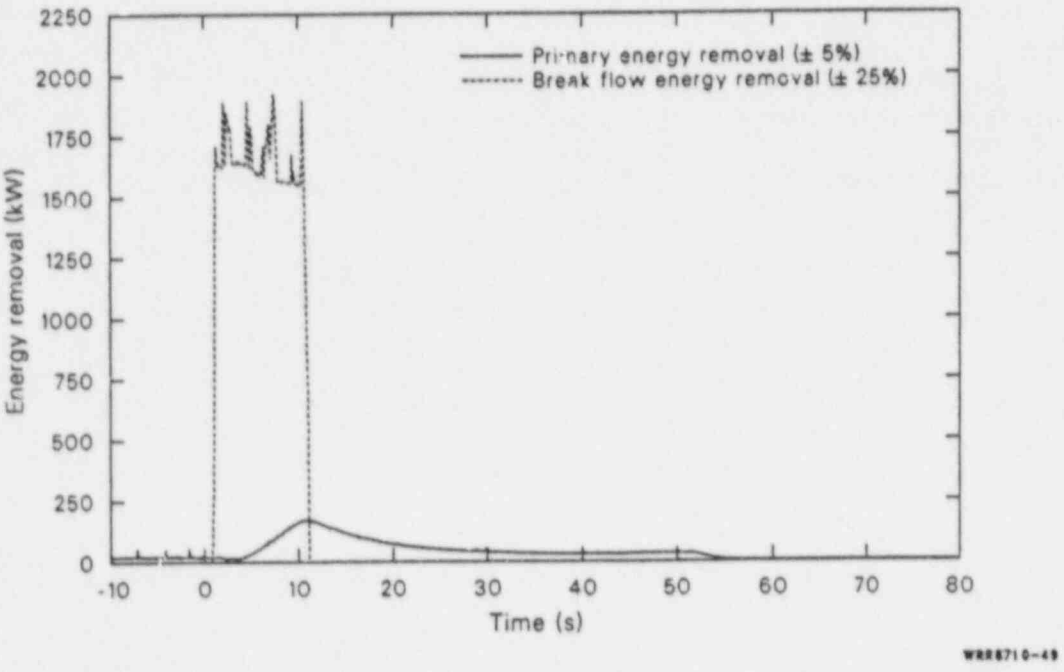

Figure 49. Unaffected loop steam generator primary-to-secondary heat transfer and break flow energy during the blowdown phase of MSLB Test S-FS-2 (-10 to 80 s).

The unaffected loop steam generator primary-to-secondary heat transfer during both tests was obviously limited by some mechanism, since the primary energy removal was at least an order of magnitude below the energy removal capacity associated with the break flow. During both tests, the primary-to-secondary heat transfer during the initial part of the blowdown was limited by the conduction heat transfer across the U-tube wall, as with the affected loop steam generator. However, the primary-to-secondary heat transfer was next limited by the secondary convective heat transfer, due to the isolation of the secondary at MSIV closure. The primary-to-secondary heat transfer was then limited during the pump coastdown part of the blowdowns by the secondary and primary convective heat transfer.

In both MSLB transients, the unaffected loop steam generator provided significant cooling of the primary coolant system, which added to the cooling provided by the affected loop steam generator. This substantially increased the cooling of the primary coolant system in both cases. Therefore, the failed main steam line check valve assumption maximized primary cooling in both cases and should be considered to be a conservative assumption. However, when considering what break size will produce the best match between the conduction-limited primary energy removal and the break flow energy removal, one should also consider unaffected loop steam generator break flow, since conduction limiting also occurs in this steam generator. This is evidenced by the fact that the total primary energy removal via the unaffected loop steam generator was much greater for the break downstream of the flow restrictor (Test S-FS-1) than for the break upstream of the flow restrictor (Test S-FS-2).

The initial depressurization rate of the unaffected loop steam generator secondary (Figure 29) was also affected by the initial subcooling of the secondary fluid. In both cases, the unaffected loop steam generator secondary fluid exhibited some slight stratification and subcooling in the downcomer (Figure 50) at initial conditions. The initial subcooling had the same effect on the unaffected loop steam generator secondary depressurizations as it did on the affected loop steam generator secondary depressurizations. Here again, the initial secondary depressurization rates were more rapid due to initial subcooling of the downcomer fluid.

Following the SI signal, the unaffected loop steam generator main feedwater flow was terminated, the MSIV was closed, and the auxiliary feedwater injection was initiated in both experiments. Termination of the unaffected loop steam generator main feedwater had virtually no effect on the secondary response in either case. The energy removal via the break flow completely overshadowed the loss of energy removal associated with the main feedwater termination. The MSIV closure terminated the energy removal via the break, causing the secondary to gradually heat and repressurize in both cases. The energy removal provided by the auxiliary feedwater aided in minimizing secondary heating and pressurization during both experiments.

Effects of Break Size or Location on Primary System Response. The degree of cooling of the primary fluid system depends upon the thermal-hydraulic response to the increased heat sink. Therefore it is important to understand the effects of the MSLB size and location on the primary thermal-hydraulic response in order to understand the relative severity of the resulting primary cooldown. Both of the MSLB experiments had similar basic thermal-hydraulic responses. However, several differences in the responses are worthy of note. Comparisons of the general primary system responses to the general sequences of events are discussed first. This is followed by comparisons of the primary pressure, hydraulic, and thermal responses.

General Primary Response Comparisons. In general, primary responses for the MSLB experiments exhibited similar phenomena, with differences observed mainly in the timing of events and the quantitative responses. However, one difference was noted in the qualitative response following pump coastdown. For both cases, the occurrence of the break produced severe effects in the primary fluid system. The primary fluid system experienced a rapid cooldown in response to the increased primary-to-secondary heat transfer during the secondary LOCA, causing the primary fluid to shrink and rapidly depressurize in both cases. The significantly different primary cooling which occurred during the two experiments produced a significant difference in the primary pressure and pressurizer liquid level response. For the break downstream of the flow restrictor (Test S-FS-1), the primary depressurization rate increased substantially due to the pressurizer emptying, and the primary pressure was substantially decreased. For the break upstream of the flow restrictor (Test S-FS-2),

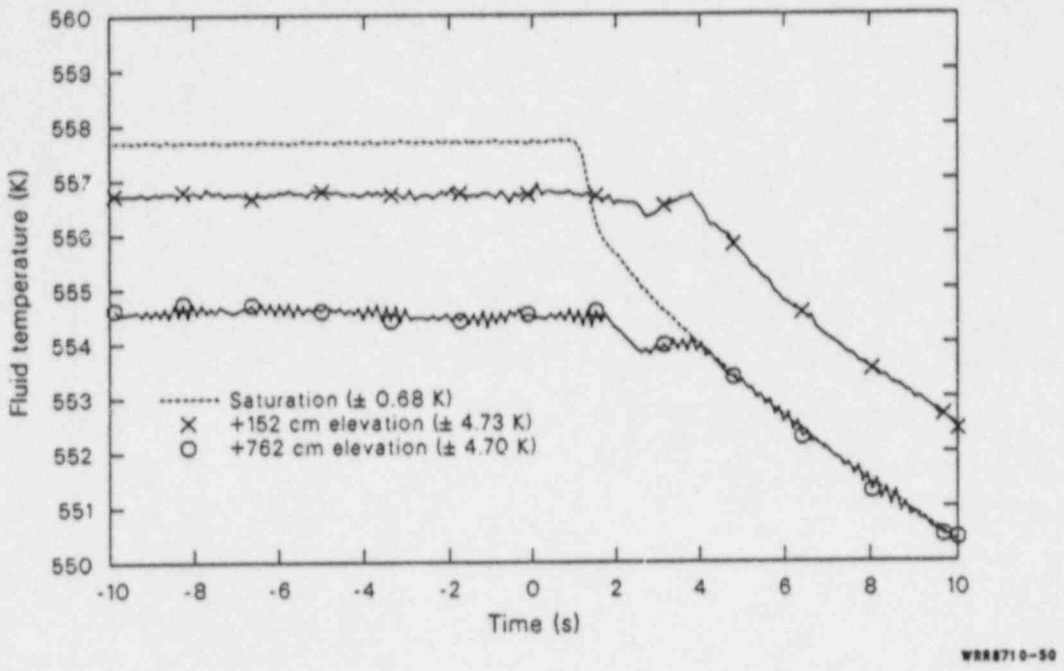

Figure 50. Unaffected loop steam generator downcomer fluid temperatures and saturation temperature during the blowdown phase of MSLB Test S-FS-2 (-10 to 10 s).

primary cooling was not sufficient to cause the pressurizer to empty. Consequently, primary depressurization was not as severe. In both cases, the cooldown and depressurization of the primary system moderated slightly following isolation of the unaffected loop steam generator due to MSIV closure at SI. However, the cooldown and depressurization continued until the primary coolant pumps coast to a stop about 52 s later (due to loss of offsite power at SI), with the minimum fluid temperature occurring in the loop cold legs.

The primary system response for the remainder of the blowdown phase of both transients is characterized by the SI flow slowly increasing the pressurizer liquid inventory and providing slight primary cooling, which aides the unaffected loop steam generator auxiliary feedwater in moderating the primary pressure and temperature. The major difference in the primary response occurred during this phase of the transient. Primary fluid system pressure and temperature increased slowly during Test S-FS-1, as the primary heated slightly and the pressurizer slowly refilled. However, during Test S-FS-2, primary fluid system pressure and temperature decreased slowly, as the primary cooled slightly and the pressurizer slowly refilled. The reason for this difference is the unaffected loop steam generator energy removal. No voiding of the primary fluid system was observed during the blowdown phase of either transient.

Primary Pressure Response Comparisons. The primary pressure responses exhibited similar basic trends for the initial phase of both tests. In both cases, the primary pressure responses are characterized by a number of inflection points associated with changes in the energy balance. As shown in Figure 51, the MSLB secondary LOCA produced a major effect on primary fluid system pressures. The primary energy balances were lost as the affected and unaffected loop steam generator primary-to-secondary heat transfer rapidly increased. The resulting increase in the primary fluid system heat sink created an energy imbalance which resulted in rapid depressurization of the primary fluid system for both break size and location cases. The depressurization of the primary fluid system continued until about 52 s after SI (i.e., about 52 s after the loss of offsite power) when the primary coolant pump impellers coasted to a stop.

The major difference between the two tests, which occurred during the initial phase of the transients, was the substantial increase in the depressurization rate during Test S-FS-1 which did not occur

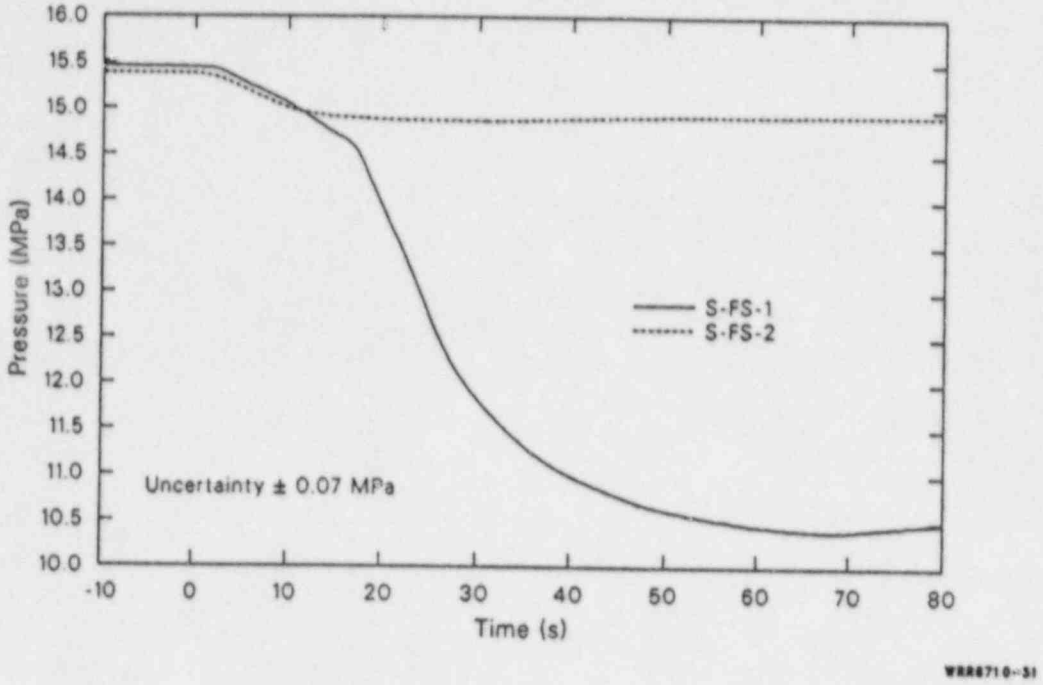

Figure 51. Comparisons of pressurizer pressures during the blowdown phases of MSLB Tests S-FS-1 and S-FS-2.

during Test S-FS-2. This was due to the pressurizer emptying during Test S-FS-1 but not during Test S-FS-2. As discussed previously, pressurizer liquid flashes and generates steam during rapid depressurization. The addition of steam mass to the pressurizer steam volume tends to moderate the rate of the steam specific volume increase which, in turn, moderates the rate of the pressurizer depressurization. When the pressurizer empties, the liquid inventory is depleted and flashing is halted. The steam volume remains essentially constant, while the steam mass decreases. Thus, the moderating effect of the vapor generation is lost; and the rate of increase for the steam-specific volume increases, which increases the rate of pressurizer depressurization. This causes the difference observed in the initial primary pressure responses for the two tests.

The pressure responses for the remainder of the transients were different due to the different primary fluid system energy balances for the two experiments. As was discussed earlier, the unaffected loop steam generator secondary mass following MSIV closure was substantially greater for the break upstream of the flow restrictor (Test S-FS-2), providing a substantially greater primary energy sink. Also, during Test S-FS-2, the primary system fluid remained at a much greater temperature following pump coastdown than occurred for Test S-FS-1. Thus, during Test S-FS-2, a substantially greater primary-to-secondary temperature gradient existed following pump coastdown, and a substantially greater primary heat sink was provided by the greater unaffected loop steam generator secondary mass. The primary energy removal via the unaffected loop steam generator secondary during Test S-FS-2 was sufficient to exceed the energy addition in the core and resulted in a gradual cooldown and depressurization of the primary fluid system. However, during Test S-FS-1, the primary-to-secondary temperature difference and the unaffected loop steam generator secondary mass inventory were not sufficient to produce a primary energy removal in excess of the core energy addition, and the primary fluid system gradually heated and pressurized.

Primary Hydraulic Response Comparisons. The primary hydraulic responses exhibited the same basic trends for both tests, but the quantitative results were significantly different. In both cases, the hydraulic response of the primary fluid system is characterized as a rapid shrinkage of fluid out of the pressurizer (Figure 52). The rate of the shrinkage was determined by the initial primary

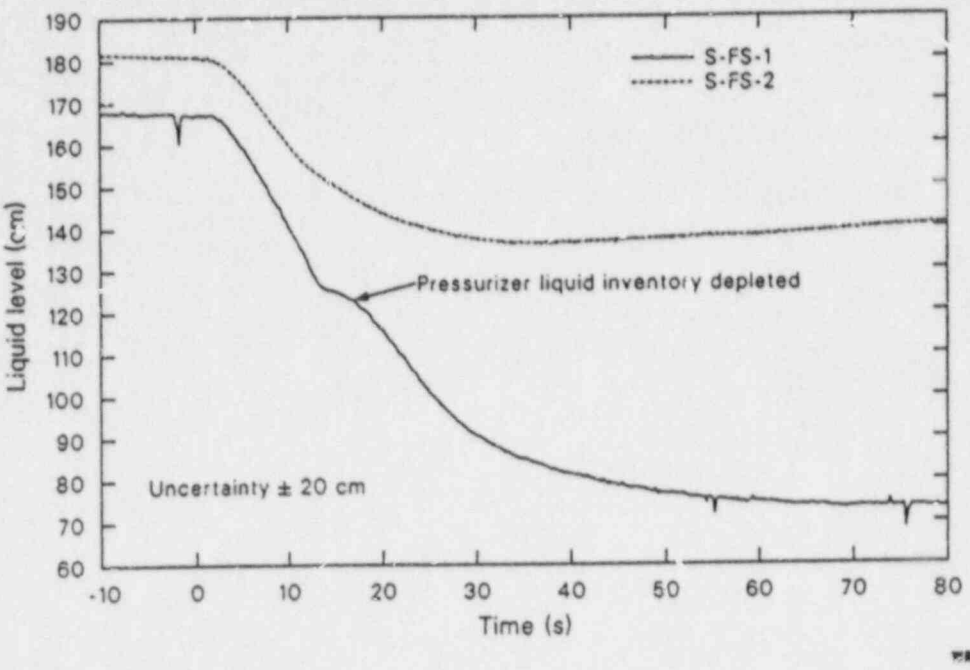

Figure 52. Comparisons of pressurizer overall collapsed liquid levels during the blowdown phases of MSLB Tests S-FS-1 and S-FS-2.

pressure and temperature, the initial pressurizer vapor volume, the energy balance, and the pressurizer surge line hydraulic resistance. All of these parameters were the same for both cases; however, the primary energy balance was significantly different for the two experiments. During Test S-FS-1, primary cooling was sufficient to shrink the primary fluid completely out of the pressurizer. However, during Test S-FS-2, primary cooling was not sufficient to shrink the primary fluid completely out of the pressurizer, causing the major difference observed in the pressurizer liquid level response. In both cases, the primary fluid shrinkage continued until the primary coolant pumps coasted to a stop about 52 s after loss of offsite power. During Test S-FS-1, the primary fluid then expanded due to primary energy addition, thus aiding the SI flow in refilling the pressurizer. During Test S-FS 2, the refilling of the pressurizer was due entirely to the mass added by SI flow, since the primary fluid system was cooling slightly and shrinking. For both tests, the above trends continued through the remainder of the blowdown phase.

Primary Thermal Response Comparisons. The primary thermal responses exhibited similar basic trends for the initial phase of both cases; however, the quantitative results were significantly different. As shown in Figure 53, primary cooling was significantly greater during Test S-FS-1 than during Test S-FS-2. In both cases, the rapid primary cooling continued until about 48 s after SI and MSIV closure, when the primary coolant pumps were tripped off and allowed to coast to a stop. The minimum downcomer fluid temperature (average cold leg fluid temperature) was significantly lower for Test S-FS-1 than for Test S-FS-2 (536 K versus 555 K), due to the substantially greater primary energy removal. Thus, for both cases, the minimum downcomer fluid temperature was well above the PTS limit of 450 K.

Similar to Test S-FS-1, primary cooling was limited somewhat during Test S-FS-2, due to the thicker U-tube walls in the Type III steam generator. However, the effect on the measured minimum average cold leg fluid temperature was also minimal for Test S-FS-2. During the initial primary cooldown for Test S-FS-2, the primary fluid average temperature (Figure 54) decreased from 560 to 556 K, while the primary fluid pressure decreased from 15.38 to 14.88 MPa. This represents a total primary fluid energy removal during the cooldown of about 3925 kJ for Test S-FS-2, as compared to 10570 kJ for Test S-FS-1. Had 0.124-cm thick

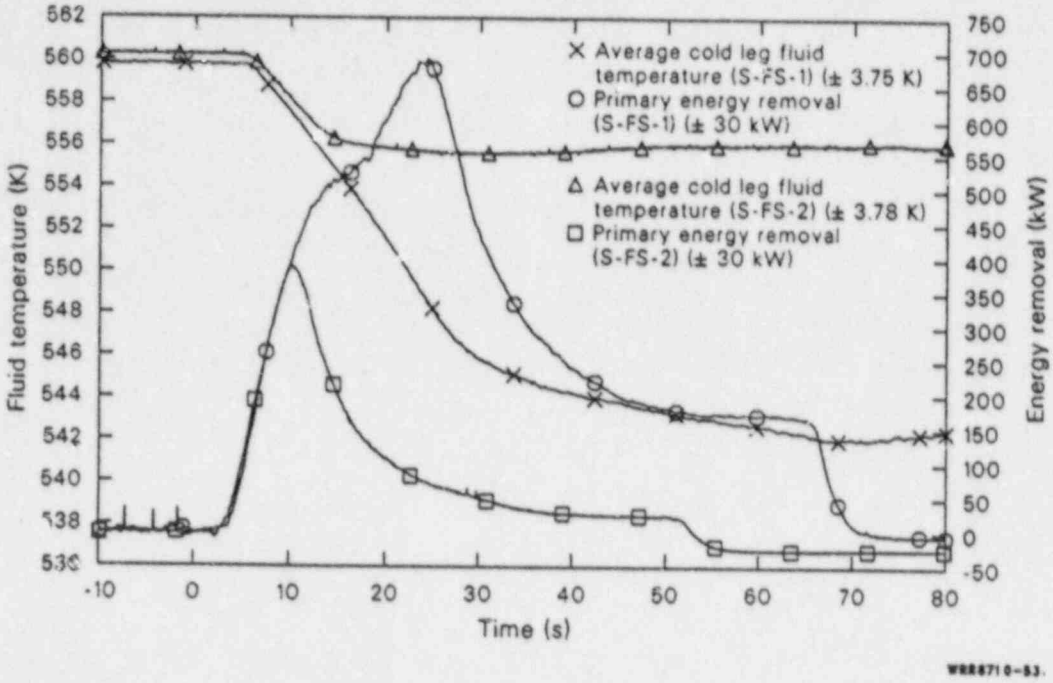

Figure 53. Comparisons of primary fluid system energy removal and average cold leg fluid temperatures during the blowdown phases of MSLB Tests S-FS-1 and S-FS-2.

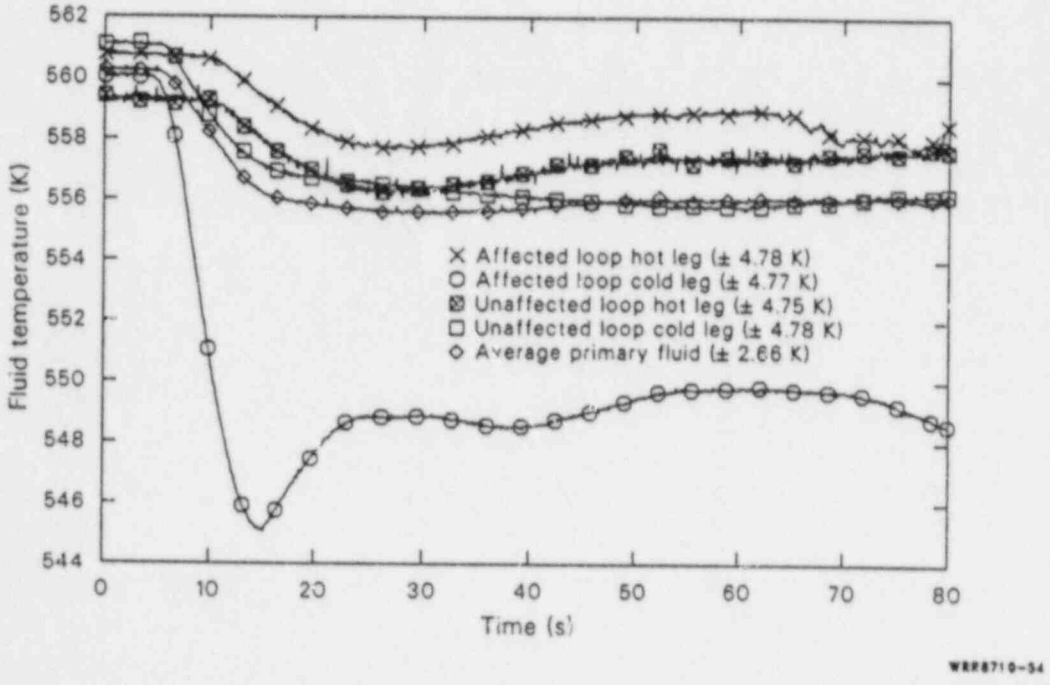

Figure 54. Affected and unaffected loop hot and cold leg and average primary fluid system temperatures during the blowdown phase of MSLB Test S-FS-2 (0 to 80 s).

U-tube walls been used for the Type III steam generator, the net primary energy removal for Test S-FS-2 would have been about 20% greater, resulting in a primary fluid energy removal of about 4430 kJ, as compared to 11490 kJ for Test S-FS-1. This would have decreased the primary fluid average temperature to about 552 K for Test S-FS-2, as compared to about 540 K for Test S-FS-1. Correspondingly, the minimum average cold leg temperature would have been about 554 K for Test S-FS-2, as compared to 534 K for Test S-FS-1. Both are still well above the PTS temperature limit. Thus, while the thicker U-tube walls in the Type III steam generator limited the primary cooling somewhat (about 14% for Test S-FS-2 and 9% for Test S-FS-1), the effect on the measured minimum downcomer fluid temperature was minimal.

The primary fluid system thermal response moderated following MSIV closure and loop flow reductions in both cases. However, a major difference was noted in the primary thermal response following primary coolant pump coastdown. During Test S-FS-1, the primary fluid system exhibited a gradual heating trend following pump coastdown; while during Test S-FS-2, the primary fluid system exhibited a gradual cooling trend following pump coastdown. This was due to greater primary energy removal via the unaffected loop steam generator for Test S-FS-2. The greater primary energy removal was due to a larger primary-to-secondary temperature difference and a greater unaffected loop steam generator secondary mass for Test S-FS-2 (Figure 55), the combined effect of which was a greater primary energy removal. The different trends were maintained throughout the remainder of the blowdown phases of the transients.

System Response to Plant Stabilization Operations

The system stabilization phase of Tests S-FS-1 and S-FS-2 was performed, for the most part, in accordance with the guidance provided in EOPs for recovery from a secondary transient for Zion Unit No. 1 (a Westinghouse four-loop plant).[11,a] The system stabilization for the tests involved SI termination, pressurizer internal heater operation, normal charging and letdown operation, and an unaffected loop steam generator steam and feed operation. The criteria for system stability were: (a) maintaining pressurizer liquid level[a] at 185 ± 10 cm, with a variance of ≤20 cm in 600 s; (b) maintaining pressurizer pressure within a variance of ≤0.276 MPa in 600 s; (c) maintaining average primary fluid temperature at ≤558 K, with a variance of ≤7 K in 600 s; (d) maintaining the unaffected loop steam generator liquid level (see footnote a) between 910 and 1010 cm; and, (e) maintaining the unaffected loop hot leg subcooled margin at ≥27.8 K.

Examination of the Semiscale Mod-2C system response to the plant stabilization operations provides invaluable insight into both the effectiveness of the EOP-specified operations in stabilizing the plant and the characteristic system response to the stabilization operations. The characteristic response to the stabilization operations was very similar for both tests; therefore, the detailed discussion of the characteristic system response to the stabilization operations will be limited to Test S-FS-1 results. Overall system response for Test S-FS-1 will be discussed first, followed by discussions of the system response to normal charging/letdown operations, pressurizer internal heater operations, and unaffected loop steam generator steam and feed operations. A brief comparison of the results for Test S-FS-2 will be made at the end of this section.

Overall System Response to Stabilization Operations. Stabilization operations were specified to be initiated at the end of the blowdown phase of the test when operator identification of the transient and operator intervention would be expected to occur. For Test S-FS-1, stabilization operations were initiated at 600 s, since MSIV closure had already occurred. At 600 s, the system was in a condition requiring no operator actions. SI continued to operate until 3900 s, when pressurizer pressure (Figure 56) reached 13.88 MPa and SI flow was terminated. At that time, the pressurizer liquid level (Figure 57) was approximately 600 cm, the unaffected loop steam generator liquid level (Figure 58) was about 980 cm, the subcooled margin (Figure 56) was 35 K, and the average primary fluid temperature (Figure 59) was 553 K.

The limiting criterion in achieving stable conditions was the reduction of the pressurizer liquid level. To reach the specified stable conditions, it

a. Zion Unit Number 1 Nuclear Plant, "Emergency Operating Procedures," Commonwealth Edison Company.

a. Collapsed liquid level is referenced to the zero reference.

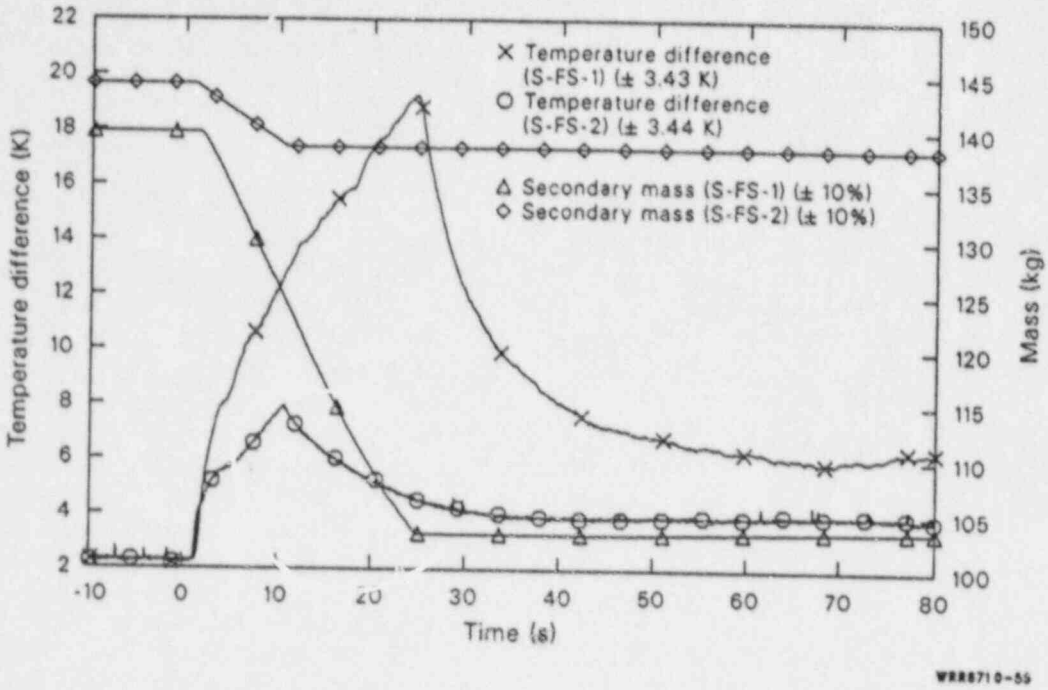

Figure 55. Comparisons of primary-to-secondary temperature differences and unaffected loop steam generator secondary masses during the blowdown phases of MSLB Tests S-FS-1 and S-FS-2

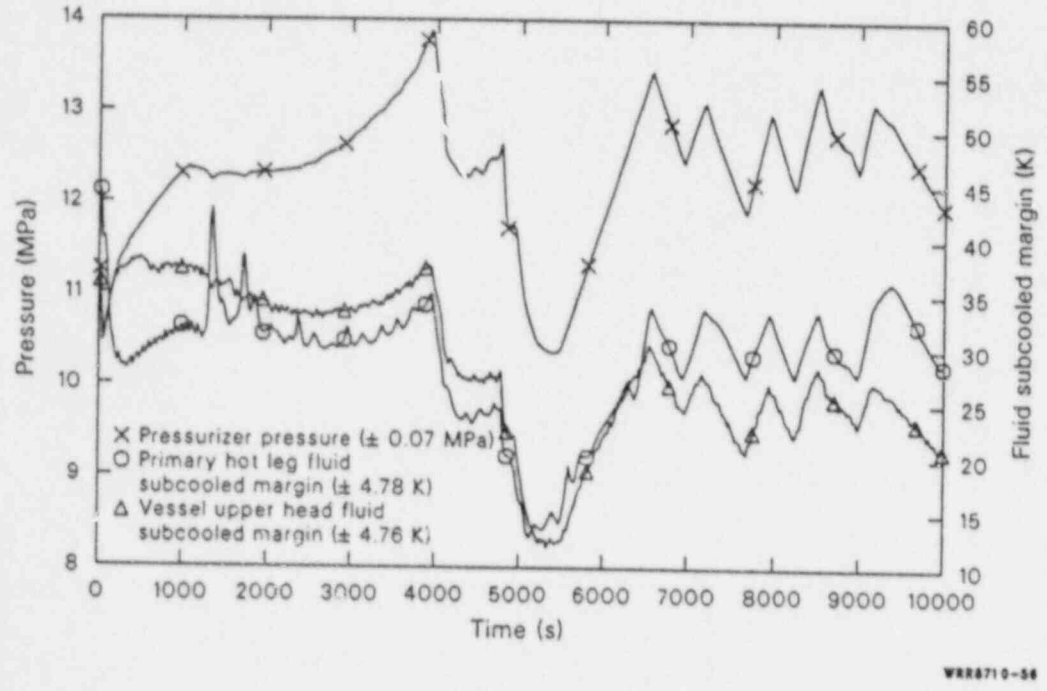

Figure 56. Pressurizer pressure, primary hot leg and vessel upper head fluid subcooled margins, and pressurizer internal heater power during the stabilization phase of MSLB Test S-FS-1 (600 to 9,900 s).

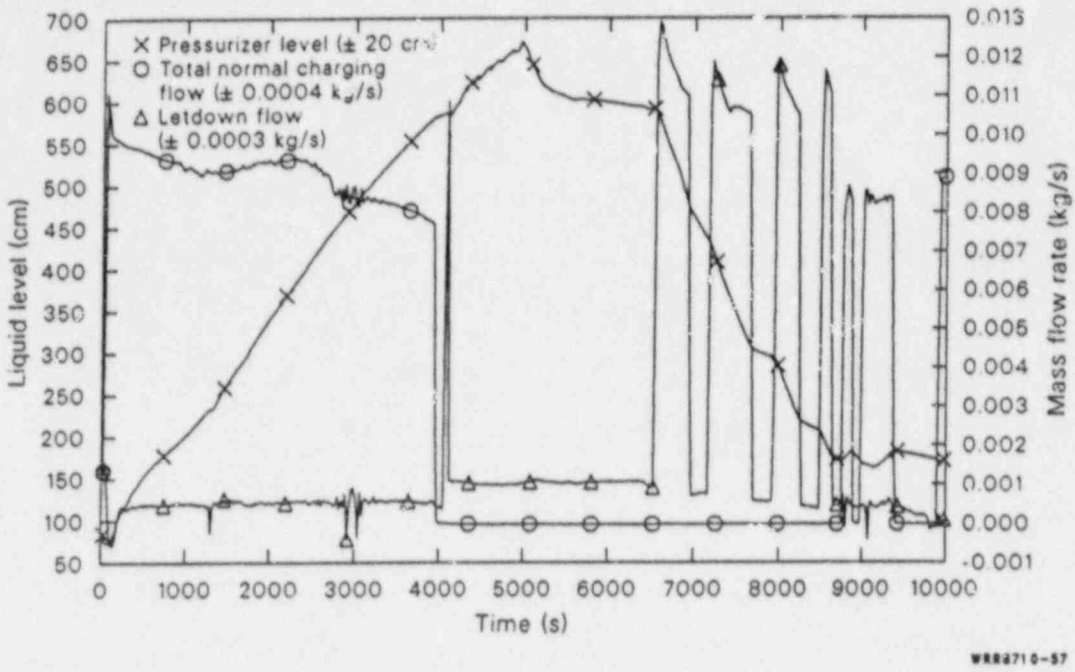

Figure 57. Pressurizer collapsed liquid level and total normal charging and letdown mass flow rates during the stabilization phase of MSLB Test S-FS-1 (600 to 9,900 s).

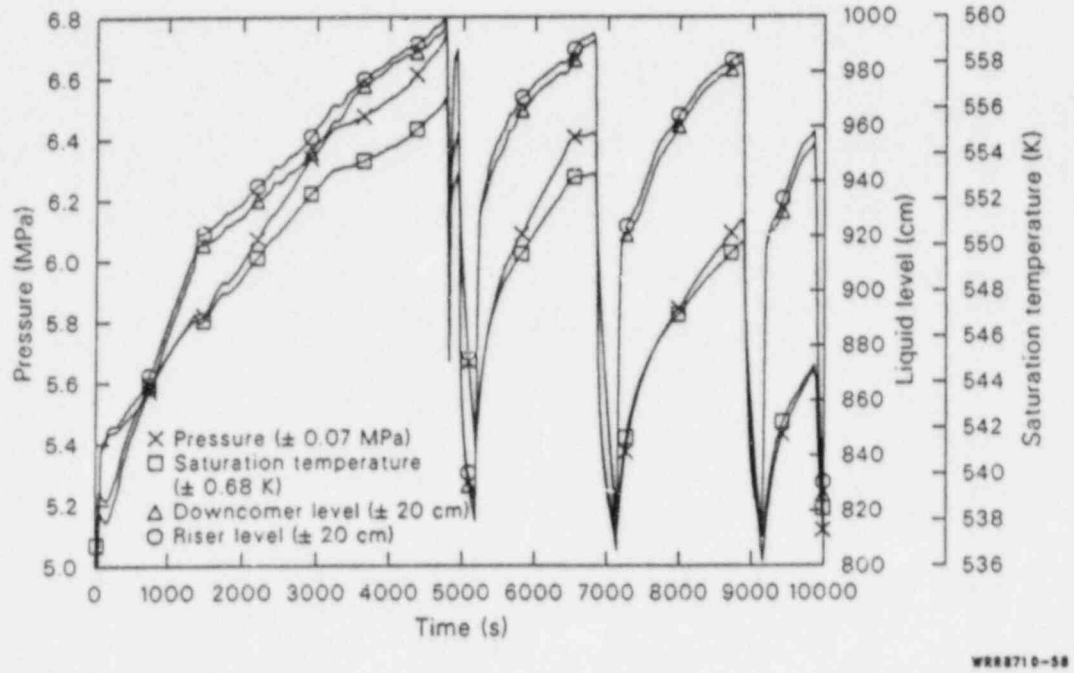

Figure 58. Unaffected loop steam generator secondary pressure, saturation temperature, and downcomer and riser overall collapsed liquid levels during the stabilization phase of MSLB Test S-FS-1 (600 to 9,900 s).

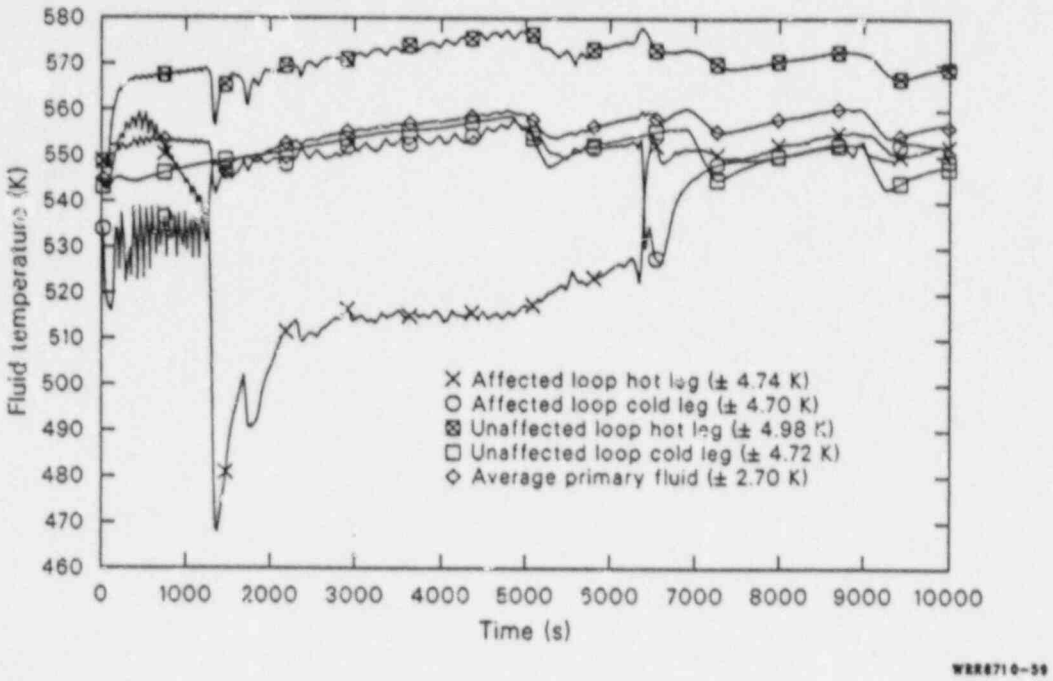

Figure 59. Affected and unaffected loop hot and cold leg and average primary fluid system temperetures during the stabilization phase of MSLB Test S-FS-1 (600 to 9,900 s).

was necessary to maintain the above conditions in the specified tolerances while the pressurizer liquid level was reduced by letdown flow (Figure 57). During the course of the pressurizer level reduction, the expanding vapor volume lowered primary pressure, reducing the primary fluid subcooled margin to the lower limit of 27.8 K. Letdown was then halted, and the pressurizer internal heaters were energized at 6.99 kW (Figure 56) to recover the primary subcooled margin. The effect of the pressurizer internal heater operation was not evident in the pressurizer pressure response until about 1500 s after energizing the heaters. This was due to the high degree of subcooling present in the pressurizer liquid prior to energizing the internal heaters. Prior to the letdown operation, the pressurizer had been filling slowly with subcooled liquid for approximately 3900 s and experiencing heat loss. This caused the pressurizer fluid to become very stratified with saturated steam and liquid at the top of the pressurizer and subcooled liquid at lower elevations (Figure 60).

Thus, operation of the pressurizer internal heater for 1500 s was required to remove the subcooling from the liquid in the pressurizer and initiate the steam mass addition to the steam volume necessary to increase the primary pressure and subcooled margin. During this period, the average primary fluid temperature increased due to the continuous 1.5% core power. The unaffected loop steam generator atmospheric dump valve (ADV) was opened, reducing the secondary pressure and saturation temperature. After a delay of approximately 70 s, due to loop transit times, the effects of the ADV operation were evident in the average primary fluid temperature response. The ADV remained open until the average primary fluid temperature returned to the specified band. Since the ADV flow was substantially greater than the auxiliary feedwater flow (Figure 61), the unaffected loop steam generator secondary liquid level decreased during the period of ADV operation. Substantial frictional flow effects are evident in the secondary level response during the period of ADV operation; however, the liquid level remained well above that required for initiating a natural circulation cooldown.

The final portions of the stabilization phase consisted of alternating cycles of letdown and pressurizer heater operation. Letdown operation reduced the pressurizer liquid level and lowered the primary subcooled margin to the lower limit. Letdown was then terminated, and the pressurizer internal heaters were energized to recover the primary subcooled

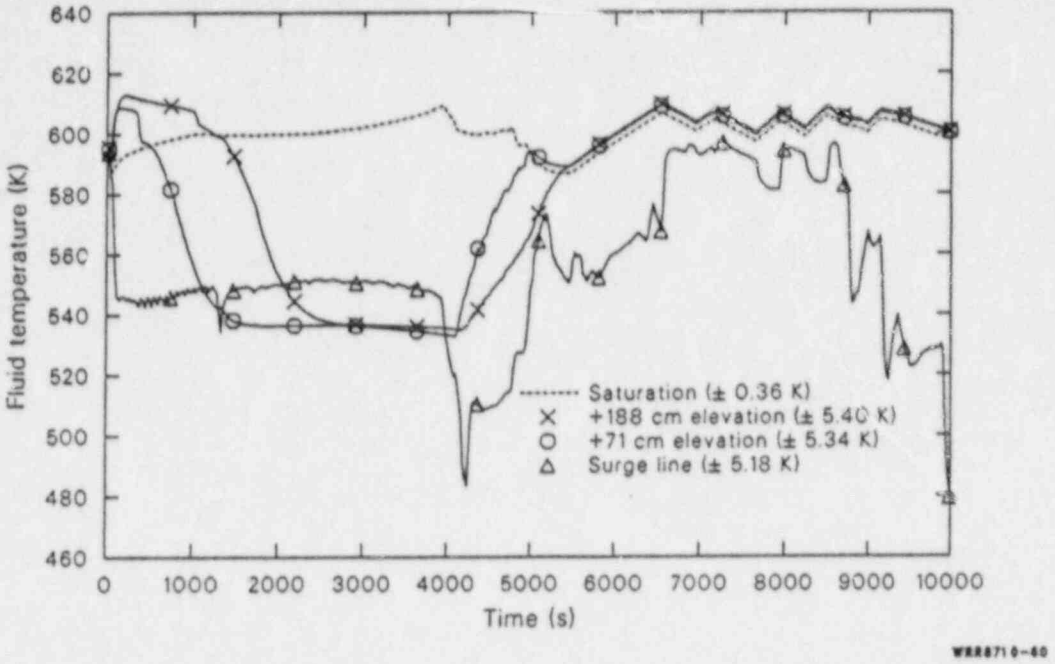

Figure 60. Pressurizer upper and lower elevation, pressurizer surge line, and saturation temperatures during the stabilization phase of MSLB Test S-FS-1 (600 to 9,900 s).

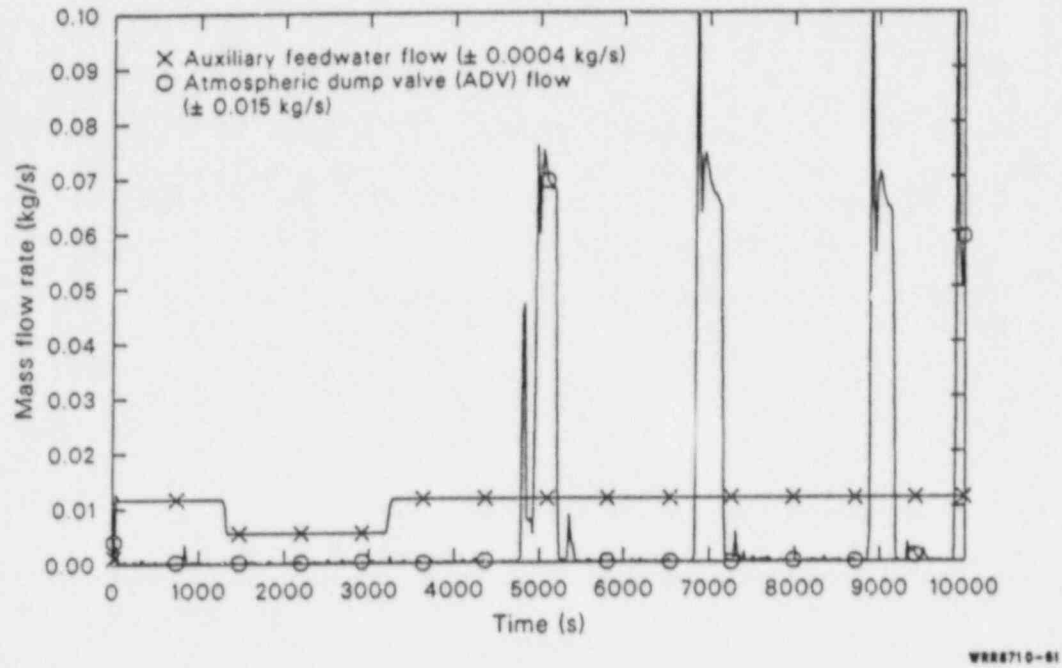

Figure 61. Unaffected loop steam generator auxiliary feedwater and atmospheric dump valve (ADV) mass flow rates during the stabilization phase of MSLB Test S-FS-1 (600 to 9,900 s).

margin to the specified range. This cycle was repeated five times until the required plant stabilization conditions were met. The system parameters were within the specified system stabilization tolerances for at least 600 s, and the system was considered to be stabilized at 9900 s.

The automatic actions performed by the plant protective systems during the blowdown phase of the test left the Semiscale Mod-2C system in a quasi-stable state but at conditions which did not ensure sufficient control of the system. The stabilization operations performed were very effective in stabilizing the Semiscale Mod-2C system at conditions which did ensure sufficient control of the system. The guidance provided by the EOPs was both appropriate and effective in stabilizing and regaining control of the system. No upper head voiding occurred, as the upper head fluid remained subcooled (Figure 56); the limiting criterion in regaining control of the system was the reduction of the pressurizer liquid level following SI termination. While the pressurizer liquid level was near the top of the pressurizer when the SI termination pressure (13.88 MPa) was reached, the pressurizer did not completely fill before SI termination. Thus, the system did not become liquid solid and did not experience the associated rapid pressurization prior to SI termination.

The effectiveness of the stabilization operations in stabilizing the plant may be better understood by considering the system response to the various operations performed. The next subsections discuss system response to the normal charging/letdown operations, pressurizer internal heater operations, and unaffected loop steam generator secondary steam and feed operations.

System Response to Normal Charging/Letdown Operation During Stabilization. Normal charging/letdown was used during the stabilization phase to establish and maintain the pressurizer collapsed liquid level within the specified tolerance. Letdown was initially used to reduce the pressurizer level from a nearly full condition (585 cm) to 185 ± 10 cm. Letdown flow was approximately 0.013 kg/s and effectively reduced the pressurizer level. The primary energy removal due to the removal of fluid via the letdown line was minimal and had no measurable effect on the average primary fluid temperature. The most significant effect of the letdown operation on system response was primary pressure reduction. Removal of liquid from the pressurizer increased the steam volume, which increased the saturated steam specific volume, thereby decreasing the saturation pressure. The reduction in primary pressure caused a reduction of the primary loop hot leg subcooled margin. It was therefore necessary to halt the pressurizer level reduction and operate the pressurizer internal heaters several times during the pressurizer liquid level reduction before the level was reduced to the specified value. Thus, care must be taken in reducing the pressurizer level to avoid saturating the primary system and inadvertently voiding the vessel upper head.

Normal charging flow (Figure 57) was approximately 0.009 kg/s at the stabilization pressure of 11.0 MPa. The flow was adequate to make up for primary fluid shrinkage and leakage, thereby maintaining control of the pressurizer liquid inventory. The primary fluid cooling (due to the addition of cold charging water) did not have a significant effect on the loop temperatures.

System Response to Pressurizer Internal Heater Operation During Stabilization. Pressurizer internal heaters were used to maintain the primary system subcooled margin by maintaining primary pressure control in the pressurizer. Initially, the pressurizer internal heater operation had no effect on the primary fluid system pressure. When the pressurizer internal heaters were first energized at 4100 s, significant stratification existed in the pressurizer, as shown in Figure 60. The lower portion of the pressurizer contained liquid at about 536 K, while the upper portion contained saturated steam at about 600 K. As a result, a long period of pressurizer internal heater operation (1500 s) at 6.99 kW was required to remove the subcooling from the liquid in the lower portions of the pressurizer. Once the subcooling was removed from the pressurizer liquid, steam mass addition to the steam space was initiated by vapor generation. From that point on, the pressurizer internal heaters were very effective in controlling primary pressure. An average of 225 s was required to raise the subcooled margin from 27.8 K to 33.3 K. Each subsequent cycle of pressurizer internal heater operation required increasingly more time to raise the subcooled margin from 27.8 to 33.3 K. This was due to the pressurizer liquid level being lower for each heater operation. The lower liquid level produced greater steam space. Therefore, more steam mass had to be added to the steam volume at each cycle in order to recover the saturated steam specific volume sufficiently to raise the saturation pressure and temperature to that necessary for the 33.3 K primary subcooled margin condition. Overall, the

pressurizer internal heaters were very effective in maintaining control of the primary fluid system pressure and subcooled margin.

System Response to Unaffected Loop Steam Generator Steam and Feed Operation During Stabilization. The unaffected loop steam generator steam and feed operation was used to maintain the primary system average fluid temperature within the specified tolerances. The unaffected loop steam generator auxiliary feedwater operated throughout the stabilization phase at a flow rate of 0.012 kg/s. The auxiliary feedwater flow provided cooling for the primary fluid system and provided mass to replace mass lost from the secondary during ADV operations. The unaffected loop steam generator ADV was cycled three times during the stabilization phase to maintain the average primary fluid temperature between 556 and 560 K. During each ADV operation, the secondary liquid level was reduced (Figure 58) due to the ADV flow greatly exceeding the auxiliary feedwater flow (Figure 61). The unaffected loop steam generator ADV operation was very effective in reducing the primary fluid average temperature (Figure 59). The loss of steam from the secondary via the ADV reduced the secondary saturation pressure and temperature (Figure 58), thereby increasing the primary to secondary temperature difference. This increased the unaffected loop natural circulation flow (Figure 62) and heat transfer, greatly enhancing the primary-to-secondary heat transfer.

Comparison of Stabilization Phase Responses. The system stabilization phase of Tests S-FS-1 and S-FS-2 involved the same recovery operations and stabilization criteria. The basic response of the system to the stabilization operations was the same for both tests, with differences primarily due to the difference in the system conditions following the blowdown phase of the tests. Figures containing the pertinent parameters (the same parameters as those presented for Test S-FS-1) for Test S-FS-2 may be found in Appendix B (Figures B-15 through B-21).

The initiation of stabilization operations was to begin at the end of the blowdown phase of the test when operator identification of the transient and operator intervention would be expected to occur. For both tests, the stabilization phase was initiated at 600 s. The first operation performed in both tests was SI termination; however, the timing of this operation was quite different. In Test S-FS-2, the primary pressure remained above 13.88 MPa, so that SI termination was allowed at 600 s. During Test S-FS-1, SI termination was delayed until 3900 s, due to the primary pressure being below 13.88 MPa. Earlier termination of SI flow during Test S-FS-2 left the pressurizer liquid level below the specified upper value for stable operations, precluding the need for letdown flow. Thus, the cycles of letdown operation, followed by pressurizer internal heater operation, which were necessary during Test S-FS-1 were not necessary during Test S-FS-2. In both tests, following SI termination, it was necessary to initiate an unaffected loop steam generator steam and feed operation to reduce the average primary fluid temperature to within the specified stable operation range. The unaffected loop steam generator ADV was cycled once (from 735 to 1135 s) during Test S-FS-2, whereas during Test S-FS-1 it was necessary to cycle the ADV three times (from 4,790 to 5,230 s; 6,825 to 7,190 s; and, 8,880 to 9,190 s). In both tests, the effects of the ADV operations were evident in the unaffected loop steam generator secondary pressure and liquid level responses and (after a delay of about 70 s due to the loop transit time) the average primary fluid temperature response. The primary cooling provided by the ADV operations was also evident in the pressurizer liquid level response for both tests. During Test S-FS-1, the primary fluid shrinkage aided the letdown flow in reducing the pressurizer liquid inventory. During Test S-FS-2, despite normal charging operation, the pressurizer fluid inventory decreased due to primary fluid shrinkage. The gradual decrease in pressurizer level continued during Test S-FS-2 until the unaffected loop steam generator ADV was closed, leaving the pressurizer level at about 145 cm. The pressurizer level then began to increase due to the normal charging flow.

The limiting criterion in achieving stable conditions for both tests was the recovery of the pressurizer liquid level. However during Test S-FS-1, the limiting criterion was the *reduction* of the pressurizer level; whereas during Test S-FS-2, it was the *increase* of the pressurizer level. During Test S-FS-2, the primary hot leg fluid subcooled margin remained above 27.8 K, so that operation of the pressurizer internal heaters was not necessary. During Test S-FS-1, the pressurizer internal heaters were cycled several times during the pressurizer liquid level reduction operations. The stabilization criteria were satisfied and the system stabilization phase was considered to be completed 600 s after the pressurizer liquid level was recovered to the specified range for both tests (9,900 s for

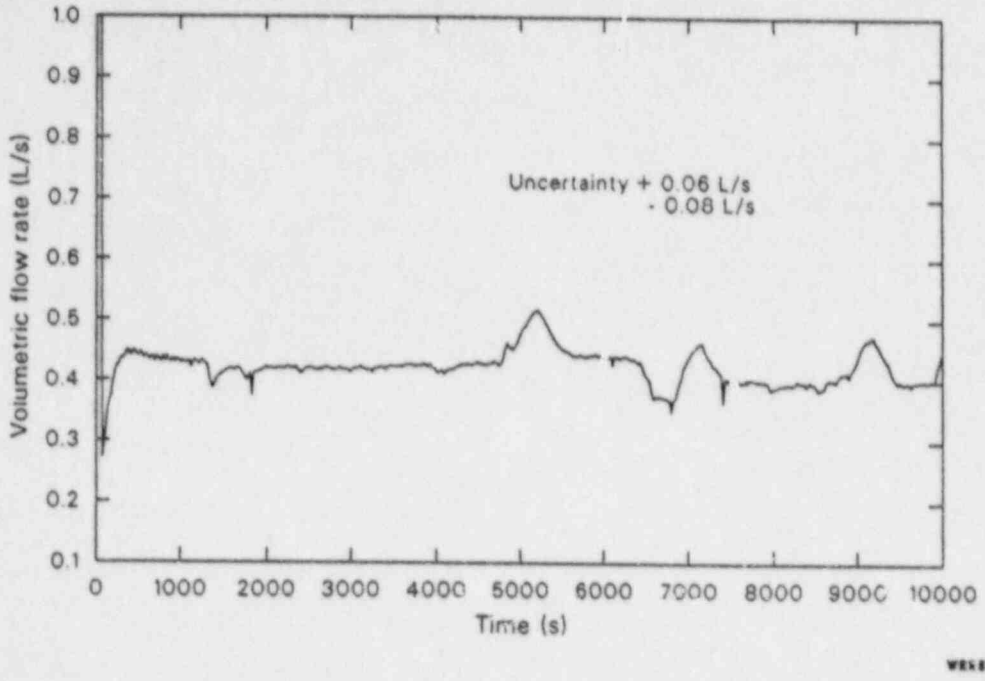

WRK8710-82

Figure 62. Unaffected loop hot leg volumetric flow rate during the stabilization phase of MSLB Test S-FS-1 (600 to 9,900 s).

Test S-FS-1 and 2,150 s for Test S-FS-2). Test S-FS-2 was then terminated at 2,220 s.

The system response to the normal charging and unaffected loop steam generator steam and feed operations was similar for both tests, with the main differences occurring in the timing of events. No upper head voiding occurred during the stabilization phase of either experiment, and the primary and secondary systems remained under operator control. For both tests, the automatic actions performed by the plant protective systems left the system in a quasi-stable condition. The EOP-specified recovery operations were very effective in stabilizing the Semiscale Mod-2C system, and no unexplainable or unsatisfactory conditions were encountered during either experiment.

System Response to Plant Cooldown and Depressurization Operations (Test S-FS-1)

The objective of the cooldown and depressurization phase was to reduce the average primary fluid temperature to 500 K while maintaining the pressurizer liquid level at 185 ± 10 cm, the primary hot leg fluid subcooled margin between 27.8 and 33.3 K, and the unaffected loop steam generator downcomer collapsed liquid level ≥ 600 cm. This was accomplished using combined operations of pressurizer internal heaters, normal charging/letdown, pressurizer auxiliary spray, and unaffected loop steam generator steam and feed operation.

The cooldown and depressurization were also performed in accordance with the guidance provided in EOPs for a natural circulation cooldown for Zion Unit No. 1 (a Westinghouse four-loop PWR plant).[11,a] Minor deviations from the EOP guidelines consisted of: adjustments to the unaffected loop steam generator auxiliary feedwater flow; an inadvertent vessel upper head void formation; and, a pressurizer auxiliary spray operation performed at the end of the cooldown. The adjustments to the auxiliary feedwater mass flow rate were undertaken in light of the limited test time. The vessel upper head void formation was due to heat loss makeup via external heaters in excess of the actual heat loss for the vessel upper head. The pressurizer auxiliary spray operation was undertaken to provide data to assess the effectiveness of pressurizer auxiliary spray in controlling primary

a. Zion Unit Number 1 Nuclear Plant, "Emergency Operating Procedures," Commonwealth Edison Company.

pressure. The overall response to the cooldown and depressurization operations will be discussed first, followed by discussions of the effects of unaffected loop steam generator steam and feed operations and combined pressurizer auxiliary spray and internal heater operations on the system response.

Overall System Response to Plant Cooldown and Depressurization Operations. System stabilization criteria were met and cooldown operations were begun 9,900 s after transient initiation. Normal charging was cycled on and off throughout this period to make up for the slight primary leakage and maintain the pressurizer collapsed liquid level at 185 ± 10 cm (Figure 63). At 10,600 s, the controlled unaffected loop steam generator secondary depressurization was initiated by opening the ADV. Figure 64 shows the secondary pressure and illustrates the stairstep secondary depressurization at the specified rate of 0.71 MPa per decrement. The secondary pressure was maintained at the lower pressure for at least 600 s after each stairstep.

The unaffected loop steam generator secondary depressurization resulted in a primary system cooldown and gradual depressurization, as shown in Figures 65 and 66. The primary system cooled down initially at a rate of approximately 26 K/h. The rapid pressure increases shown in Figure 66 are the result of pressurizer internal heater operation to maintain the primary hot leg subcooled margin within the specified band. Throughout the early cooldown period, the unaffected loop steam generator secondary liquid level continued to decrease as ADV flow exceeded auxiliary feedwater flow (Figure 67). At 12,000 s, the unaffected loop steam generator secondary liquid level decreased to below 600 cm, the lowest allowable level for ADV operation. The primary cooldown had to be temporarily halted by closing the unaffected loop steam generator ADV while auxiliary feedwater slowly reestablished the liquid level. To ensure completion of the test before data acquisition time was expended, it was deemed necessary to increase the auxiliary feedwater flow. The auxiliary feedwater flow was therefore increased to 0.0173 kg/s, the scaled[2,3] maximum flow from a single auxiliary feedwater pump. This flow was adequate to maintain the unaffected loop steam generator secondary pressure at the current value, but was not adequate to maintain the secondary liquid level during a subsequent depressurization. The auxiliary feedwater flow was therefore increased again to the Semiscale maximum capacity of 0.030 kg/s, which was close to the scaled maximum flow for the two

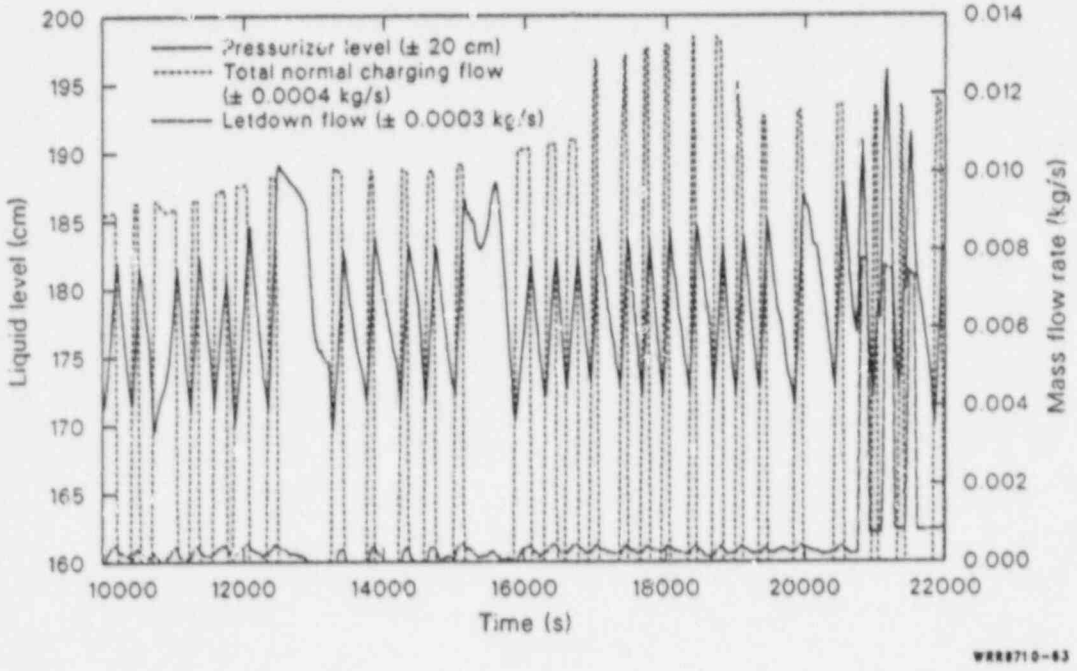

Figure 63. Pressurizer overall collapsed liquid level, total normal charging, and letdown mass flow rates during the plant cooldown and depressurization phase of MSLB Test S-FS-1 (10,000 to 22,000 s).

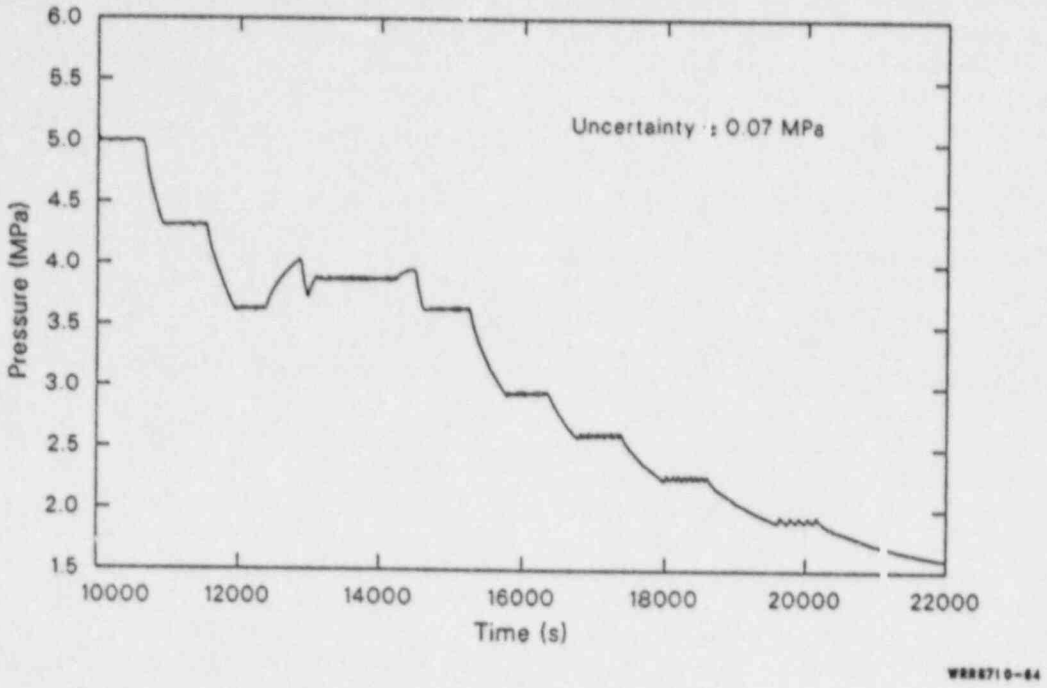

Figure 64. Unaffected loop steam generator secondary pressure during the plant cooldown and depressurization phase of MSLB Test S-FS-1 (10,000 to 22,000 s).

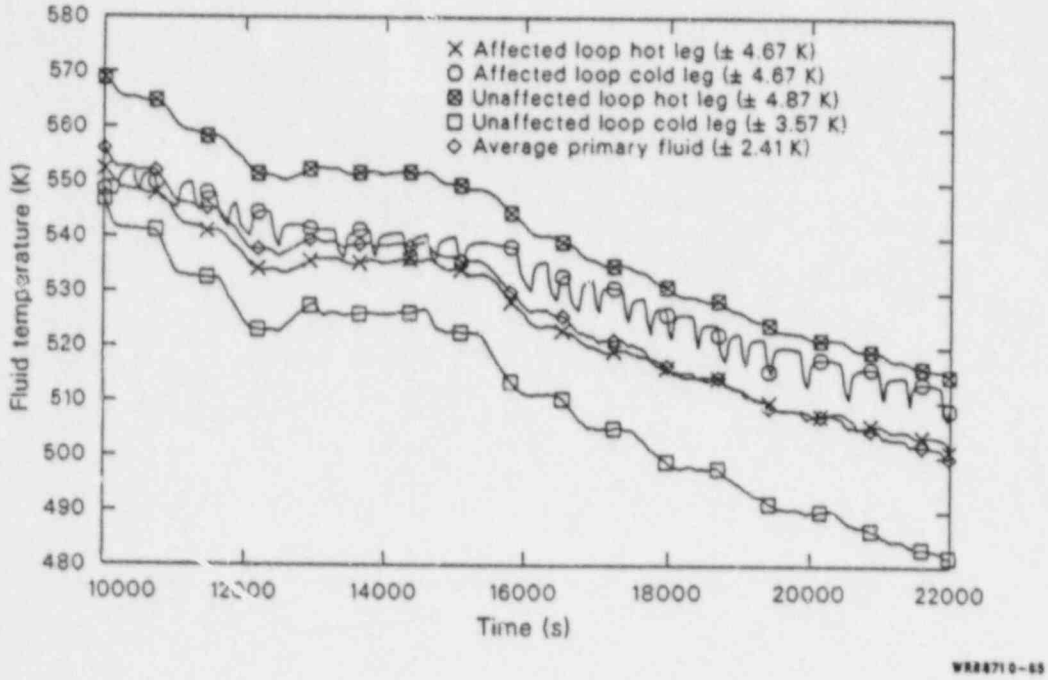

Figure 65. Affected and unaffected loop hot and cold leg and average primary fluid temperatures during the plant cooldown and depressurization phase of MSLB Test S-FS-1 (10,000 to 22,000 s).

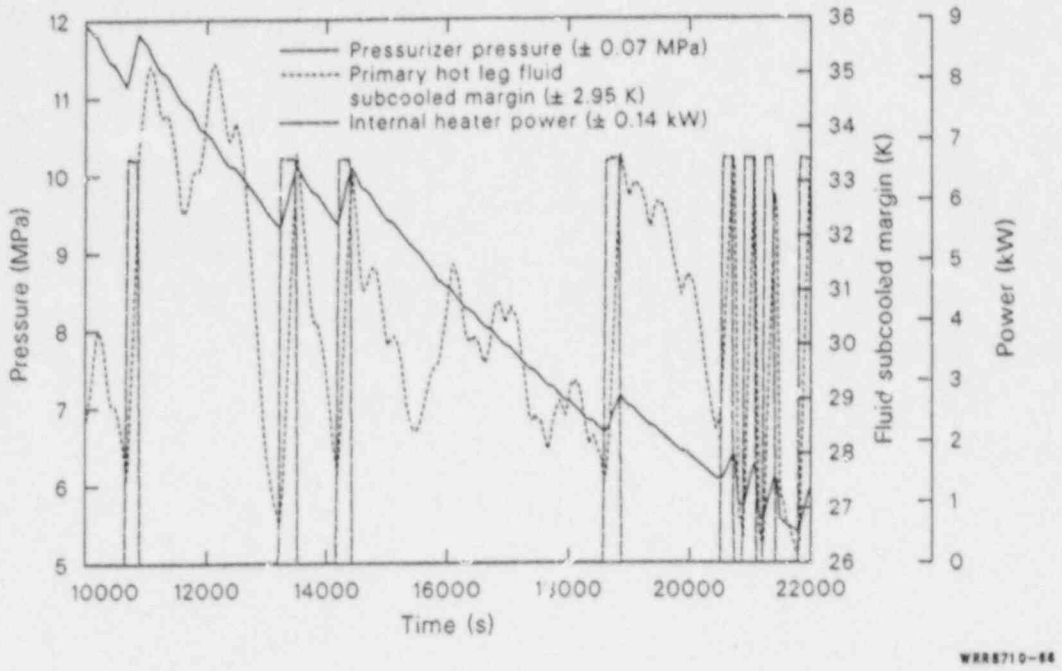

Figure 66. Pressurizer pressure, primary hot leg fluid subcooled margin, and pressurizer internal heater power during the plant cooldown and depressurization phase of MSLB Test S-FS-1 (10,000 to 22,000 s).

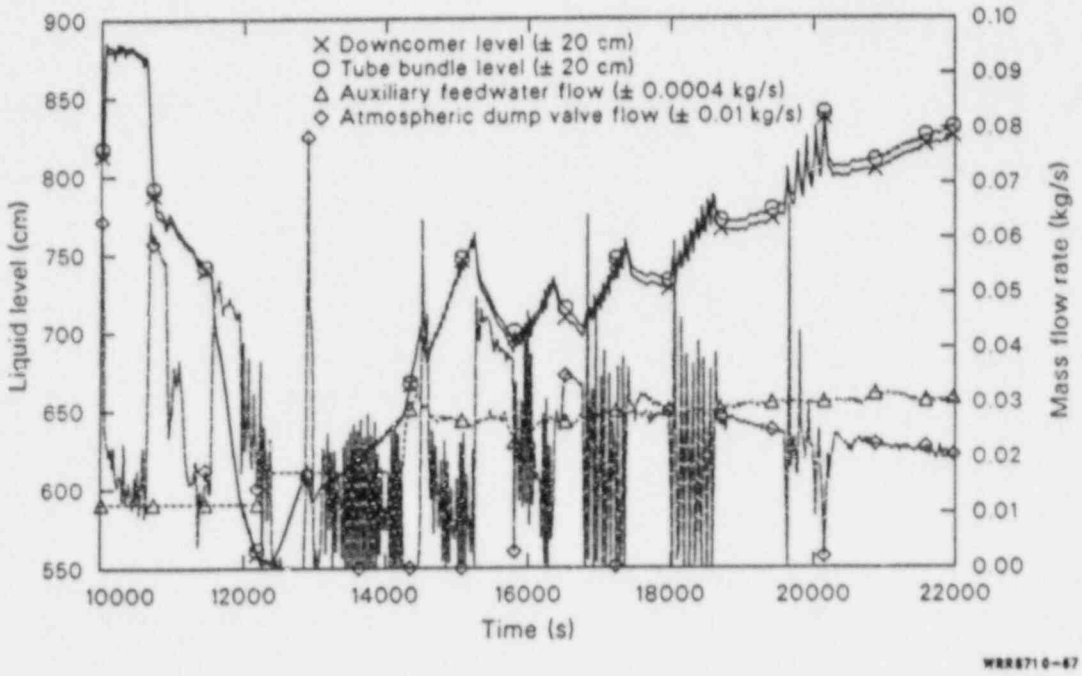

Figure 67. Unaffected loop steam generator downcomer and tube bundle overall collapsed liquid levels and auxiliary feedwater and ADV mass flow rates during the plant cooldown and depressurization phase of MSLB Test S-FS-1 (10,000 to 22,000 s).

diesel-driven auxiliary feedwater pumps of a full scale PWR.[2,3] The increased auxiliary feedwater flow was sufficient to reestablish the unaffected loop steam generator secondary liquid level at 700 cm, and the unaffected loop steam generator secondary pressure was stabilized at the pressure achieved before the primary cooldown was suspended (approximately 3.6 MPa). The primary system cooldown was then resumed at 15,400 s. The unaffected loop steam generator secondary pressure stairstep reductions (Figure 64) continued at 0.71 MPa per decrement until the secondary pressure reached 3.07 MPa. The decrement was then changed to 0.34 MPa for each subsequent secondary stairstep pressure reduction. The auxiliary feedwater flow at the maximum flow rate was adequate to maintain the unaffected loop steam generator secondary mass inventory, providing adequate secondary level control.

Concurrent with the resumption of primary system cooldown at 15,400 s, a steam bubble was produced in the vessel upper head (vessel upper head void), as shown in Figure 68. This was a result of the primary pressure reduction reducing the upper head fluid saturation temperature, while the upper head fluid and metal temperatures were not decreasing. The vessel upper head external heater power exceeded the environmental heat loss for the upper head. This, combined with the reduced flow through the vessel upper head, caused the upper head fluid temperature to be maintained at 577 K (Figure 69). As the primary pressure decreased, the saturation temperature decreased to the vessel upper head fluid temperature, the upper head fluid saturated, and a void formed in the upper head. To correct for this atypical vessel upper head void formation, the power to the vessel upper head external heater bank was terminated at 15,540 s. The vessel upper head void began to collapse, and the upper head level immediately began to recover. The unaffected loop steam generator secondary stairstep pressure reduction continued throughout the period, cooling and depressurizing the primary and secondary systems.

The pressurizer auxiliary spray was cycled when the average primary fluid temperature reached 505 K to assess its effect on primary system pressure. The auxiliary spray was cycled three times between 20,000 and 22,000 s. Each cycle produced a substantial reduction in the primary pressure, as shown in Figure 70. Pressurizer internal heaters were alternately used to maintain the primary hot leg fluid subcooled margin (Figure 70). The combined operation of pressurizer auxiliary spray and internal heaters demonstrated effective control of the primary system pressure and subcooled margin.

Effects of Unaffected Loop Steam Generator Steam and Feed Operation on Plant Cooldown and Depressurization. The unaffected loop steam generator steam and feed operation consisted of steaming through the ADV and feeding with auxiliary feedwater. The intention of the stairstep secondary pressure reduction was to reduce the secondary saturation temperature in a controlled manner, thereby producing a controlled primary system cooldown. The 0.71-MPa stairstep pressure decrements shown in Figure 64 produced an average primary fluid temperature reduction of about 26 K/h, between 10,000 and 12,500 s. The cooldown was suspended between 12,500 and 14,500 s while the auxiliary feedwater flow was increased to the maximum available. The 0.34-MPa stairstep secondary pressure reductions produced a 17.5-K/h primary fluid system cooldown rate. As the secondary pressure decreased, the ADV mass flow and steam enthalpy also decreased. The decreasing ADV flow allowed the auxiliary feedwater flow to exceed the ADV flow at about 18,000 s. The combined ADV mass flow and steam enthalpy reduction greatly reduced the energy removal capacity of the secondary ADV (Figure 71). As a result, much longer intervals of ADV operation were required to reduce the secondary pressure by the desired stairstep decremental value.

Effects of Combined Pressurizer Auxiliary Spray and Internal Heater Operation on Plant Cooldown and Depressurization. Late in the system cooldown and depressurization phase (20,000 to 22,000 s), the pressurizer auxiliary spray was cycled three times to assess its effectiveness in reducing primary pressure. The average depressurization rate produced by using auxiliary spray was 0.01 MPa/s during an average total pressure decrease of approximately 0.65 MPa (Figure 70). The subcooled margin was reduced to about 26 K during each spray cycle (Figure 72). The pressurizer internal heaters were then used to increase the primary hot leg fluid subcooled margin to at least 33.3 K. The pressurization rate produced by the pressurizer internal heaters at 6.99 kW was about 0.003 MPa/s during an average total pressure increase of 0.58 MPa. The combined pressurizer auxiliary spray and pressurizer internal heater operation demonstrated excellent control of the primary fluid system pressure and the primary hot

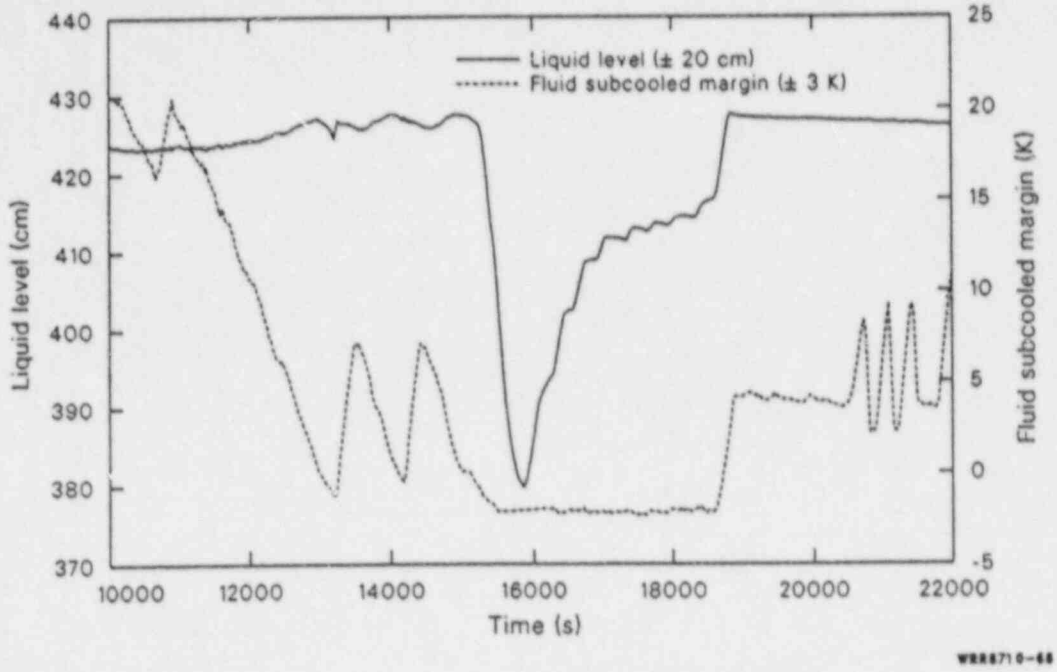

Figure 68. Vessel upper head collapsed liquid level and fluid subcooled margin during the plant cooldown and depressurization phase of MSLB Test S-FS-1 (10,000 to 22,000 s).

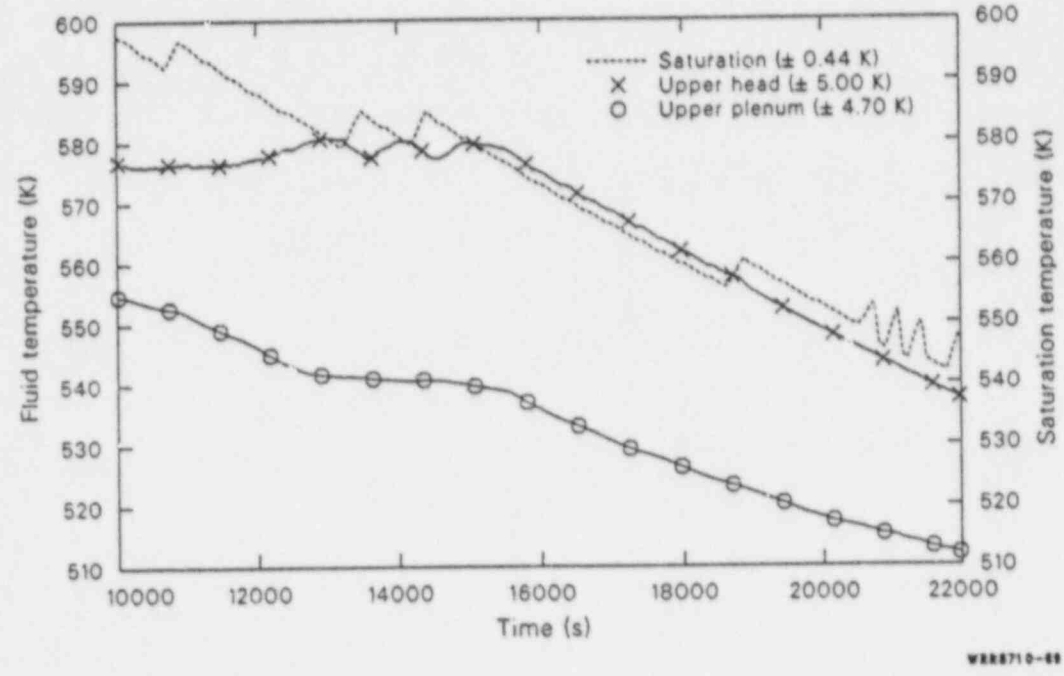

Figure 69. Vessel upper head, upper plenum, and saturation fluid temperatures during the plant cooldown and depressurization phase of MSLB Test S-FS-1 (10,000 to 22,000 s).

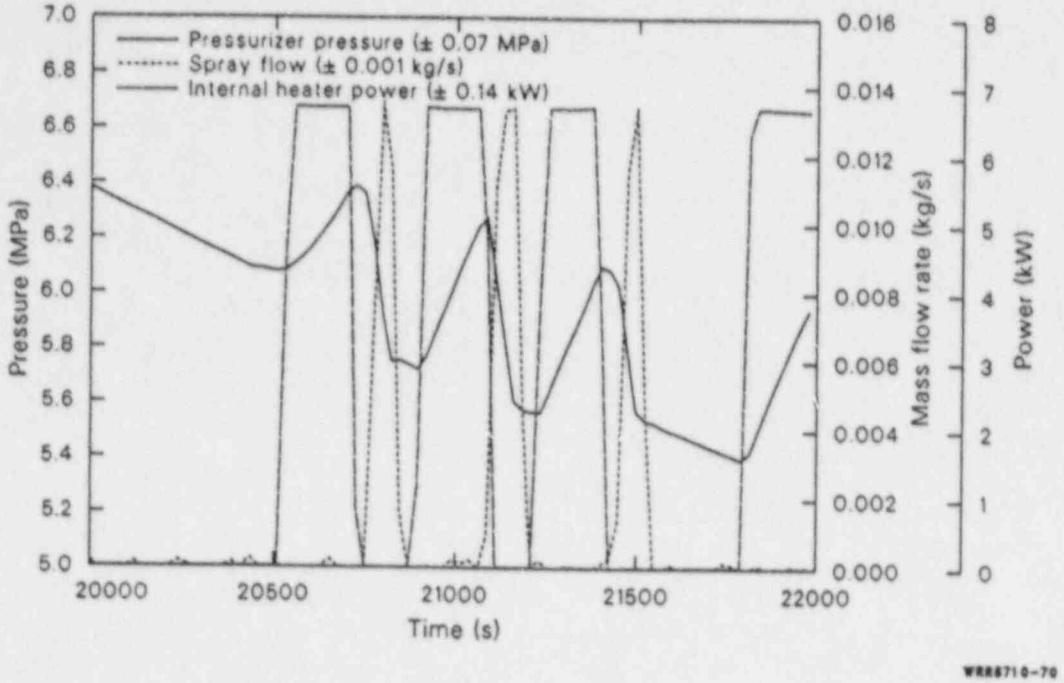

Figure 70. Pressurizer pressure, auxiliary spray mass flow rate, and internal heater power during the final portion of the plant cooldown and depressurization phase of MSLB Test S-FS-1 (20,000 to 22,000 s).

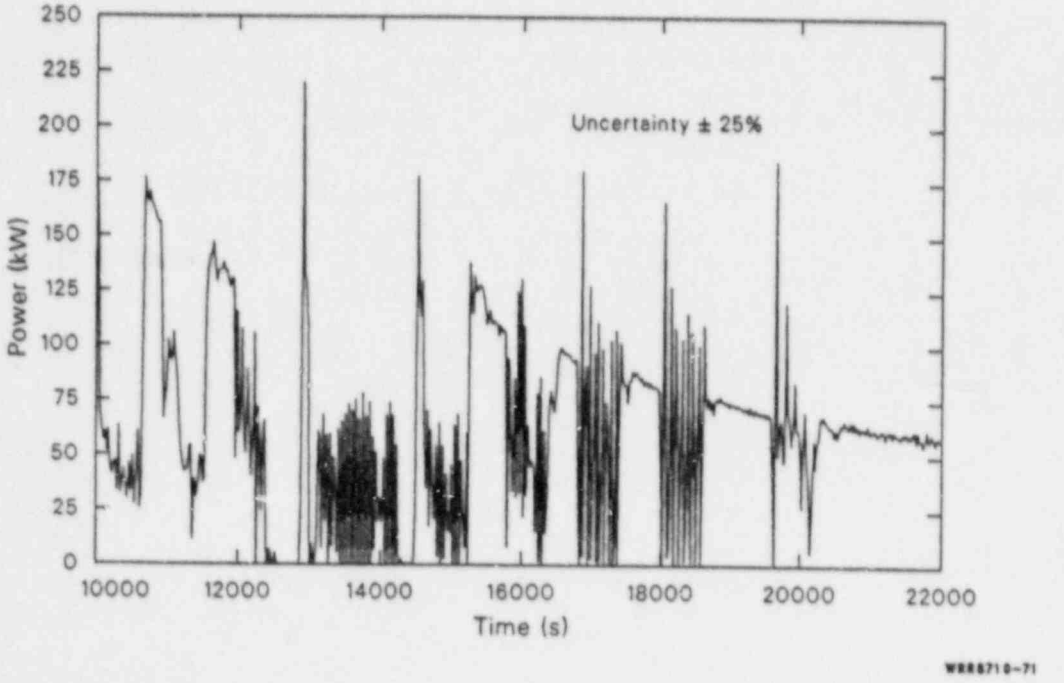

Figure 71. Unaffected loop steam generator ADV energy removal during the plant cooldown and depressurization phase of MSLB Test S-FS-1 (10,000 to 22,000 s).

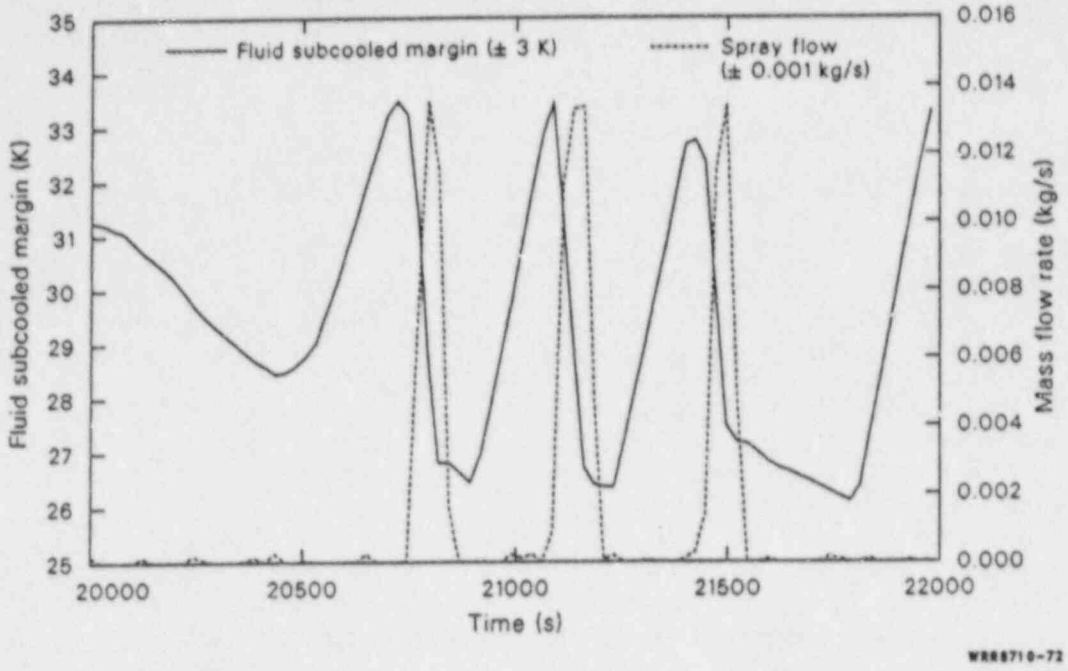

Figure 72. Primary hot leg fluid subcooled margin and pressurizer auxiliary spray mass flow rate during the final portion of the plant cooldown and depressurization phase of MSLB Test S-FS-1 (20,000 to 22,000 s).

leg fluid subcooled margin during the system cooldown and depressurization phase.

Relevance to Main Steam Line Break Issues

One of the objectives for performing these MSLB experiments was to provide data to assist the NRC in addressing the various concerns regarding these kinds of events. The major concerns are: the minimum primary system temperature; the relative effects, conservatisms, or applicability of several FSAR calculation assumptions; and, the effectiveness of EOP-specified procedures for recovering and cooling down the plant. This section contains a discussion of these major concerns in light of the results of these experiments. The implications of the experimental results relative to FSAR assumption concerns are discussed first. This is followed by a discussion of the implications of the experimental results relative to the minimum primary system temperature predicted for a full-scale PWR plant. Finally, the implications that the experimental results provide regarding the effectiveness of the EOP-specified procedures for recovering and cooling down the plant are discussed.

FSAR Assumption Conservatisms. As discussed in the section on historical background, due to the limited data base on steam generator MSLBs, a large number of assumptions and simplifications are made when performing transient calculations for FSARs. Because the calculations performed for FSARs predict primary system temperatures close to those required for PTS occurrences, questions were raised regarding the degree of conservatism inherent in the calculations. While the vendors and utilities consider the calculations to be highly conservative, such a large number of assumptions and simplifications were utilized that the degree of conservatism inherent in the calculations is unknown. The intent of this subsection is to provide some insight into the effects of the major assumptions and simplifications utilized for the FSAR calculations on the transient severity, based on the results of these MSLB experiments. In this manner, the degree of conservatism inherent in the FSAR calculations may be partially addressed. However, the final determination of the degree of conservatism inherent in the FSAR calculations will require comparisons of the FSAR-calculated parameters to best-estimate parameters calculated using a code which has been assessed and verified against these experimental results. The

assumptions and simplifications addressed in this report are limited to: the assumed separator performance; the assumed break size and location; the assumed main steam line check valve failure; the assumed loss of offsite power at scram; and the response of the secondary liquid level differential pressure measurements and their utilization for reactor trip signals.

The assumption made for FSAR Appendix 15 MSLB calculations regarding separator performance (i.e., perfect separation during the entire transient) is only mildly conservative for the Semiscale Type III steam generator. Because primary-to-secondary heat transfer is conduction-limited during the blowdown, it is at least an order of magnitude less than the break flow energy removal capacity. Therefore, the greater secondary energy removal associated with 100% steam exiting the secondary has no major effect on the primary energy removal. The greatest effects of the assumed perfect separation are that it minimizes the rates of secondary depressurization and mass depletion for a given break size. Minimizing the rate of secondary depressurization minimizes the rate of secondary saturation temperature reduction, thereby minimizing the conduction limiting for a given break size. Minimizing the rate of secondary mass depletion maximizes the timing of primary energy removal, thereby maximizing the total primary energy removal for a given break size. The assumed separator performance is therefore considered to be only mildly conservative, based on Semiscale Mod-2C experimental results.

MSLB calculations performed for FSARs typically assume the break to consist of a double-ended offset shear of the main steam line either upstream or downstream of the flow restrictor. These break size and location combinations were chosen because they produce the largest possible flow of effluent from the secondary, and it was thought that the associated greater break flow energy removal would result in the maximum possible primary cooling. However, as shown in the Semiscale experimental results, primary-to-secondary heat transfer is conduction-limited during the secondary blowdown. Also, the Semiscale results show that primary cooling provided by the affected loop steam generator is greater for the smaller-break-size case. Thus, there is no direct correlation between break flow energy removal and primary energy removal. The greatest primary cooling will occur for cases where the break flow energy removal is closely matched by the conduction-limited primary-to-secondary heat transfer. This allows the magnitude of the primary energy removal to approach that for the break flow energy removal and maximizes the effect of the secondary LOCA on primary fluid cooling. Hence, FSAR assumptions of greater primary cooling for larger break sizes are not conservative. The Semiscale experimental results indicate that the most conservative break size assumption would be a break size which produced a break flow energy removal capacity as close as possible to the conduction-limited primary-to-secondary heat transfer.

The failed affected steam generator main steam line check valve assumption utilized for FSAR Appendix 15 MSLB calculations is a conservative assumption based on the results of the Semiscale Mod-2C experiments. The additional primary energy removal provided by the loss of inventory from the unaffected loop steam generators prior to MSIV closure significantly increases the amount of total primary cooling. Semiscale results indicate that for calculations utilizing this assumption, consideration should be given to utilizing a break size which produces break flow energy removals that match the conduction-limited, primary-to-secondary heat transfer for all of the secondaries. In any case, the Semiscale Mod-2C experimental results indicate that the assumed failure of the main steam line check valve is a conservative assumption based on the increased primary cooling which results.

The FSAR Appendix 15 MSLB calculation assumption regarding the loss of offsite power at SI signal generation is not conservative based on the results of the Semiscale Mod-2C experiments. The loss of offsite power caused loop flow reductions, which reduced the cooling of the primary fluid system by the affected and unaffected loop steam generators following SI signal generation. This limited the amount of primary fluid temperature reduction and left the primary fluid system at a higher energy state following SI and MSIV closure, which in turn provided less restrictive conditions from which plant recovery had to be initiated. However, the continued loss of offsite power provided limiting conditions and capabilities for recovering the plant. Hence, the loss of offsite power assumption is not a conservative assumption for the blowdown phase of the transient, but is a conservative assumption for the recovery phase of the transient. Therefore, consideration should be given to delaying the assumed loss of offsite power until the blowdown phase of the transient is completed (i.e., the affected loop steam generator is empty). In any case, the assumed loss of offsite power at SI signal

generation is not a conservative assumption based on its effect on the amount of the primary cooling.

The expected responses of the secondary liquid level differential pressure measurements during a MSLB accident vary depending on the downcomer fluid hydraulic response and the differential pressure measurement tap connection orientation. With the positive side of the differential pressure transducer connected to the higher elevation tap, the frictional pressure drop (due to upflow through the downcomer) produces indicated liquid levels which are higher than the actual level. Thus, as the downcomer liquid inventory is depleted during the transient (if the downcomer flow reverses as it did during the Semiscale experiments), the indicated liquid level will decrease at a slower rate than the liquid inventory. This kind of response would produce conservative results with regard to generating SI signals. If, however, the differential pressure transducer is connected in the opposite manner (i.e., the negative side connected to the higher elevation tap), then the frictional pressure drop (due to upflow through the downcomer) produces an indicated liquid level which is lower than the actual liquid level. For this case, as the downcomer liquid inventory is depleted during the transient (if the downcomer flow reverses as it did during the Semiscale experiments), the indicated liquid level will decrease at a faster rate than the liquid inventory. This kind of response would produce nonconservative results with regard to generating SI signals. For this discussion, conservative means relative to the expected "best-estimate" responses. However, from the standpoint of the overall transient severity, the most conservative assumption with regard to SI generating signals continues to be the low affected loop steam generator secondary pressure SI signal generation setpoint. The configurational and fluid hydraulic dependencies of the downcomer liquid levels makes them suspect for conservative assumption candidates.

Minimum Primary Temperature. The major concern with regard to a MSLB accident is the minimum vessel downcomer fluid temperature resulting from excessive primary cooling. Excessive cooling can lead to the occurrence of PTS phenomena, leading to rupture of the reactor vessel. Direct extrapolation of the Semiscale Mod-2C results relative to those expected for a full-scale PWR plant is not adequate to fully answer this concern. However, the Semiscale results can be utilized to provide some indication of the actual temperatures which might be expected.

The extrapolation of results from a scaled experimental facility requires consideration of the effects of scaling distortions on the measured results. Extrapolation of the Semiscale Mod-2C MSLB experiment primary fluid thermal response results to a full-scale PWR plant requires consideration of the effects of excessive metal mass on the system thermal response. First, the amount of metal energy removal which occurred during the Semiscale Mod-2C experiments was estimated and compared to the total (primary fluid plus metal) energy removed by the secondaries. Then, by estimating the relative metal mass effects for Semiscale versus a full-scale PWR plant, the effects of the excessive metal mass can be accounted for and the expected thermal response (without the excessive metal mass) can be extrapolated. This method, outlined in the following discussions, was used to extrapolate the Semiscale Mod-2C MSLB experimental results and provide some indication of the minimum primary fluid temperature which might occur in a full-scale PWR plant.

The energy removed from the primary fluid during the Semiscale Mod-2C MSLB experiments was less than the total energy transferred to the secondaries. The difference between the two was primarily due to the system metal transferring energy to the primary fluid. With the correct scaled metal mass, there would have been less energy addition to the fluid from the metal; and the energy removed from the primary fluid would have been closer to the total energy transferred to the secondaries. The first step in determining the effect of the larger-than-scaled metal mass was to estimate the energy removed from the metal during the blowdown phase of each experiment. This was estimated as the difference between the total energy transferred to the secondaries and the energy removed from the primary fluid. The total energy transferred to the secondaries was obtained by integrating the affected and unaffected loop steam generator primary-to-secondary heat transfer. The energy removed from the primary fluid was estimated based on the primary fluid mass and the change of enthalpy of the primary fluid during the blowdown.

Energy addition from the metal to the primary fluid will also occur in a full-scale PWR plant during a MSLB accident. Hence, reasonable indication of the actual temperature response which might occur in a full-scale plant requires consideration of the metal mass effects. The next step was to estimate the effect of the overscaled metal mass in the Semiscale Mod-2C system relative to the

full-scale PWR plant. The larger-than-scaled metal mass in Semiscale produces surface-area-to-metal-mass and surface-area-to-primary-fluid-volume ratios greater than those for a full-scale plant. As discussed in Reference 14, these ratios were used to determine an average metal mass distortion factor (2.98) for the Semiscale Mod-2C facility (the actual full-height, full-pressure, water facility discussed in Reference 14). This distortion factor is an estimate of the relative effect of the overscaled metal mass on the primary system response. Thus, the energy addition to the primary fluid from the metal was about three times greater than would have occurred relative to a full-scale PWR plant. About two-thirds of the energy removed from the metal during the Semiscale Mod-2C experiments would have actually been removed from the primary fluid if the facility were perfectly scaled.

One additional consideration for this analysis was the effect of the thicker-than-scaled U-tube walls in the Type III affected loop steam generator. As discussed in the subsection on secondary thermal response, the thicker tube walls reduce the conduction through the walls by about 20%. Since the primary-to-secondary heat transfer during these MSLB experiments was conduction-limited, the affected loop steam generator primary energy removal was about 20% less than it should have been. Thus, the total primary energy removal must be increased by about 20% of the affected loop steam generator primary energy removal to account for the effect of the thicker U-tubes.

The undistorted primary fluid energy removal was estimated by first increasing the affected loop steam generator portion of the total primary fluid energy removal by 20%. Next, the estimated metal energy removal was increased to preserve the ratio of metal energy removal to total energy removal. This accounted for the distortion due to the thicker U-tube walls in the Type III affected loop steam generator. Next, the metal energy removal was decreased by two-thirds to account for the metal mass distortion. The reduced metal energy removal was then subtracted from the total energy removal to obtain an estimate of the undistorted primary fluid energy removal. The undistorted primary fluid energy removal was then used in conjunction with the primary fluid mass and the initial primary fluid enthalpy to determine the undistorted minimum primary fluid enthalpy. Assuming the same primary fluid pressure as occurred in the test, the pressure and undistorted fluid enthalpy were then used to estimate the undistorted minimum primary fluid temperature.

The estimated minimum average cold leg (downcomer) fluid temperatures (Table 1) represent temperatures much closer to, but still above, the PTS minimum temperature limit (450 K). It is recognized that this analysis included a number of simplifications. However, the relative proximity to the PTS temperature limit for Test S-FS-1 and the indicated trend in minimum temperature with break size points out the need to perform best-estimate calculations with a thermal-hydraulic computer code that has been assessed against and verified for the results of these experiments.

Effectiveness of EOPs. The major concern with regard to system recovery from a MSLB accident is the effectiveness of the operations specified in the plant EOPs in recovering and maintaining control of the plant. Due to inherent scaling distortions (such as atypical metal-mass-to-volume ratios, heat loss/heat loss mitigation, and timing distortions)[13,14] and facility limitations, the results of these experiments are not a precise replication of full-scale PWR response. However, the experiments provided thermal-hydraulic behavior sufficiently representative of full-scale PWR behavior to preserve important phenomena and allow quantification of the effectiveness of the EOP-specified operations in recovering the system from a MSLB accident.

The automatic actions performed by the plant safety systems (i.e., SI initiation and MSIV closure) were effective in mitigating the consequences of the MSLB accident. The automatic actions left the Semiscale Mod-2C system in a quasi-stable condition, which aided in the stabilization and recovery of the system.

The stabilization operations performed following operator identification of the transient (i.e., SI termination, pressurizer internal heater operations, normal charging/letdown operations, and unaffected loop steam generator steam and feed operations) were effective in stabilizing the system at conditions which would permit a natural circulation cooldown and depressurization to begin. The limiting criterion in achieving stable conditions was the recovery of the pressurizer liquid inventory to a level which would ensure adequate level control during the natural circulation cooldown.

The primary fluid system natural circulation cooldown and depressurization operations performed following system stabilization in Test S-FS-1 (i.e., pressurizer auxiliary spray operations, pressurizer internal heater operations, normal charging/letdown operations, and unaffected loop

Table 1. Minimum primary fluid temperatures predicted for a full-scale PWR plant based on extrapolation of Semiscale Mod-2C data

Main Steam Line Break Size and Location	Minimum Primary Fluid Temperature (K)	Predicted Margin Above PTS Limit 450 (K)
Double-ended offset shear upstream of the flow restrictor	544	94
Double-ended offset shear downstream of the flow restrictor	522	72

steam generator steam and feed operations with stairstep reductions in the secondary pressure) were very effective in cooling down and depressurizing the primary fluid system in a controlled manner. An inadvertent void formation in the vessel upper head was due to the external heater energy addition in the upper head exceeding the upper head heat loss (not to inappropriate recovery operations). It was necessary to increase the unaffected loop steam generator auxiliary feedwater flow rate to the maximum scaled flow for two diesel-driven auxiliary feedwater pumps. However, the maximum flow was sufficient to maintain control of the secondary inventory.

All in all, the EOP-specified operations were shown to be very effective in maintaining control of the Semiscale Mod-2C system during these experiments. Scale effects (atypical metal-mass-to-fluid-volume ratio and heat loss/heat loss mitigation) had little effect on the system response.

The atypically large metal-mass-to-fluid-volume ratio had little effect because the system stabilized at temperatures very close to the initial condition temperatures. During the course of the transient, the change in system temperatures was very gradual. If anything, the atypically large metal mass provided an additional energy source which slowed the system cooldown and depressurization, providing conservative system recovery responses.

The heat loss/heat loss mitigation had little effect because the primary fluid system remained subcooled during the transients, making the external heaters very effective in mitigating the heat loss. (The vessel upper head for a portion of Test S-FS-1 and the pressurizer were the only components which saturated.) The largest heat loss/heat loss mitigation effect was observed in the vessel upper head during Test S-FS-1. Under natural circulation conditions, fluid flow through the upper head is minimal. The energy added to the upper head fluid by the external heaters remains in the upper head and is not transferred to the rest of the system. Because the external heater energy addition was greater than the upper head heat loss, the upper head fluid was gradually heated and reached saturation during the primary depressurization, causing a void formation.

The metal-mass and heat-loss scale effects on the system response were minimal. In addition, the effects offset each other such that the overall system response should be a reasonable indicator of the general response expected for a full-scale PWR plant. In any case, the atypically large metal-mass-to-fluid-volume ratio and the system heat loss/heat loss mitigation have been well characterized and can be modeled. Hence, the data are useful for the thermal-hydraulic code verification required prior to utilizing the code to predict full-scale PWR plant response.

CONCLUSIONS

The following conclusions have been drawn, based on analyses of the experimental data from the Semiscale Mod-2C feedwater and steam line break experiment (S-FS) series.

1. A simplistic extrapolation of Semiscale Mod-2C experimental results to those expected for a full-scale PWR plant indicates significant cooling of the primary fluid, particularly for the break downstream of the flow restrictor. While the predicted temperatures do not reach the PTS limit of 450 K, their relative proximity to the PTS limit and the indicated trend in minimum temperature with break size provides substantial evidence in support of the need to perform best-estimate calculations with a code verified against these experimental data.

2. FSAR assumptions of perfect separator performance are only mildly conservative. The measured response of the Semiscale Type III affected loop steam generator indicates a very brief period of separator flooding and separator performance degradation, followed by essentially perfect separator performance. Due to conduction-limiting of the primary-to-secondary heat transfer, the measured primary cooling is substantially smaller than the cooling potential associated with the break flow energy removal. The greatest contribution of the assumption to the conservatism of the calculated response, therefore, lies not in maximizing the break flow energy removal but in maximizing the length of the blowdown and minimizing the rate of secondary depressurization.

3. The break size and location are significant in determining the severity of the event. A double-ended offset shear downstream of the flow restrictor produces much greater cooling of the primary than one upstream of the flow restrictor. This trend in primary cooling versus break size is due to the conduction limiting which occurs across the U-tube walls during the secondary MSLB LOCA.

4. The automatic actions (MSIV closure, SI initiation and auxiliary feedwater injection) performed by the plant protective safety systems were effective in mitigating the consequences of the MSLB accident in the Semiscale experiments. The actions left the system in a quasi-stable condition which minimized the amount of operator intervention required to stabilize the plant.

5. The EOP-specified stabilization operations (SI termination, pressurizer internal heater operation, normal charging/letdown operation, and unaffected loop steam generator steam and feed operation) were effective in stabilizing the Semiscale Mod-2C system at conditions which permit initiation of natural circulation cooldown and depressurization. SI termination based upon a pressurizer pressure of 13.88 MPa presented no real threat of significant pressurization of the primary fluid system. Termination of the SI flow occurred before the pressurizer went liquid solid. Also, the SI flow was small enough that even with the pressurizer liquid solid, the rate of primary pressurization would not be sufficient to cause significant pressurization prior to SI termination.

6. The EOP-specified natural circulation cooldown and depressurization operations (pressurizer auxiliary spray operation, pressurizer internal heater operation, normal charging and letdown operation, and unaffected loop steam generator steam and feed operation with stairstep secondary pressure reductions) were effective in maintaining a controlled cooldown and depressurization of the Semiscale Mod-2C system. Inadvertent vessel upper head voiding occurred due to excessive upper head heat loss makeup, not inappropriate recovery operations.

7. The assumed separator performance for FSAR calculations is only mildly conservative. Coupled with a break size which provides appropriate break flow energy

removal, however, this assumption may prove beneficial to both FSAR and best-estimate calculations.

8. The break size and location assumptions utilized for FSAR calculations resulted in the largest break sizes being utilized to maximize the break flow energy removal. These assumptions are not conservative. The greatest primary cooling will occur for cases where the break flow energy removal is closely matched to the conduction-limited primary-to-secondary heat transfer. Future FSAR and best-estimate calculations should not utilize this assumption, but should investigate smaller break sizes which produce break flow energy removal rates as close as possible to the conduction-limited primary-to-secondary heat transfer.

9. Further analysis for smaller break sizes is warranted in light of the indicated trend in overcooling versus break size.

10. The failed affected steam generator main steam line check valve assumption utilized for FSAR calculations is conservative. The additional primary energy removal provided by the loss of inventory from the unaffected loop steam generator significantly increases the amount of the total primary cooling.

11. The assumed loss of offsite power at SI signal generation, utilized for FSAR calculations, is not conservative. The resulting loop flow reductions reduce the cooling of the primary fluid system, limiting the amount of the primary fluid temperature decrease. However, loss of offsite power provides limiting conditions and capabilities for recovering the plant. Therefore, consideration should be given to delaying the assumed loss of offsite power until the blowdown phase of the transient is completed.

12. Downcomer liquid-level response dependencies on the measurement configuration and the secondary fluid hydraulic response makes them suspect for conservative assumption trip generating candidates. However, with appropriate consideration of the differential pressure measurement configuration and accurate modeling and calculation of the secondary fluid hydraulic responses, they could prove to be the actual trip signal generators for best-estimate calculations.

13. The data obtained during these MSLB experiments satisfy the stated objectives for the experiments. The data are of sufficient detail and quality to allow verification of thermal-hydraulic computer codes for MSLB accident, system stabilization, and system cooldown and depressurization calculations. The analyses of the experimental results have provided invaluable insight into the phenomena and driving mechanisms evidenced in the experiments and applicable to full-scale PWR plants.

RECOMMENDATIONS

During the course of analyzing the results of these experiments, a number of deficiencies were identified in the current methods of computer code simulations for secondary transients. These deficiencies need to be corrected before an accurate estimate of the actual full-scale plant response (an accurate best-estimate calculation) can be obtained.

Foremost in the deficiencies is the assumed primary cooling due to break flow energy removal. The primary-to-secondary heat transfer during these experiments was conduction-limited, negating the effect of the large break flow energy removal rate. The primary energy removal during the secondary blowdown is a rate-controlled process. Therefore, substantial consideration must be given to smaller break sizes which produce break flow energy removal rates as close as possible to the conduction-limited primary-to-secondary heat transfer. Future best-estimate calculations with smaller break sizes should provide invaluable insight into the maximum amount of primary cooling which could actually occur during a MSLB secondary LOCA.

Another deficiency identified was in the existing correlations for predicting secondary convective heat transfer coefficients. As discussed in the S-FS series feedwater line break test results report,[15] the Semiscale Type III steam generator measured local secondary convective heat transfer coefficient dependence on the local vapor void fraction exhibits a trend which is exactly the opposite of that predicted by the existing boiling heat transfer correlations. This deficiency is sure to exist for MSLB calculations as well as feedwater line break calculations, since the same correlations are utilized. Accurate prediction of the secondary convective heat transfer coefficients will be important as the steam line break size is reduced, alleviating the conduction limiting observed for the larger steam line break sizes.

Improvements in secondary convective heat transfer calculation methodology will be required in order for thermal-hydraulic computer codes to accurately calculate the actual primary-to-secondary transient heat transfer for smaller MSLBs, since secondary convective heat transfer will play a major role in determining primary-to-secondary heat transfer. This will require either modifications to existing, or development of new, boiling convective heat transfer correlations based on the Semiscale Type III steam generator heat transfer data, as discussed in the S-FS series feedwater line break test results report.[15]

Finally, a deficiency exists in the FSAR calculation assumption regarding loss of offsite power. The Semiscale Mod-2C bottom main feedwater line break experiment results show that the assumed loss of offsite power at SI signal generation severely limits the amount of primary fluid temperature reduction. Future calculations should consider delaying the loss of offsite power until after the blowdown phase of the transient is completed (i.e., the affected loop steam generator is empty).

The capabilities and accuracy of codes used for best-estimate MSLB calculations should be established using these experimental data or similar integral system experimental data before they can be used with confidence or to satisfy the proposed revision to the ECCS rule (10 CFR Part 50). For future best-estimate calculations, smaller break sizes should be considered, the loss of offsite power should be delayed until after the affected loop steam generator has emptied, and consideration may be given to utilizing the secondary liquid level obtained from the downcomer differential pressure as a possible trip generating signal if the measurement configuration and secondary fluid component hydraulic response can be accurately simulated.

REFERENCES

1. T. J. Boucher, J. R. Wolf, *Experiment Operating Specification for the Semiscale Mod-2C Feedwater and Steam Line Break Experiment Series*, EGG-SEMI-6625, May 1984.

2. T. J. Boucher, W. A. Owca, *Appendix S-FS-1 of the Experiment Operating Specification for the Semiscale Mod-2C Feedwater and Steam Line Break Experiment Series*, EGG-SEMI-6783, January 1985.

3. W. A. Owca, T. H. Chen, *Quick Look Report for Semiscale Mod-2C Test S-FS-1*, EGG-SEMI-6858, May 1985.

4. T. J. Boucher, *Appendix S-FS-2 of the Experiment Operating Specification for the Semiscale Mod-2C Feedwater and Steam Line Break Experiment Series*, EGG-SEMI-6761, December 1984.

5. T. J. Boucher, T. H. Chen, *Quick Look Report for Semiscale Mod-2C Test S-FS-2*, EGG-SEMI-6827, March 1985.

6. Office for Analysis and Evaluation of Operational Data, USNRC, *Power Reactor Events, 4*, 5, NUREG/BR-0051, July-August 1982, p. 4.

7. R. C. Kryter et al., *Evaluation of Pressurized Thermal Shock*, NUREG/CR-2083, ORNL/TM-8072, October 1981.

8. D. J. Shimeck, *Experiment Operating Specification for Semiscale Mod-2A Steam and Feedwater Line Break Series*, EGG-SEMI-5830, March 1982.

9. G. R. Berglund, D. J. Shimeck, *Quick Look Report for Semiscale Mod-2A Main Steam Line Break Tests S-FS-4 and S-FS-5*, EGG-SEMI-6079, November 1982.

10. M. Y. Young, et. al., *Prototypical Steam Generator (MB-2) Transient Testing Program*, NUREG/CR-3661, EPRI-NP-3494, WCAP-10475, March 1984.

11. Zion Unit Number 1 Nuclear Plant, *Final Safety Analysis Report*, Appendix 15, Commonwealth Edison Company.

12. E. Klingler, *The Semiscale Mod-2C Feedwater and Steam Line Break Configuration Report for Experiments S-FS-1, S-FS-2, S-FS-6, S-FS-6B, S-FS-7, and S-FS-11*, EGG-RTH-7445, October 1986.

13. T. K. Larsen, J. L. Anderson, and D. J. Shimeck, *Scaling Criteria and Assessment of Semiscale Mod-3 Scaling for Small Break Loss-of-Coolant Transient*, EGG-SEMI-5121, March 1980.

14. K. G. Condie, et. al., *Evaluation of Integral Continuing Experimental Capability (CEC) Concepts for Light Water Reactor Research - PWR Scaling Concepts*, NUREG/CR-4824, EGG-2494, February 1987.

15. T. J. Boucher, *Results of Semiscale Mod-2C Feedwater and Steam Line Break (S-FS) Experiment Series: Bottom Main Feedwater Line Break Accident Experiments*, NUREG/CR-4898, EGG-2503, February 1988.

APPENDIX A

DETAILED SYSTEM DESCRIPTION AND EXPERIMENTAL PROCEDURE

APPENDIX A

DETAILED SYSTEM DESCRIPTION AND EXPERIMENTAL PROCEDURE

System Description

The Semiscale test facility consists of: fluid systems (pipes, pumps, vessel, heat exchangers, etc.); control systems (power to core, pumps, valves, and instrument air and control signals); and an experimental measurement system (transducers, amplifiers, digital data system) required for integral steam and feedwater line break experiments. These systems are described in detail in Reference A-1. The fluid systems and the experimental measurement system will be summarily described here.

Fluid System Configuration. The Semiscale Mod-2C fluid system configured for the FS series steam line break tests is shown in Figure A-1. The Mod-2C system consists of the Mod-2B system with several modifications. A new Type III affected loop steam generator, new main steam line and feedwater line break assemblies, break effluent catch tanks, and refined steam generator control systems were incorporated into the system for this test series. A letdown line was added to provide better control of primary system inventory.

The primary fluid system is a 17.24-MPa (2500-psi), 616-K (650°F), 3.8- to 7.6-cm (1.5- to 3-in.) Schedule 160 stainless steel system. It consists of an unaffected loop and an affected loop, the former representing three of the four loops in a PWR. Thus, flow rates and equipment sizes are in the ratio of 3:1 for the two loops. The pressurizer is connected by a surge line to the unaffected loop hot leg. Scaled emergency core coolant from an accumulator and high- or low-pressure injection system pumps is routed to the loop cold legs.

The secondary fluid system consists of an unaffected loop steam generator and an affected loop steam generator, the former representing three of the four steam generators in a PWR. Feedwater was supplied from a heated tank to the upper downcomer of the affected loop steam generator and the lower downcomer of the unaffected loop steam generator, and the steam was routed through control valves to the atmosphere; i.e., an open loop secondary coolant system was used. Auxiliary feedwater was routed to the upper downcomer of both steam generators at approximately the top U-tube bend elevation.

In Semiscale, the annular downcomer of the PWR vessel is replaced with an external pipe to permit extensive instrumenting of both the core and downcomer regions, as shown in Figure A-2. Most of the fluid system components are full height, including the core that consists of a 5 x 5 array of electrically heated, 3.66-m-long rods that simulate the fuel rods in a 15 x 15 PWR core. The number of turns per inch of the electrically heated coil is varied along the rod length to give the staircase approximation of a cosine axial heat flux shape. Total core power is nominally 2 MW.

The upper head, upper plenum, and core flow bypass arrangement in the Semiscale reactor vessel simulates a Westinghouse inverted top hat, upper-head internals package design.

The steam generators incorporate 2.22-cm (7/8-in.) OD Inconel inverted U-tubes, six in the unaffected loop generator and two in the affected loop unit. The tube lengths cover the range found in a PWR generator. Two tubes in each generator are supplied with small-diameter, Inconel-sheathed thermocouples brazed to the tubes, which provide primary and secondary coolant temperatures and tube wall temperatures at various elevations in the upflow and downflow legs. It should be noted that the major portion of the unaffected loop steam generator secondary flow area and volume is taken up by filler pieces in order to obtain the approximately correct secondary side liquid volume and velocity.

Assessment of computer code capabilities to predict secondary side transient response requires accurate measurement of important parameters, such as local primary-to-secondary heat transfer and fluid condition data and component mass inventories. The Type III affected loop steam generator design incorporates a downcomer that is external to the tube bundle and riser sections (Figure A-3). In this manner, component mass inventory and fluid property (including density and void fraction) information was obtained. The design also entails a steam dome with separator equipment that provides steam exit qualities of approximately 90% during full-power, steady-state operations.

Component flow areas, volumes, lengths, and pressure drops were sized to simulate a Westinghouse Model 51 steam generator. Table A-1 contains both

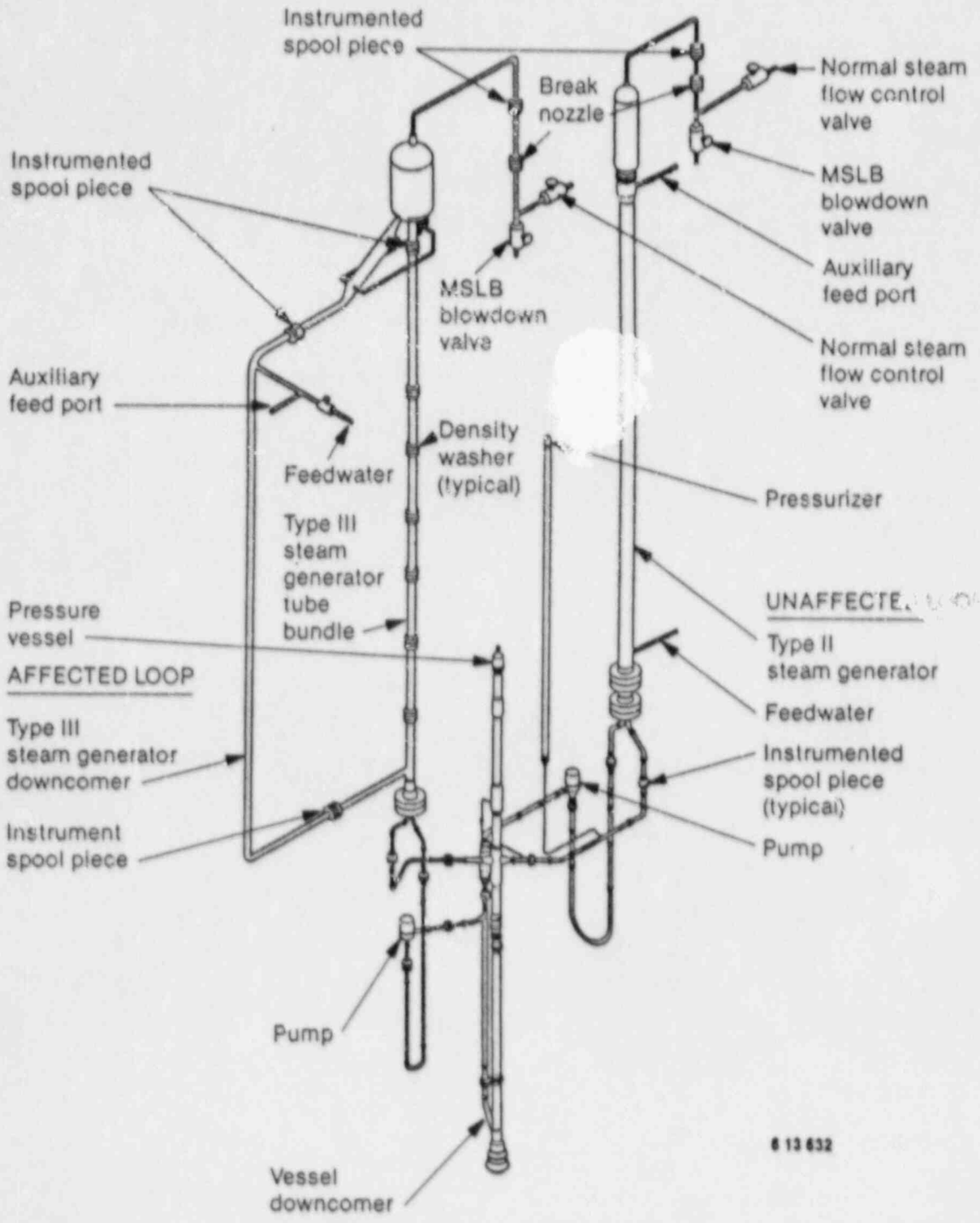

Figure A-1. The Semiscale Mod-2C facility as configured for the FS series steam line break experiments.

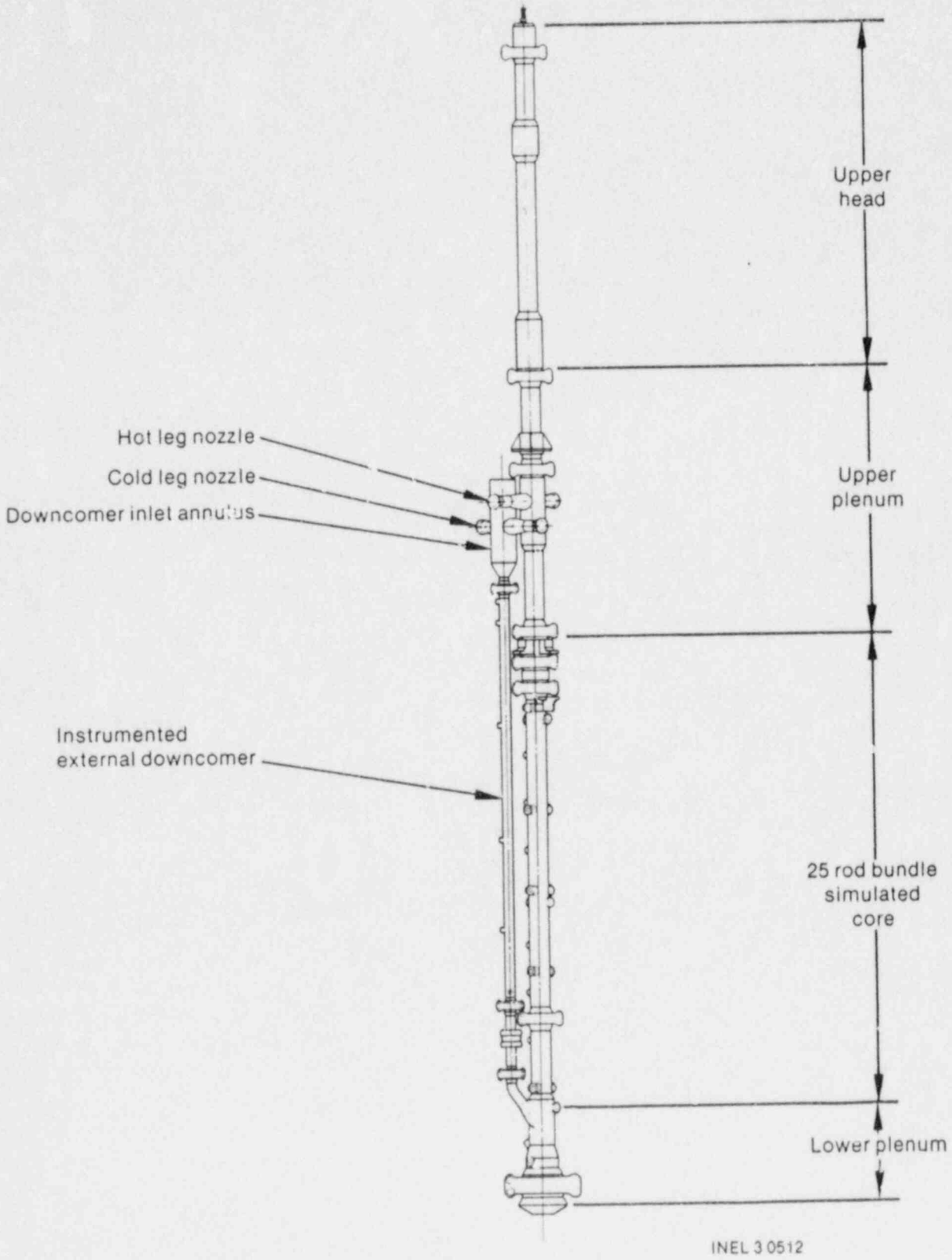

Figure A-2. The Semiscale Mod-2C pressure vessel.

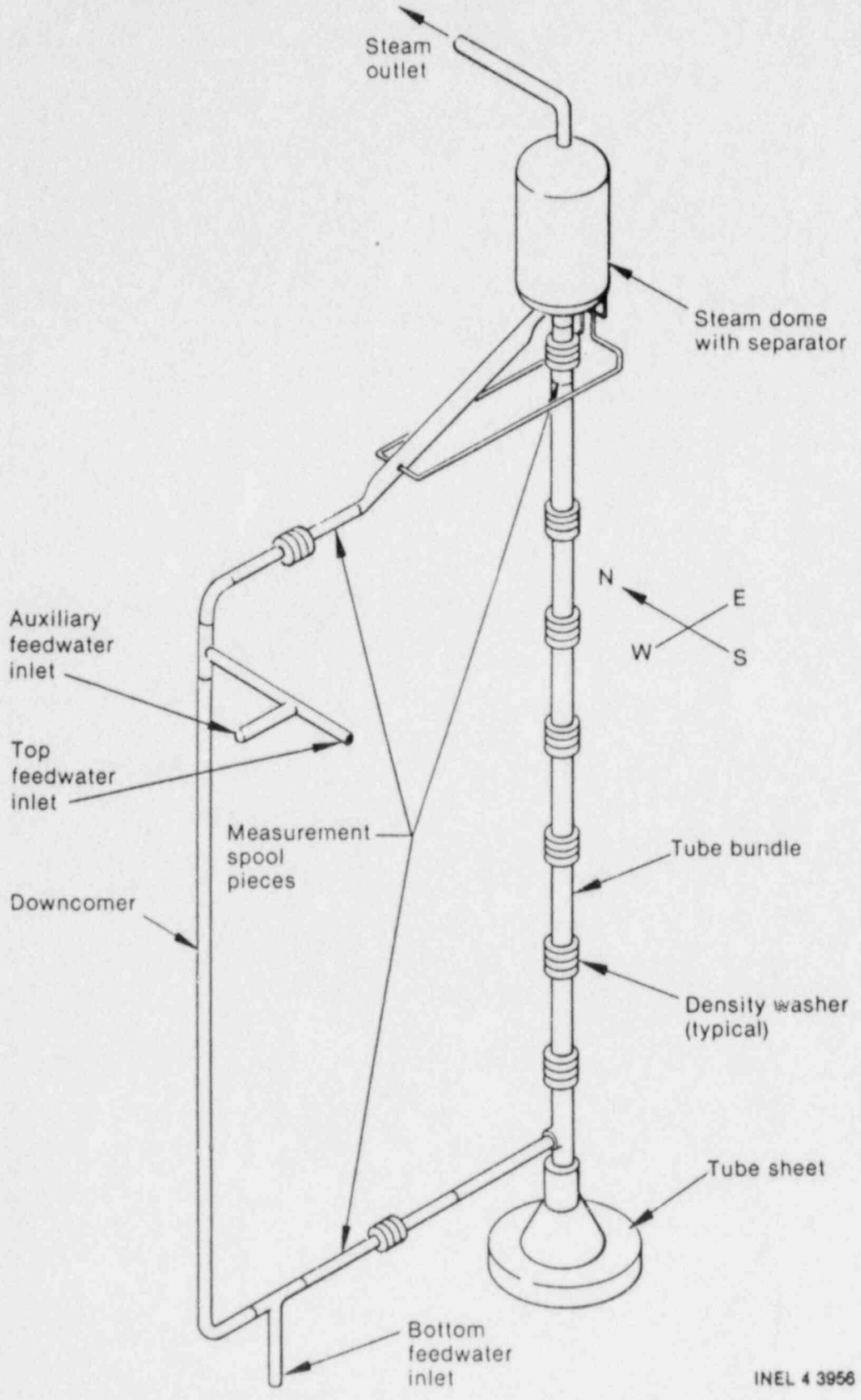

Figure A-3. The Semiscale Type III affected loop steam generator configuration.

Table A-1. Comparison of Westinghouse Model 51 steam generator design values, scaled design values, and Semiscale Type III affected loop steam generator design values

Parameter	Westinghouse Model 51 Steam Generator		Semiscale Type III Affected Loop Steam Generator Values
	Design Values	Volume-Scaled[a] Design Values	
Flow area, m^2, in constant area region of:			
Downcomer	0.658	0.000386	0.000965
Tube bundle	5.100	0.002990	0.003039
Elevation, m, of:[b]			
U-tubes	10.59	10.59	9.93
Riser	11.21	11.21	10.54
Downcomer	13.91	13.91	11.31
Total secondary volume, m^3, below top of:			
U-tubes	65.5	0.0384	0.0439
Riser (24 in. above top of U-tube)	73.7	0.0432	0.0502
Downcomer	112.2	0.0658	0.0712
Relative pressure drop (percentage of total flow circuit pressure drop) of:			
Downcomer	24	24	20
Tube bundle	26	26	24
Primary separator	50	50	56[c]

a. Volume scaling factor is 1705.5.

b. Relative to the top of the tube sheet.

c. Obtained by orificing the top of the riser.

the scaled and reference values for the more important performance parameters and components of the Type III affected loop generator. The tube bundle contains two 2.22-cm (7/8-in.) OD Inconel inverted U-tubes with a tube thickness of 0.165 cm (0.065 in.) to allow for more reliable temperature measurements than were possible with 0.124-cm (0.049-in.) wall tube. Design calculations indicate little difference in either heat transfer or flooding characteristics for the 0.165-cm (0.065-in.) wall tube as opposed to the 0.124-cm (0.049-in.) wall tube used in a Westinghouse Model 51 steam generator. The tubes are configured with a "square" pitch similar to a Model 51 steam generator and simulate a long and a short tube in the prototype. Tube heights were selected to maintain symmetry with the unaffected loop steam generator. A portion of the tube bundle secondary flow area and volume is taken up by two instrument tubes. However, filler tubes were not necessary to obtain the correct secondary side liquid volume and velocity. Tube bundle support baffle plates were sized to produce approximately the correct frictional pressure drop.

The downcomer flow area and volume were sized to obtain approximately the correct liquid volume and velocity, while producing approximately the correct frictional pressure drop. Either top or bottom feedwater injection and break simulation can be accommodated with the new downcomer design.

The steam dome and separator, shown in Figure A-4, were designed to simulate the behavior of the corresponding components in a Westinghouse Model 51 steam generator. Separation of the liquid from the steam occurs in three stages. The two-phase mixture exiting the riser section is deflected into the steam dome wall, where some of the liquid is separated from the mixture, flows down the wall, and is transferred to the downcomer through a connecting line. The remaining mixture continues up through the dome to the secondary separator, with some gravity-separated liquid falling back down to the bottom of the dome and mixing with the liquid separated by the deflector at the first stage ("primary" separator). The "secondary" separator, or third stage of separation, accepts the remaining two-phase mixture and imparts a centripetal motion upon it. The resulting separated liquid then flows down through the connecting lines to the downcomer. This final stage of separation produces steam dome exit qualities of approximately 90% for full-power conditions.

Failure of the check valve in the main steam line of the affected loop steam generator during a steam line break event results in flow from the unaffected, as well as the affected loop steam generator, prior to MSIV closure (see Figure A-5). To simulate this dual break flow path, the unaffected, as well as the affected, loop steam generator was allowed to blow down through a break assembly until the low affected loop steam generator secondary pressure MSIV closure signal was generated. The unaffected loop steam generator break valve was then closed to simulate the closure of the MSIV.

The MSLB assemblies for the affected and unaffected loop steam generators consisted of quick-opening valves, break-flow nozzles, and instrumentation to measure single-phase and two-phase break mass flows, as well as fluid densities, pressures, and temperatures. The break nozzles were interchangeable to allow simulation of steam line breaks upstream or downstream of the flow restrictor. Information on the nozzle geometries for each test is contained in the EOS Appendices[A-2, A-3] and Reference A-1. The break assemblies were physically located in tees from the affected and unaffected loop steam generator main steam lines. To provide a history of mass exiting from the systems, the break flows were routed to tanks where they were collected in liquid pools and measured. Special feedwater and steam lines with smaller control valves, smaller measurement orifices, and heat tracing to compensate for environmental heat losses were installed on both steam generators for steady-state "hot standby" operations. The main steam lines were connected into the break assemblies between the break nozzles and the break valves and were routed to atmosphere. Transient initiation was realized via rapid (nominally 1 s) closure of the valves in the lines to atmosphere at the same time that the valves in the lines to the collecting tanks were rapidly (nominally 1 s) opened.

Letdown simulation in the Semiscale system consisted of a valved line connected to the unaffected loop cold leg. A flow control valve in the Semiscale letdown simulation line provided a letdown flow rate of 0.01081 kg/s for fluid conditions typical of the cold leg fluid at initial conditions.

Heat loss makeup was accomplished by using external heaters distributed fairly uniformly throughout the Semiscale system. These heaters are controlled by six separate power supplies, including: vessel, hot legs, cold legs, unaffected loop pump suction, affected loop pump suction, and pressurizer. The total power provided by these heaters is about 44 kW (excluding the pressurizer). An additional 15 kW of heat loss makeup was provided by augmenting core power throughout the transient. Control of the heaters was as follows: if the maximum allowable temperature (755 K) was reached on the inside surface of the pipe insulation, external power to that component was reduced by half. If the temperature trip limit continued to be exceeded, power to that component was terminated. To maximize the amount of the depressurization during the blowdown phase of the transients, the pressurizer external heaters were not used during the steam line break experiments.

Pressurizer internal heater simulation in the Semiscale system for these tests consisted of use of the system pressurizer warm-up heaters. These heaters were controlled manually, supplying 6.99 kW to three of the six warm-up heater rods. The internal heaters were operated in an on/off mode to maintain primary system subcooling.

Measurement System Configuration. The measurement system consists of primary and secondary system measurement hardware and the software utilized for measurement manipulation and recording. The general hardware configuration is discussed in the following text. Description of the

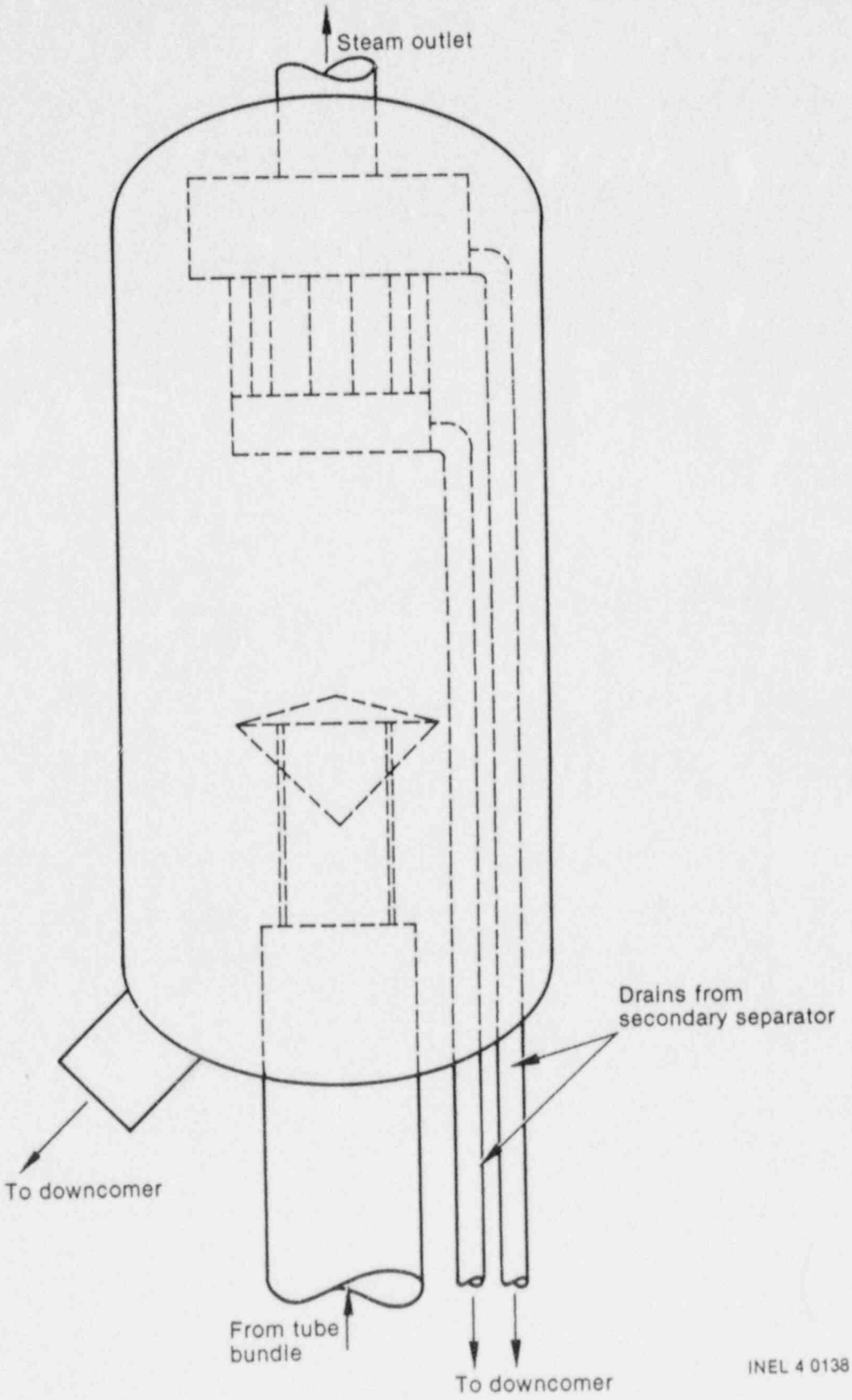

Figure A-4. The Semiscale Type III affected loop steam generator steam dome and separator configuration.

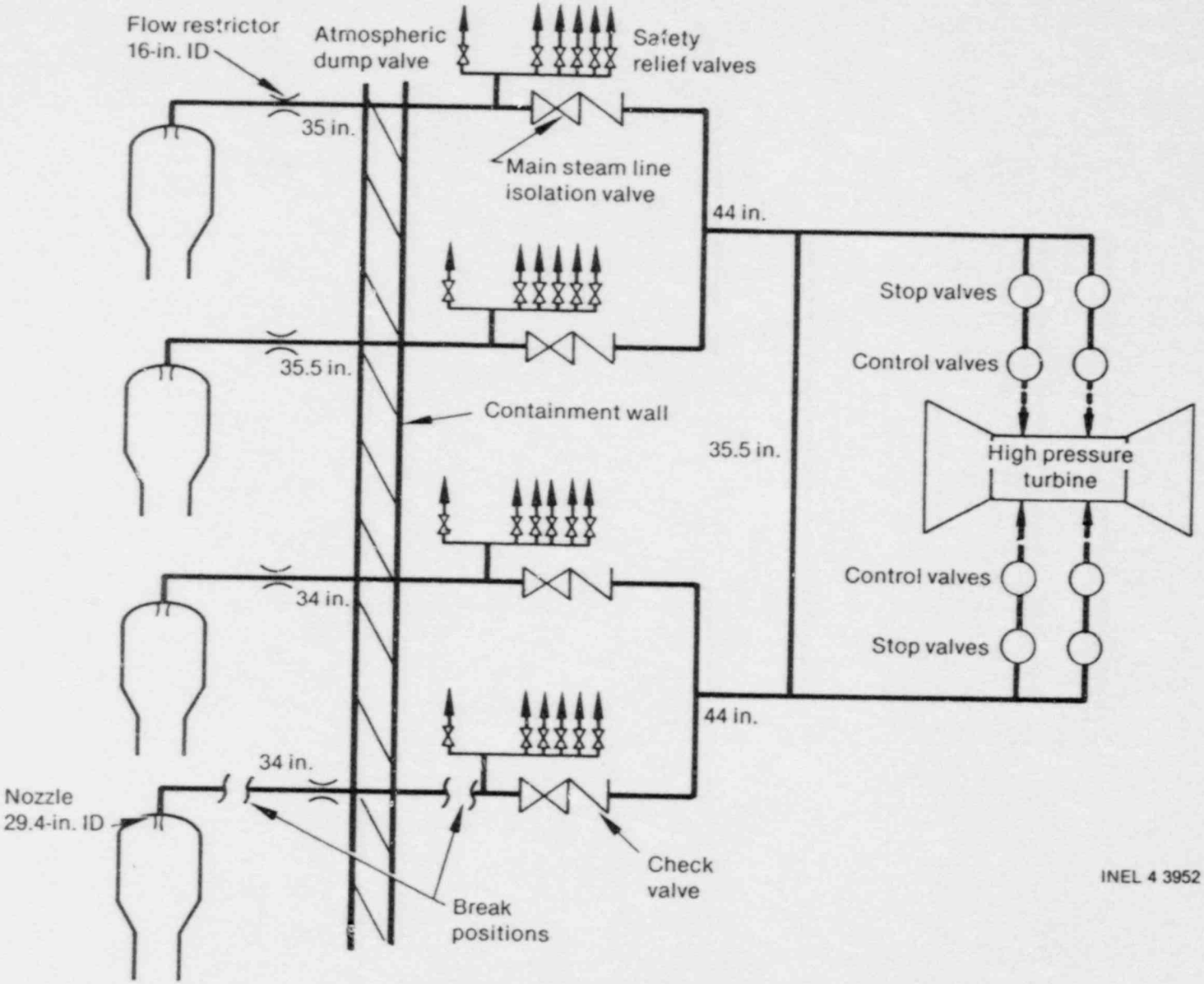

Figure A-5. Typical main steam line piping configuration for a full-scale four-loop PWR plant.

measurements made for each steam line break test in the series are given in the Appendix for that test.[A-2, A-3]

Experiment instrumentation transducers included thermocouples, resistance temperature detectors, absolute and differential pressure cells, full-flow turbine rotors (each with one or two external magnetic or R.F. blade sensors to measure bidirectional flow), full-flow drag screens (each with one deflection sensor), multiple-beam densitometer detectors with radioactive sources, and (for unidirectional flow of single-phase fluids) orifice plates or nozzles with differential pressure cells.

The approximately 350 instruments, along with further detailed information regarding the particular configuration for each test of the series, were documented in the final instrumentation log sheet.[A-1] Measurements were chosen to provide information on fluid conditions at key points throughout the primary, secondary, and support systems. A number of measurements were included to provide redundancy so that instrument failures were accommodated without compromising the test objectives. Included in the secondary measurements category were special measurements involving instrumentation development.

New measurement system capabilities were provided for the FS series to allow for more accurate assessment of secondary transient phenomena. The changes included measurement of global, local, and component data for the new Type III affected loop steam generator and break flow measurements, expected to allow break effluent characterization.

The measurements on the Type III affected loop steam generator for the FS series provided thermal-hydraulic data about the steam generator during steady-state and transient conditions. The measured data can be grouped into three categories; global, local, and component data. The global data were used to determine the overall mass and energy balances for the affected loop steam generator. Since performing these mass and energy balance calculations requires knowledge of the input, output, and storage terms for the steam generator, break flow measurement, discussed later, can be considered as part of the global data measurement category. The local data are utilized to determine local heat transfer coefficients and fluid conditions, and, as such, include the local fluid and material states (primary fluid, U-tube outside wall, secondary fluid temperature triplets and densities) as well as local mass-flow rates (secondary mass-flow rates and U-tube primary mass-flow rates). Data on the mass and energy transfer rates between, and the mass distribution and fluid states within, components of the new Type III affected loop steam generator, component data, were used to analyze the interaction of the components during secondary transients. Determination of break flow conditions was provided by two-phase mass-flow measurements upstream of the break nozzle.

Experimental Procedure

As a general procedure before initiation of the transient, the primary system was filled with demineralized water and vented to ensure a liquid-full system. Instrumentation was calibrated and zeroed as necessary. The primary system was heated to initial conditions using core power and pumped flow and was pressurized using the pressurizer internal heaters to draw a steam bubble. The steam generators, after being heat-soaked, dissipated the core power to atmosphere by steaming. The Semiscale initial conditions (Table A-2) were typical of, or scaled from, the Zion Unit 1 Nuclear Plant FSAR, Appendix 15,[A-4] steam line break calculation initial conditions.

During the period of primary system heating, a procedure was performed to acquire data to allow for normalization of the Type III affected loop steam generator temperature triplets. The procedure involved bringing the primary-to-secondary heat transfer through zero (i.e., gradually reversing the direction of energy transfer) for three different absolute temperatures. By determining the difference between the triplet temperatures at the point of no heat transfer (i.e., where the temperature difference should be zero), the correction required to match the triplets to the average temperature was determined. By performing the procedure for three different absolute temperatures, three different correction-versus-temperature points were obtained for each temperature measurement. The three correction-versus-temperature points were then curve-fit to obtain a linear correction-versus-temperature function for each temperature measurement. The linear correction functions were then applied to the temperature measurements to obtain the normalized temperature triplet data.

The transient was initiated at time zero ($t = 0$ s) by opening the valves in the unaffected and affected loop steam generator break assemblies at the same time that the valves in the lines to atmosphere were closed. The simulated MSLB, in conjunction with the simulated affected loop steam generator main

Table A-2. Initial conditions for the MSLB experiments in the S-FS test series

Parameters	Test S-FS-1	Test S-FS-2
Pressurizer pressure, MPa	15.44	15.38
Core power, kW	30.00	30.00
Core power augmentation, kW[a]	14.9	14.8
Core ΔT, K	0.7	0.4
Pressurizer liquid level [collapsed liquid level relative to zero reference elevation (bottom of pressurizer)], cm	167	181
Cold leg fluid loop-to-loop temperature difference (absolute), K	2.4	1.0
Cold leg fluid temperature (nominal), K	560	561
Primary flow rates (nominal), L/s		
Unaffected loop cold leg	9.9	9.1
Affected loop cold leg	3.1	3.3
Initial bypass flow (% of total loop flow)	2.50	2.50
Steam generator secondary pressures, MPa		
Unaffected loop	6.79	6.78
Affected loop	6.76	6.86
Steam generator secondary side masses, kg		
Unaffected loop	140	144
Affected loop	46.2	42.0
Steam generator feedwater flow rates (nominal), kg/s		
Unaffected loop	0.0195	0.0106
Affected loop	0.0	0.0
Steam generator feedwater temperatures (nominal), K		
Unaffected	370	375
Affected	—	—
Pretest measured leakage, kg/s		
Primary	0.0028	0.0028
Affected loop secondary	0.00028	0.00028

a. Core power augmentation is used to compensate for environmental heat loss.

steam line check valve failure, produced pressure reductions and inventory losses in both steam generator secondaries and rapid cooling of the primary system. The affected loop steam generator secondary pressure response caused signals to be generated, which triggered automatic responses[a] by various systems. The safety injection (SI) signal was generated by a low affected loop steam generator secondary pressure of 4.14 MPa and triggered:

- Closure of the main feedwater flow control valves, with a 1-s valve closure time simulated;
- Loss of offsite power, producing primary coolant pump coastdowns (with a 2-s delay to simulate transformer decay time) and delaying the availability of safety injection and auxiliary feedwater flows by 25 s (the time required to start the diesel generators that power the pumps);
- Closure of the unaffected loop steam generator MSLB blowdown valve (MSIV closure action with a 4-s valve closure time simulated); and
- Initiation of the auxiliary feedwater and SI signals.

The completion of these automatic actions and operator identification of the event (assumed to require a minimum of 600 s) represented the end of the blowdown phase of the test. The timing of events for the blowdown phase of the tests are contained in Table A-3.

Various recovery operations were performed for Tests S-FS-1 and S-FS-2, based on the guidance provided by Emergency Operating Procedures.[a] The recovery procedures for Test S-FS-1, specified to simulate expected operator actions in response to a steam line break, consisted of: (a) stabilizing the plant at specified pressures, temperatures, and levels, using normal charging/letdown operation, pressurizer heater operation, and unaffected loop steam generator steam and feed operations; and (b) performing a natural circulation cooldown and depressurization using pressurizer auxiliary spray operation, pressurizer heater operation, normal charging/letdown operation, and unaffected loop steam generator steam and feed operations. The recovery procedures for Test S-FS-2 consisted of stabilizing the plant as was done for Test S-FS-1. The specific requirements for these recovery procedures were outlined in References A-2, A-3, A-5, and A-6.

---

a. The automatic events were specified to simulate those used for the Zion Unit 1 Nuclear Plant FSAR calculations.

a. Zion Unit Number 1 Nuclear Plant, "Emergency Operating Procedures," Commonwealth Edison Company.

Table A-3. Timing of events for the blowdown phase of the S-FS Series MSLB experiments

Event	Specified Time (s)	Test S-FS-1 (s)	Test S-FS-2 (s)
Transient initiation	0.0	0.0	0.0
Affected and unaffected loop MSLB blowdown valves fully open	1	1	1
Normal steam valves fully closed			
Unaffected loop	—	2	2
Affected loop	—	0	0
Affected loop steam generator steam dome pressure = 4.14 MPa	$T = T_{SIS}$	21.0	7.6
Main feedwater valves fully closed			
Unaffected loop	$T = T_{SIS} + 1$	22.0	8.0
Affected loop	$T = T_{SIS} + 1$	0	0
Affected and unaffected loop pumps begin coastdown	$T = T_{SIS} + 2$	24	10
Unaffected loop MSLB blowdown valve fully closed	$T = T_{SIS} + 4$	21	11.3
HPIS/charging flows initiated; unaffected loop steam generator auxiliary feedwater flow initiated	$T = T_{SIS} + 25$	47	33
Power to both pumps tripped	$T = T_{SIS} + 43$	69	51
Operator identification of transient (blowdown over)	$T \geq 600$ and $T \geq T_{SIS} + 4$	600	600

REFERENCES

A-1. E. Klingler, *The Semiscale Mod-2C Feedwater and Steam Line Break Configuration Report for Experiments S-FS-1, S-FS-2, S-FS-6, S-FS-6B, S-FS-7, and S-FS-11*, EGG-RTH-7445, October 1986.

A-2. T. J. Boucher, W. A. Owca, *Appendix S-FS-1 of the Experiment Operating Specification for the Semiscale Mod-2C Feedwater and Steam Line Break Experiment Series*, EGG-SEMI-6783, January 1985.

A-3. T. J. Boucher, *Appendix S-FS-2 of the Experiment Operating Specification for the Semiscale Mod-2C Feedwater and Steam Line Break Experiment Series*, EGG-SEMI-6761, December 1984.

A-4. Zion Unit Number 1 Nuclear Plant, *Final Safety Analysis Report*, Appendix 15, Commonwealth Edison Company.

A-5. W. A. Owca, T. H. Chen, *Quick Look Report for Semiscale Mod-2C Test S-FS-1*, EGG-SEMI-6858, May 1985.

A-6. T. J. Boucher, T. H. Chen, *Quick Look Report for Semiscale Mod-2C Test S-FS-2*, EGG-SEMI-6827, March 1985.

APPENDIX B

ADDITIONAL INFORMATIVE DATA

APPENDIX B

ADDITIONAL INFORMATIVE DATA

Additional data obtained in Semiscale Mod-2C Tests S-FS-1 and S-FS-2 are presented in Figures B-1 through B-21.

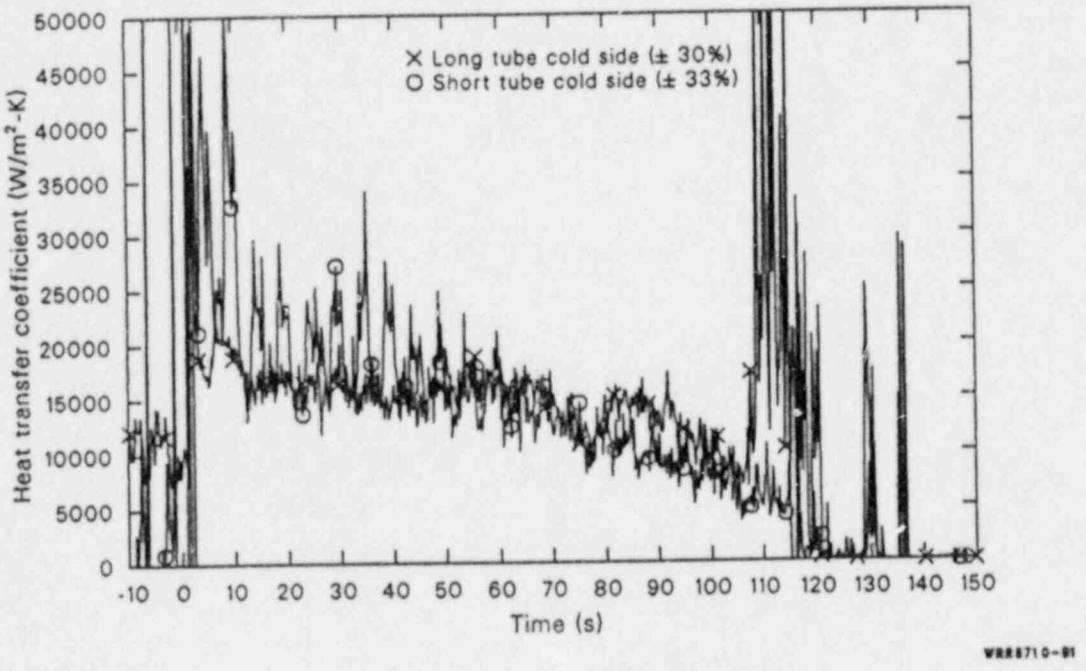

Figure B-1. Affected loop steam generator secondary convective heat transfer coefficients at the 99-cm elevation during the blowdown phase of MSLB Test S-FS-1 (-10 to 150 s).

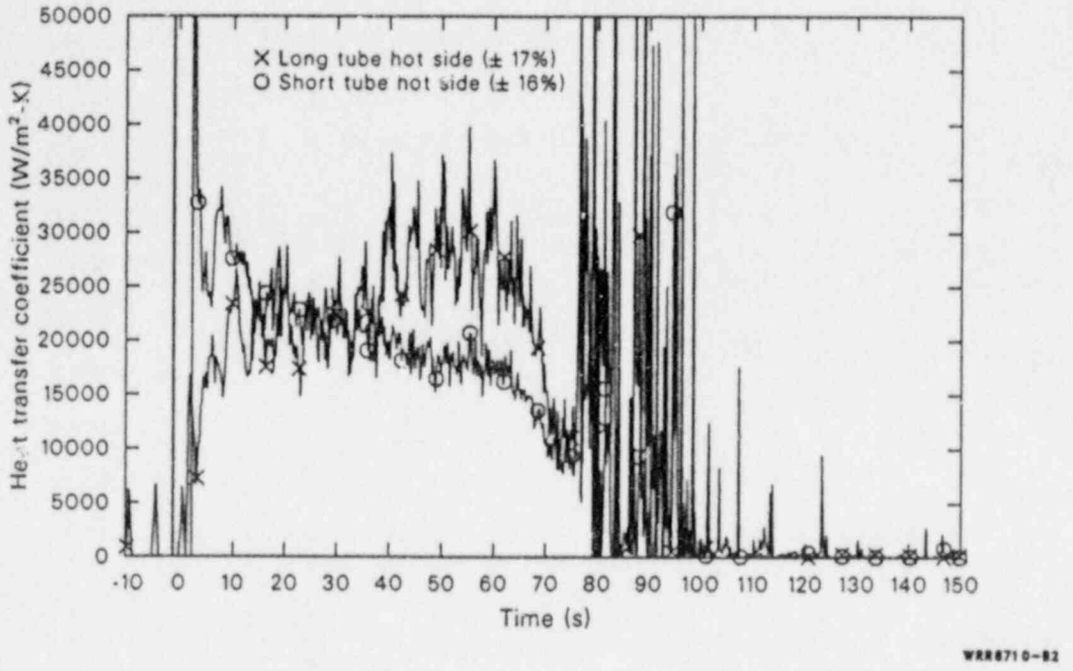

Figure B-2. Affected loop steam generator secondary convective heat transfer coefficients at the 137-cm elevation during the blowdown phase of MSLB Test S-FS-1 (-10 to 150 s).

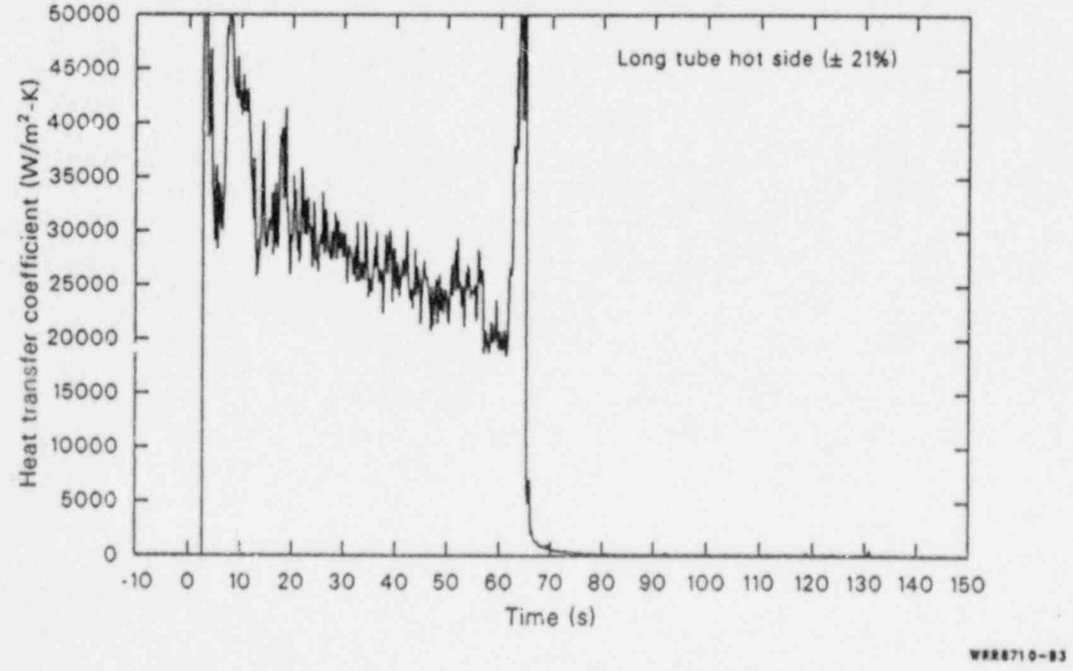

Figure B-3. Affected loop steam generator secondary convective heat transfer coefficients at the 213-cm elevation during the blowdown phase of MSLB Test S-FS-1 (-10 to 150 s).

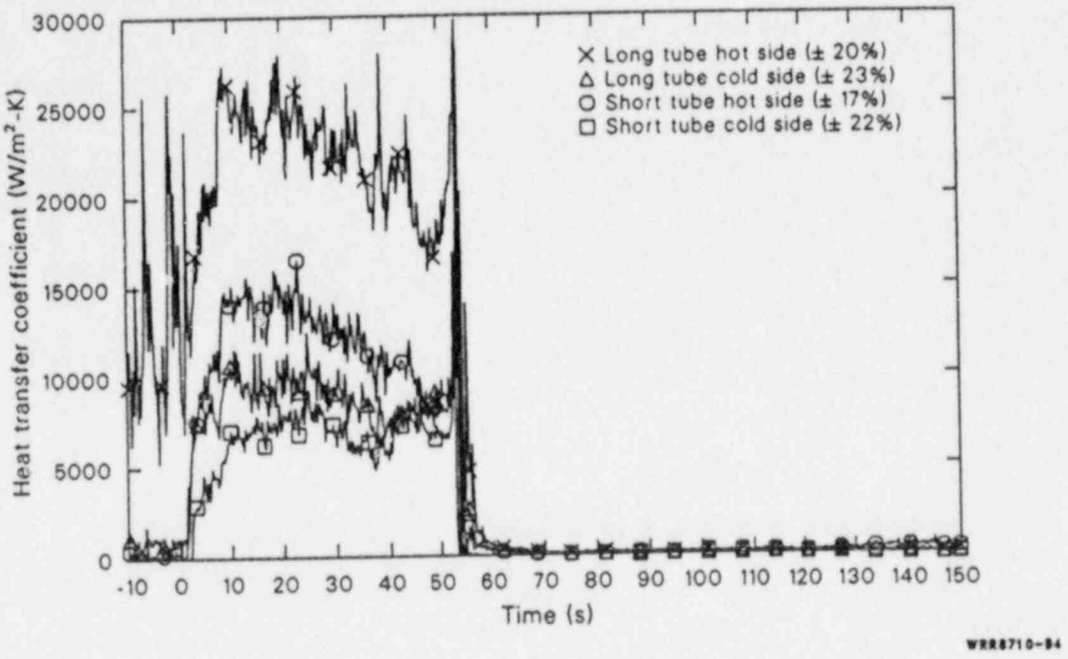

Figure B-4. Affected loop steam generator secondary convective heat transfer coefficients at the 404-cm elevation during the blowdown phase of MSLB Test S-FS-1 (-10 to 150 s).

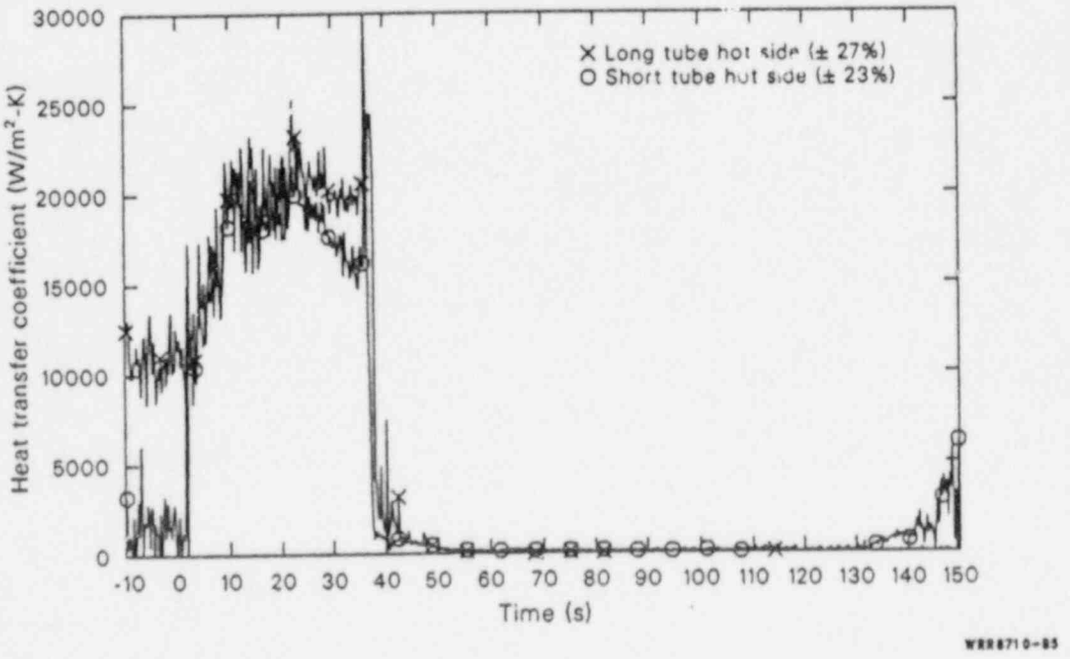

Figure B-5. Affected loop steam generator secondary convective heat transfer coefficients at the 556-cm elevation during the blowdown phase of MSLB Test S-FS-1 (-10 to 150 s).

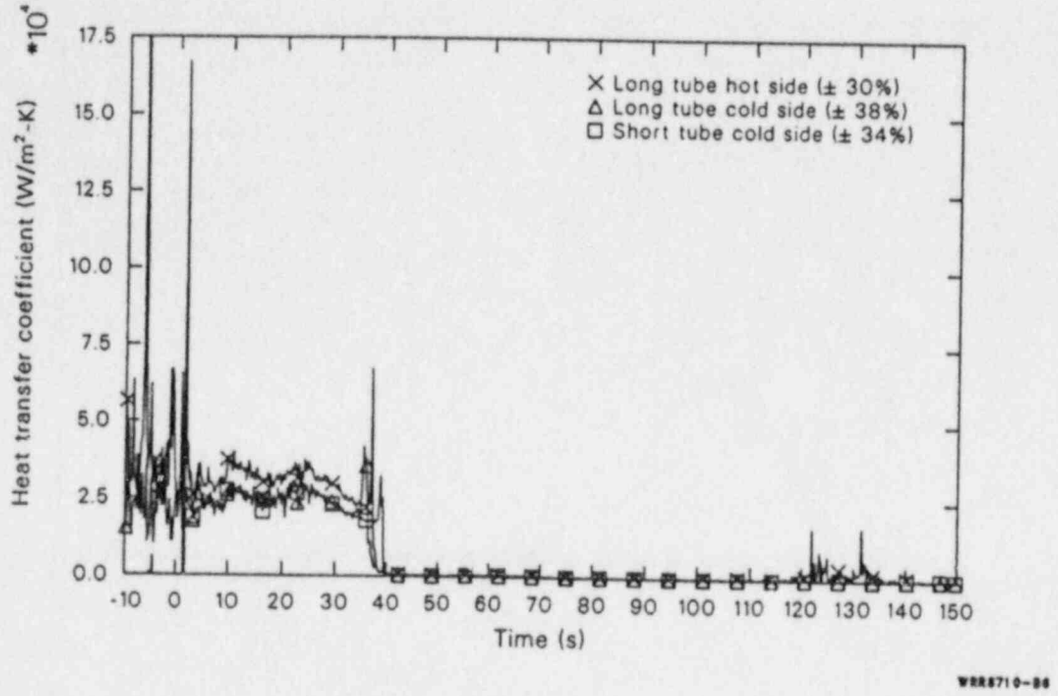

Figure B-6. Affected loop steam generator secondary convective heat transfer coefficients at the 709-cm elevation during the blowdown phase of MSLB Test S-FS-1 (-10 to 150 s).

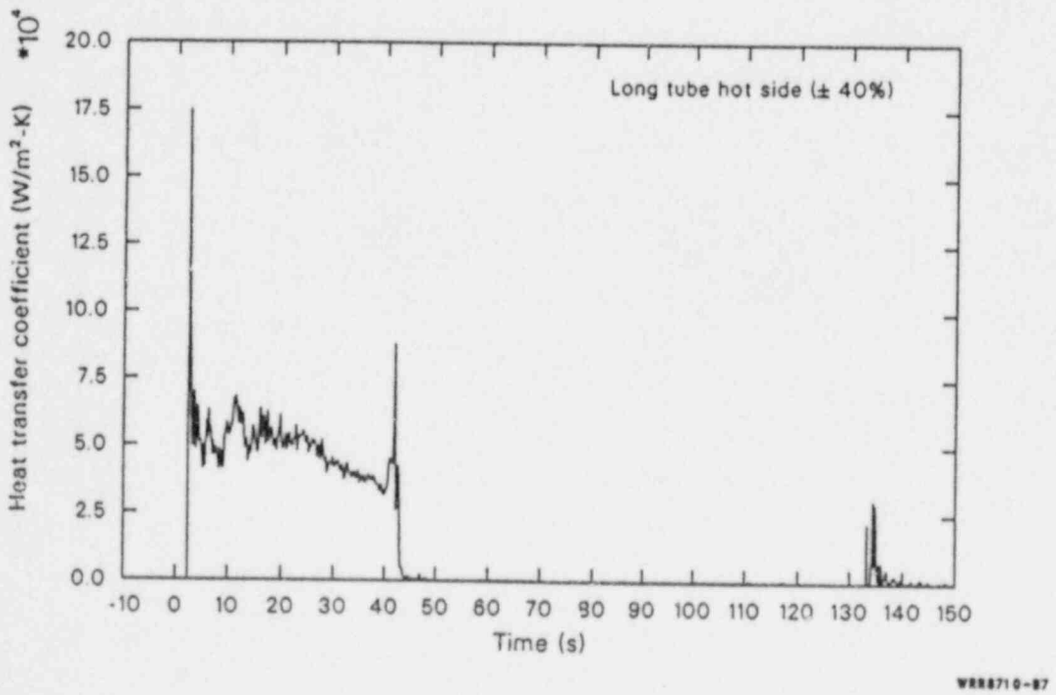

Figure B-7. Affected loop steam generator secondary convective heat transfer coefficient at the 886-cm elevation during the blowdown phase of MSLB Test S-FS-1 (-10 to 150 s).

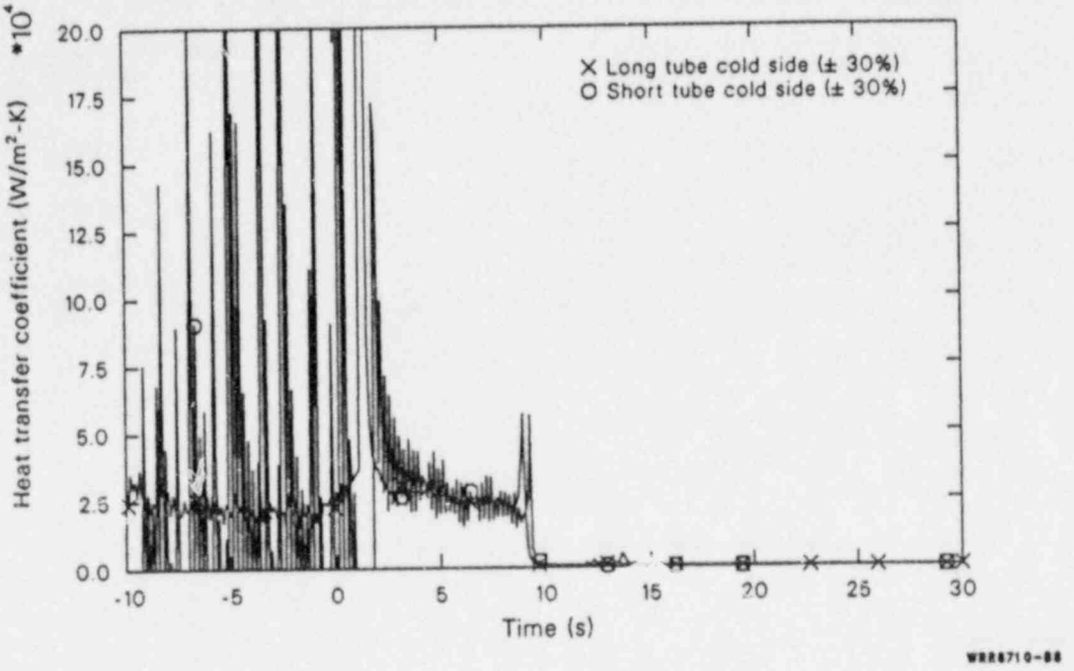

Figure B-8. Affected loop steam generator secondary convective heat transfer coefficients at the 99-cm elevation during the blowdown phase of MSLB Test S-FS-2 (-10 to 30 s).

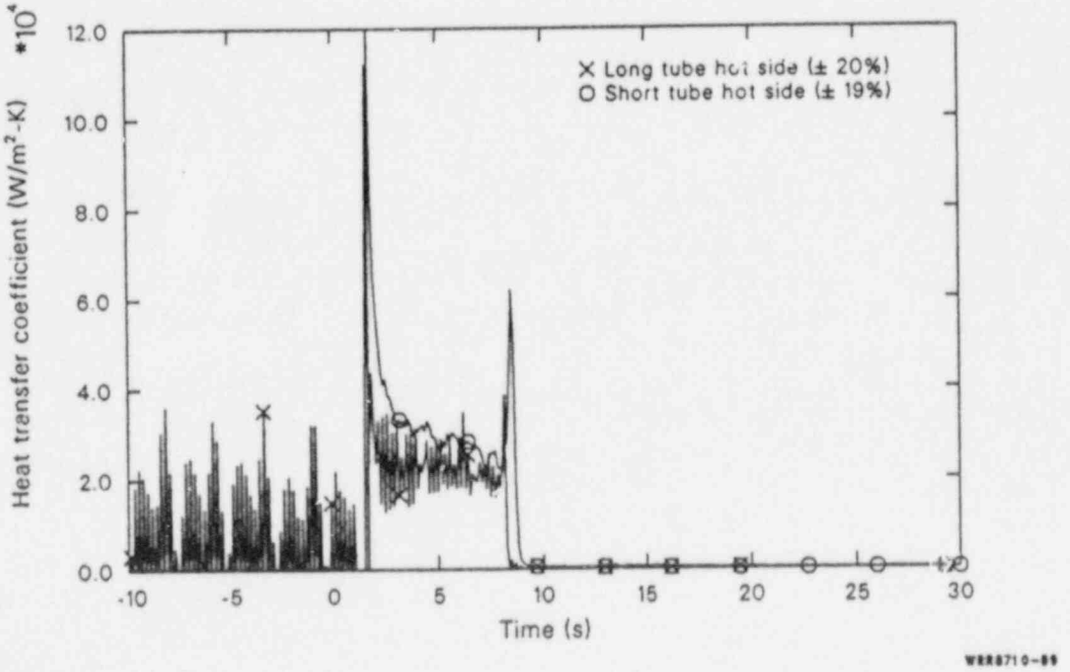

Figure B-9. Affected loop steam generator secondary convective heat transfer coefficients at the 137-cm elevation during the blowdown phase of MSLB Test S-FS-2 (-10 to 30 s).

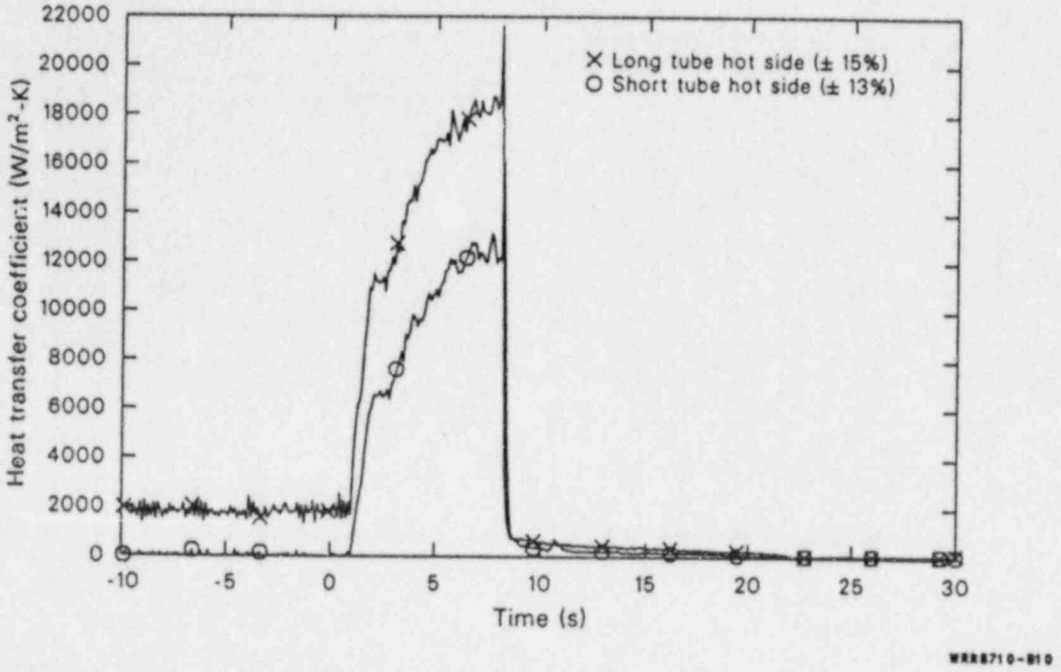

Figure B-10. Affected loop steam generator secondary convective heat transfer coefficients at the 213-cm elevation during the blowdown phase of MSLB Test S-FS-2 (-10 to 30 s).

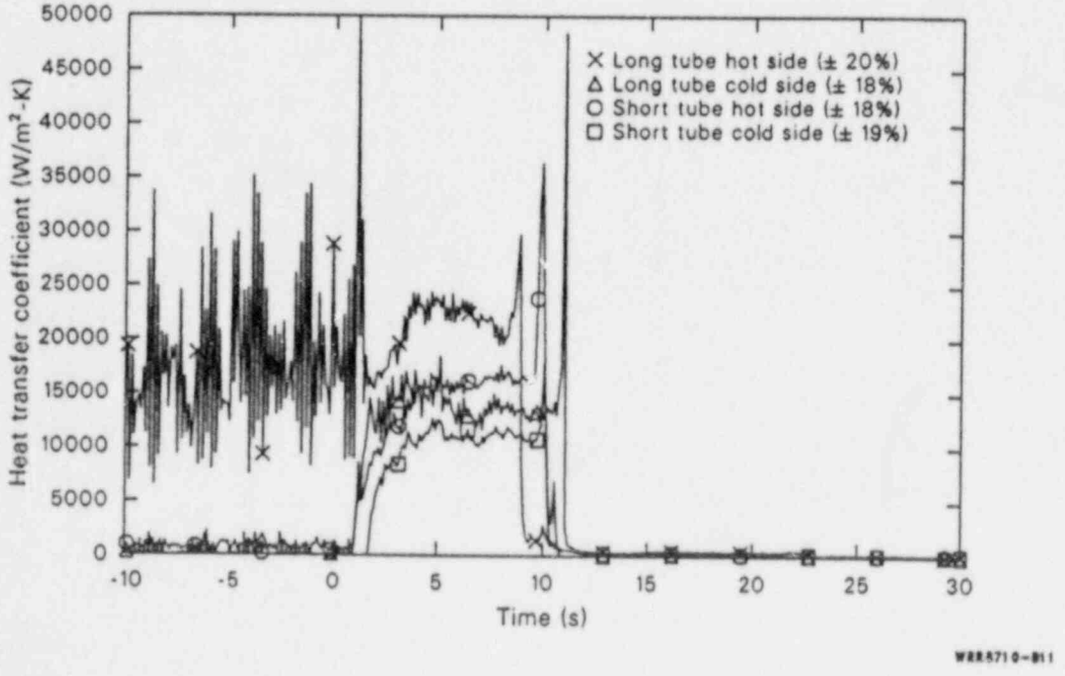

Figure B-11. Affected loop steam generator secondary convective heat transfer coefficients at the 404-cm elevation during the blowdown phase of MSLB Test S-FS-2 (-10 to 30 s).

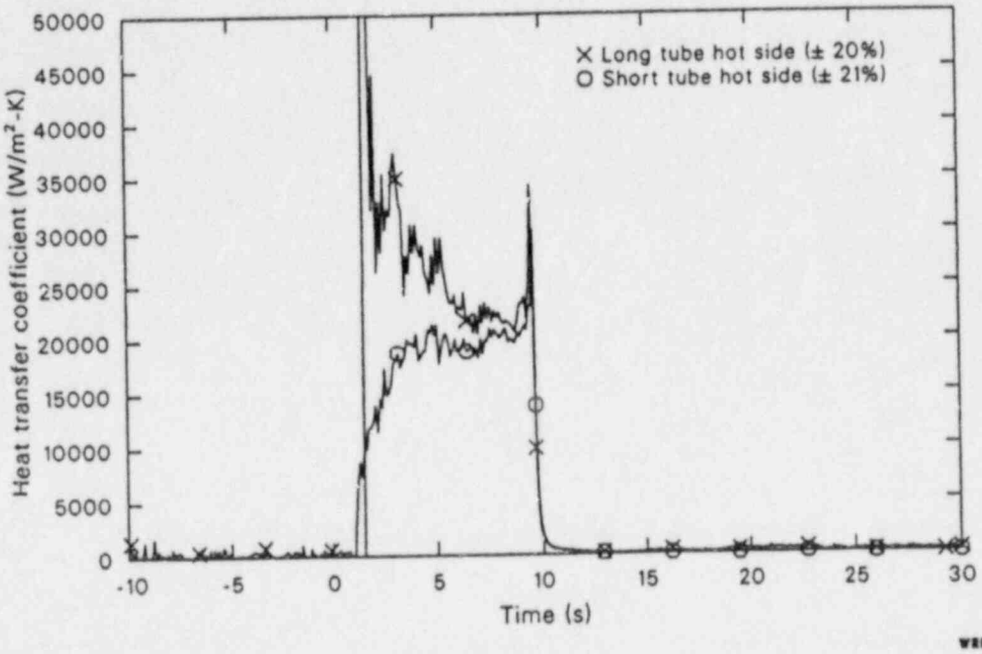

Figure B-12. Affected loop steam generator secondary convective heat transfer coefficients at the 556-cm elevation during the blowdown phase of MSLB Test S-FS-2 (-10 to 30 s).

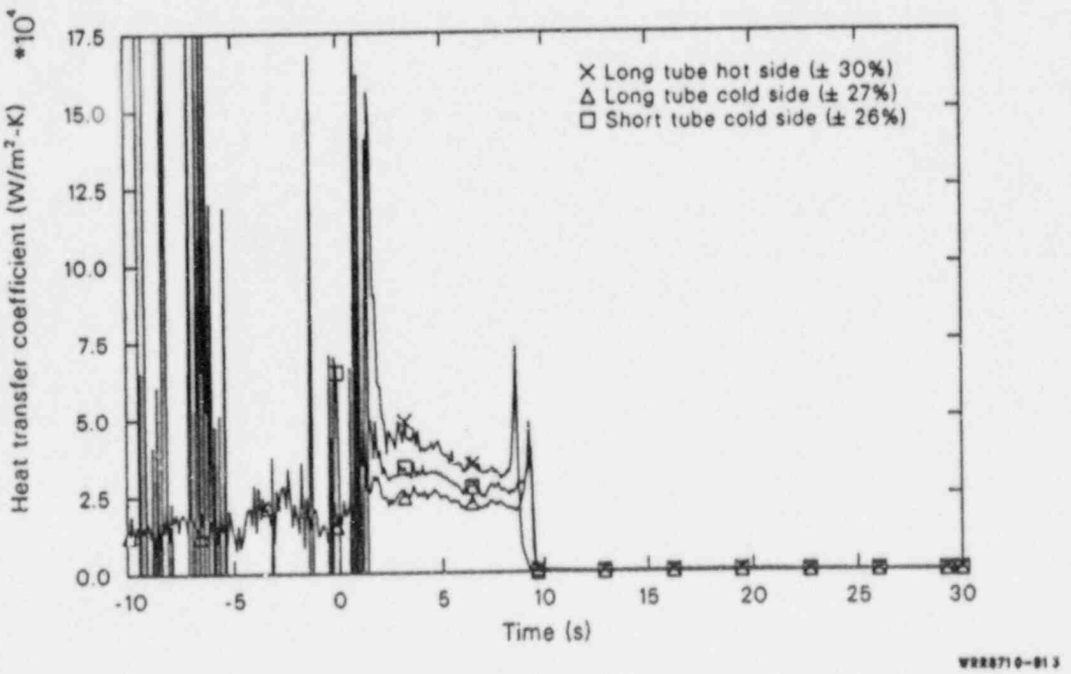

Figure B-13. Affected loop steam generator secondary convective heat transfer coefficients at the 709-cm elevation during the blowdown phase of MSLB Test S-FS-2 (-10 to 30 s).

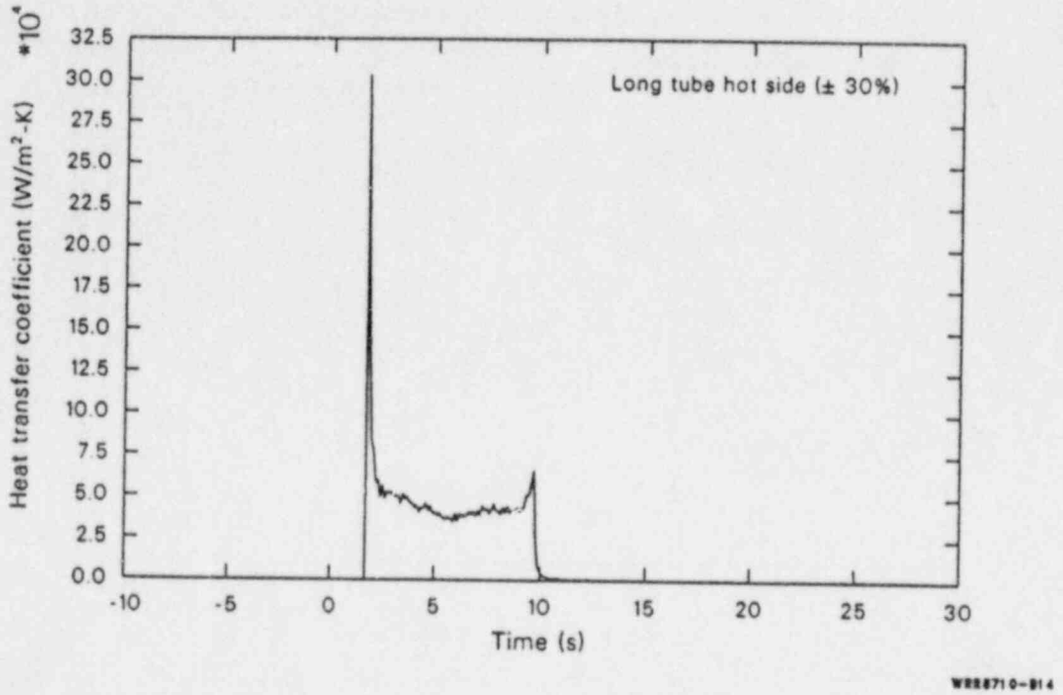

Figure B-14. Affected loop steam generator secondary convective heat transfer coefficient at the 886-cm elevation during the blowdown phase of MSLB Test S-FS-2 (-10 to 30 s).

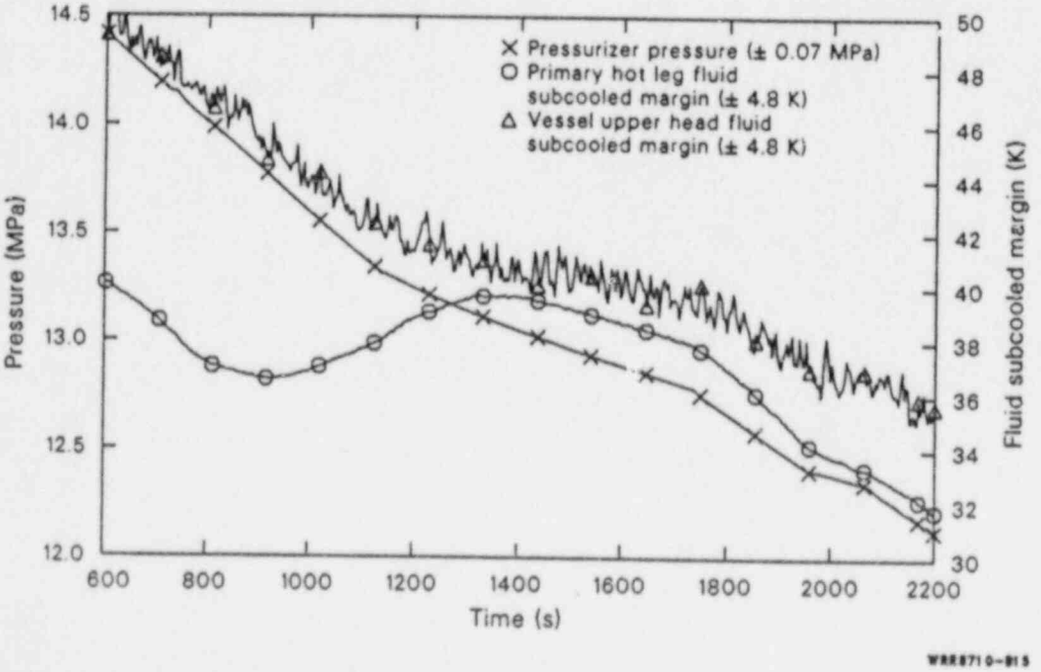

Figure B-15. Pressurizer pressure, primary hot leg and vessel upper head fluid subcooled margins, and pressurizer internal heater power during the stabilization phase of MSLB Test S-FS-2 (600 to 2,220 s).

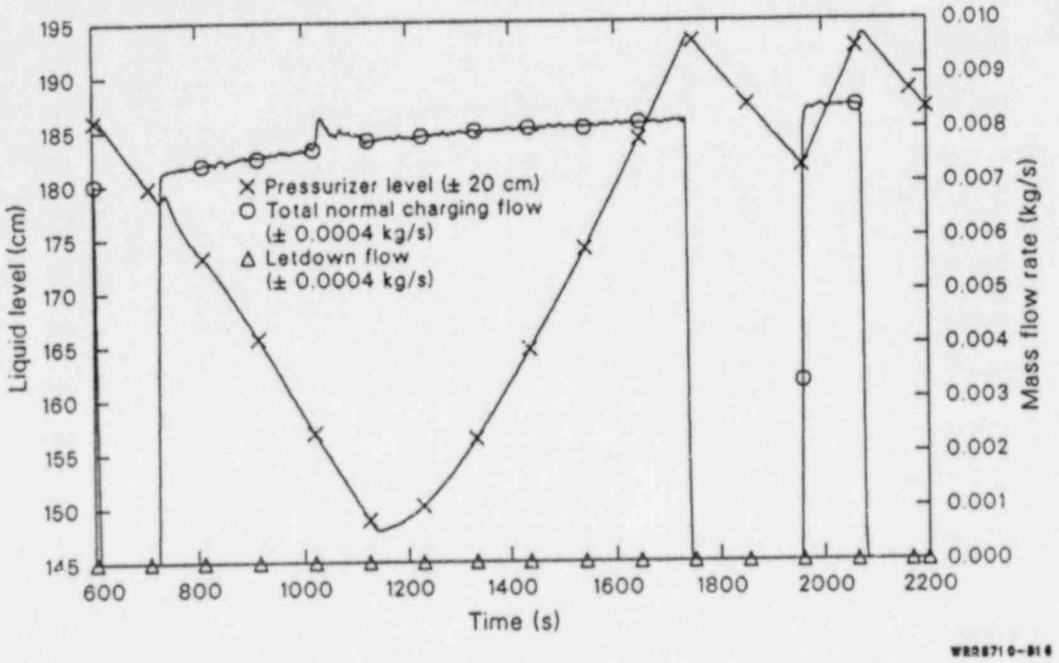

Figure B-16. Pressurizer collapsed liquid level, and total normal charging and letdown mass flow rates during the stabilization phase of MSLB Test S-FS-2 (600 to 2,220 s).

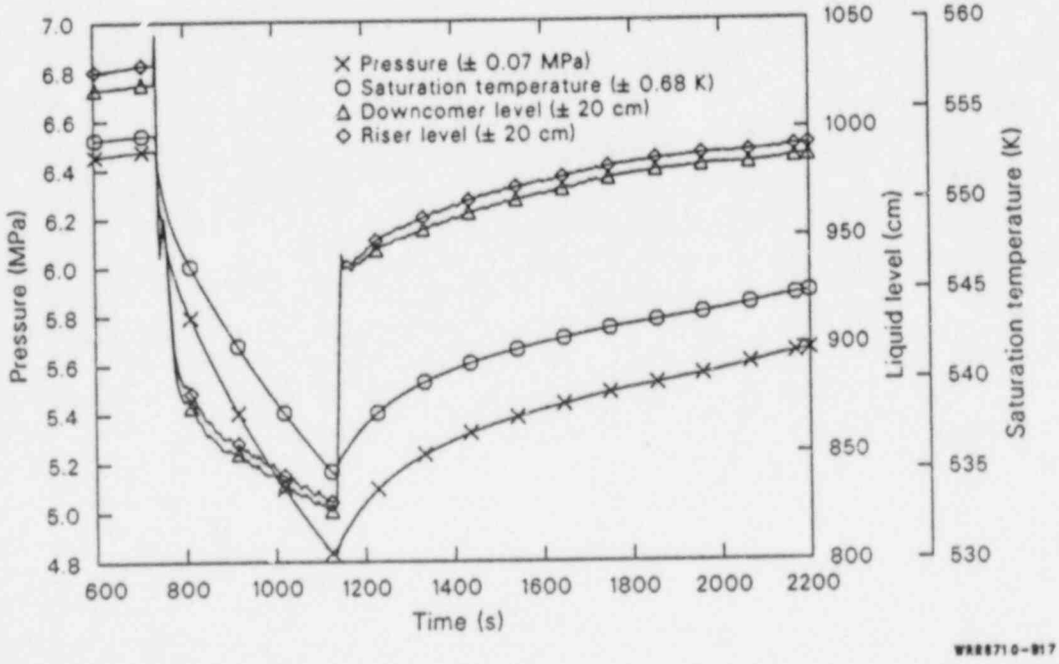

Figure B-17. Unaffected loop steam generator secondary pressure, saturation temperature and downcomer and riser overall collapsed liquid levels during the stabilization phase of MSLB Test S-FS-2 (600 to 2,220 s).

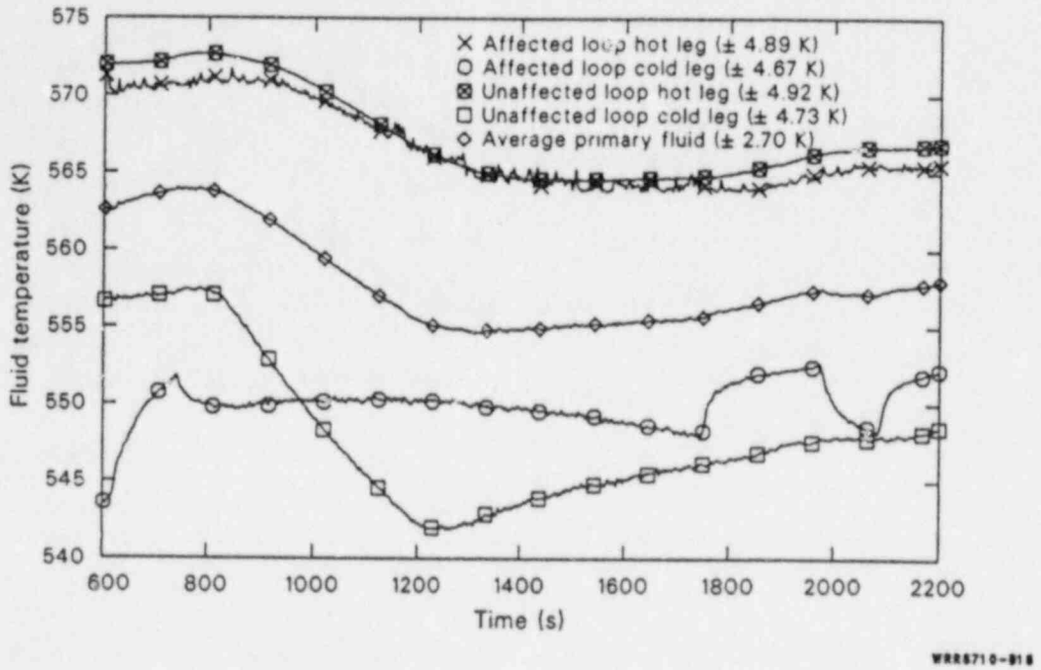

Figure B-18. Affected and unaffected loop hot and cold leg and average primary fluid system temperatures during the stabilization phase of MSLB Test S-FS-2 (600 to 2,220 s).

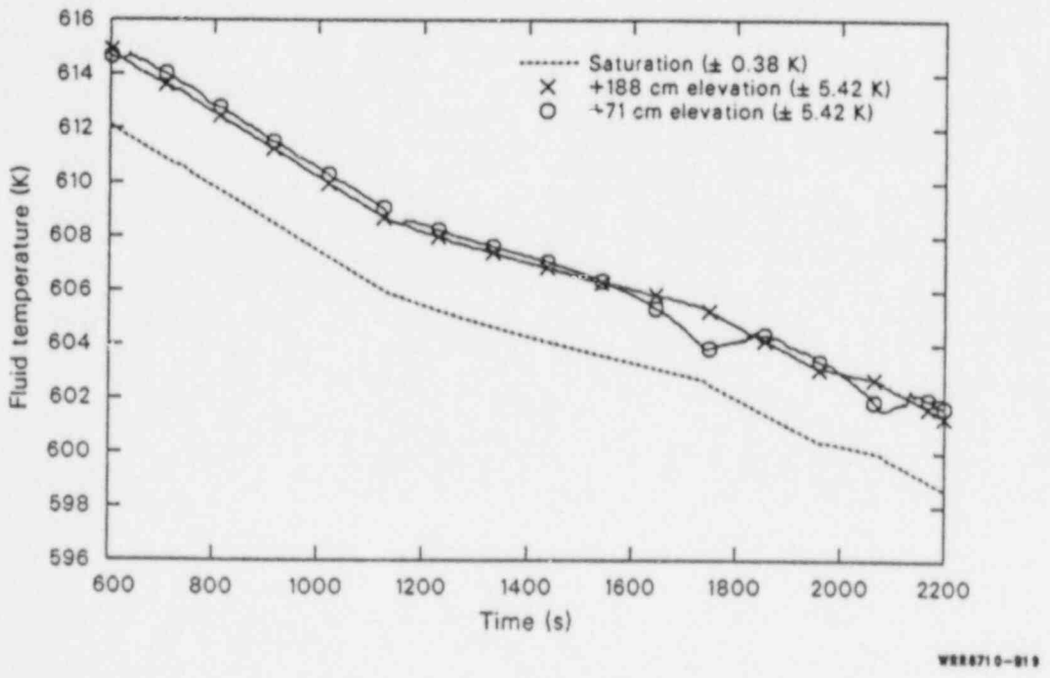

Figure B-19. Pressurizer upper and lower elevation and saturation temperatures during the stabilization phase of MSLB Test S-FS-2 (600 to 2,220 s).

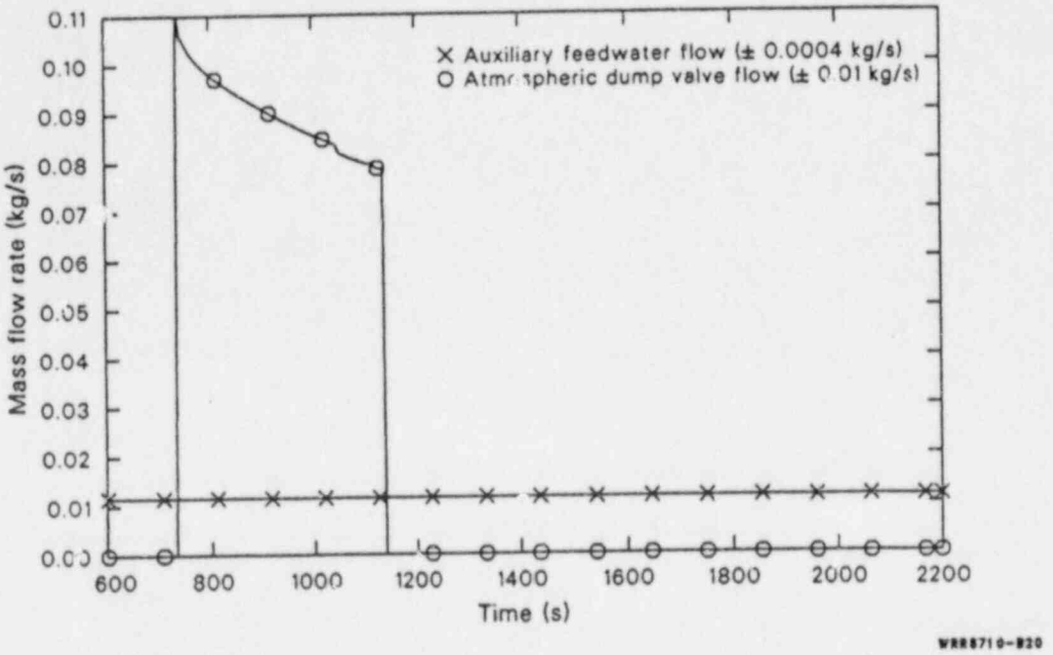

Figure B-20. Unaffected loop steam generator auxiliary feedwater and atmospheric dump valve (ADV) mass flow rates during the stabilization phase of MSLB Test S-FS-2 (600 to 2,220 s).

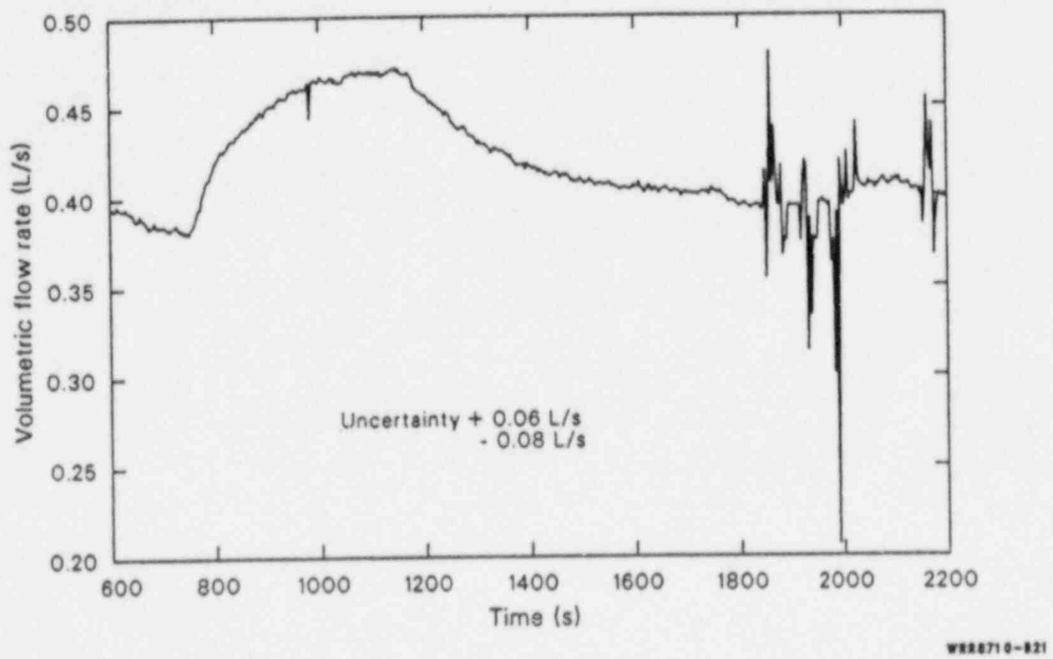

Figure B-21. Unaffected loop cold leg volumetric flow rate during the stabilization phase of MSLB Test S-FS-2 (600 to 2,220 s).

NRC FORM 335 (2.84) NRCM 1102 3201, 3202

U.S. NUCLEAR REGULATORY COMMISSION

SEE INSTRUCTIONS ON THE REVERSE

BIBLIOGRAPHIC DATA SHEET

1 REPORT NUMBER (Assigned by TIDC and Vol. No., if any)

2 TITLE AND SUBTITLE

Results of Semiscale Mod-2C Feedwater and Steam Line Break (S-FS) Experiment Series: Main Steam Line Break Accident Experiments

3 LEAVE BLANK

4 DATE REPORT COMPLETED

MONTH: March YEAR: 1988

5 AUTHOR(S)

Timothy J. Boucher

6 DATE REPORT ISSUED

MONTH: March YEAR: 1988

7 PERFORMING ORGANIZATION NAME AND MAILING ADDRESS (Include Zip Code)

EG&G Idaho, Inc.
Idaho Falls, ID 83415

8 PROJECT/TASK/WORK UNIT NUMBER

9 FIN OR GRANT NUMBER

A6038

10 SPONSORING ORGANIZATION NAME AND MAILING ADDRESS (Include Zip Code)

U.S. Nuclear Regulatory Commission
Washington, D.C., 20555

11a TYPE OF REPORT

Research

b PERIOD COVERED (Inclusive dates)

12 SUPPLEMENTARY NOTES

13 ABSTRACT (200 words or less)

This report presents the results of two experiments conducted in the Semiscale Mod-2C facility which simulated main steam line break accidents at high pressure and temperature. Tests S-FS-1 and S-FS-2 simulated double-ended offset shears of the main steam line downstream and upstream, respectively, of the flow restrictor. Initial and boundary conditions were scaled from, and compounding failures and assumptions simulated, those conditions utilized for Final Safety Analysis Report (FSAR) calculations.

Primary and secondary thermal-hydraulic responses are characterized, and the influence of the break size or location on the responses is discussed. The limiting of primary-to-secondary heat transfer by conduction heat transfer is shown to produce a trend of increased primary cooling with decreased break size, pointing out the need for further analysis for smaller break sizes. The degree of conservatism inherent in FSAR separator performance and break size and location assumptions is shown to be questionable, and the FSAR assumption of a loss of offsite power is shown to be nonconservative. The effectiveness of the recovery operations in regaining and maintaining control of the system is addressed; and main steam line break issues are discussed. Finally, conclusions are drawn and recommendations are made for further utilization of the data.

14 DOCUMENT ANALYSIS a KEYWORDS/DESCRIPTORS

b IDENTIFIERS/OPEN-ENDED TERMS

15 AVAILABILITY STATEMENT

16 SECURITY CLASSIFICATION

(This page) Unclassified

(This report) Unclassified

17 NUMBER OF PAGES

18 PRICE

EG&G Idaho
P.O. Box 1625
Idaho Falls, Idaho
83415